2019

Development of Hybrid Ion Exchange Processes Driven by Carbon Dioxide (HIX-CO2)

HANG DONG
Lehigh University

Development of Hybrid Ion Exchange Processes Driven by Carbon Dioxide (HIX-CO_2)

by

Hang Dong

A Dissertation

Presented to the Graduate and Research Committee

Of Lehigh University

In Candidacy for the Degree of

Doctor of Philosophy

in

Environmental Engineering

Lehigh University

May 2019

Approval of the Doctoral Committee

Approved and recommended for acceptance as a dissertation in partial fulfillment of the requirements for the degree of Doctor of Philosophy in Environmental Engineering on this date of _____.

_____

Derick G. Brown, Ph.D.
Committee Chairperson and Co-Advisor
Department of Civil and Environmental Engineering
Lehigh University

_____

Arup K. SenGupta, Ph.D.
Dissertation Advisor
Department of Civil and Environmental Engineering
Lehigh University

_____

Kristen Jellison, Ph.D.
Committee Member
Department of Civil and Environmental Engineering
Lehigh University

_____

John T. Fox, Ph.D.
Committee Member
Department of Civil and Environmental Engineering
Lehigh University

_____

James E. Roberts. Ph.D.
External Committee Member
Department of Chemistry
Lehigh University

Date Accepted: _____

Acknowledgment

Words are powerful to record the moments, to share the knowledge, and to create beautiful poetry, however, it seems powerless to describe the deep emotion from the heart. *Appreciation* and *thanks* are never enough to express my gratitude at this moment, even with thousands of "*many*" in front. To my parents and all my family members, friends, colleagues, teachers and advisor, appreciation and thanks are far beyond the letters.

I want to thank my Mom and Dad, who educated me since the very beginning of my life, who made the person who I am. Nothing could happen without you and this achievement belongs to both of you. Your unconditional great love and support are the most grateful thing I have had.

I want to thank my advisor, Dr. SenGupta, who guides me to accomplish this achievement, leads me to the scientific world, and throws the light on my way to the future. Your input of knowledge, thoughts, and humanity inspired me to a passionate and meaningful future. That is the power and influence just like Tagore, and Mother Teresa had.

I want to thank Jerrie Chen, who makes me a complete person fulfilled with love.

Thanks to all the friends who have presented in my life, especially lab/office mates at Lehigh for these grateful six years.

Thanks to my committee members Dr. Brown, Dr. Jellison, Dr. Fox, and Dr. Roberts, you all are important parts of this achievement. Special thanks to Dr. Brown, who guides me during master's study and initiated my journey to the Ph.D. program.

Table of Contents

List of Tables

List of Figures

Abstract

Freshwater scarcity is severely faced by humans even though our planet is full of water, being more than 97% of the water is salty water such as seawater or brackish water. And some of the brackish water is impaired by various of contaminants, such as nitrate, phosphate or fluoride, etc. There is yet an efficient and energy-saving way to recover the impaired brackish water, i.e. municipal wastewater. For removal of salts, namely, desalination, reverse osmosis (RO) and electrodialysis (ED) are truly the only water desalination processes currently in practice for the entire range of total dissolved solids (TDS) from 500 – 35,000 mg/L. For brackish water and wastewater with total dissolved solids (TDS) less than 1500 mg/L, RO is universally used. But at high recovery of 80% or more, membrane processes are energy intensive and demand significant pre-treatment to avoid salt precipitation and consequent membrane fouling. For low TDS brackish water (less than 1000 mg/L), ion exchange demineralization requires low energy input, however, multiple hazardous chemicals are employed, and hazardous wastes are produced. Ion exchange process is also commonly applied for nitrate removal. Instead of acid and base regeneration as in demineralization, a brine regeneration (10-15% NaCl) is the obstacle preventing it to be a green process due to the heavy chemical consumption and brine waste disposal. Inability to achieve multiple effects such as concurrent trace contaminants removal, i.e. fluoride and desalination also makes it less attractive.

In this study, we present for the first-time hybrid ion exchange processes (HIX-CO_2) that does not require any semi-permeable membrane and can desalinate, soften and removes contaminants (nitrate, phosphate, fluoride) from lean brackish water (TDS≤1500 mg/L) using CO_2 as the source of energy and regenerant. Hybrid anion exchanger with dispersed

ZrO_2 nanoparticles (HAIX-NanoZr) and a shell-core weak-acid cation exchange (SC-WAC) resin form the heart of the process. Pressurized carbon dioxide is the only chemical needed to sustain the process. CO_2 serves concurrently as both an acid (i.e., H_2CO_3) and a base (HCO_3^-) for the proposed process. In contrast to a conventional deionization plant, the anion exchanger, i.e., HAIX-NanoZr precedes the cation exchanger or SC-WAC to take advantage of the unique carbonate chemistry for desalination. The novel ion exchange process achieves multiple effects of desalination and nitrate removal without hazardous chemicals and brine consumption and eliminates the burden of waste disposal plus selective removal of trace ligand contaminants (i.e. phosphate, fluoride). Once appropriately developed and field tested, the HIX-CO_2 process has the attributes to be a viable alternative to RO for impaired water bodies with TDS less than 1500 mg/L or be retrofitted into existing nitrate removal facilities. Moreover, it has the potential to be integrated into existing RO systems as a CO_2 driven anti-scaling pretreatment.

CHAPTER 1 Introduction

1.1 Freshwater scarcity and viable water sources

Freshwater scarcity faced by human society is a long-existing concern. Even though our planet is surrounded by water, most of it is salty water such as seawater or brackish water. Scanty natural freshwater sources are also affected by climate changes, and not always geologically available. Alternative water sources and corresponding water reclamation strategies become urgent and necessary, such as municipal wastewater reclamation. Regardless of locations, impaired brackish water such as discharges from municipal wastewater plants are a key component for nearly every population center. Water discharge from the municipal wastewater plants, especially those located in the densely populated metropolises, is huge. The capacity of the wastewater treatment plant in Chicago achieves billions of gallons per day(Metropolitan Water Reclamatin District of Greater Chicago, 1939). Understandably, the water amount in such a water discharge approximately meets the water demand, as they are mostly collected after anthropogenic consumption. The ways human employ regulated fresh water supplies are widely similar, which renders the composition in such wastewater is steady regardless of locations. Additionally, these water discharge sources are close to the water consumption center and absent from interferences such as climate change, etc., Figure 1-1. It is obvious that attempts to utilize such a steady and abundant water discharge are attractive to all population centers. Yet, it is not practically implemented in a wide range.

The Orange County Water District (OCWD) in California has been reported to practice municipal wastewater reclamation(OCWD, 2018). After conventional treatments, i.e.

biological degradation and sedimentation to remove BODs and suspend solids, desalination for such a treated secondary water, with universally similar 500 – 1000 mg/L TDS, is necessary during the wastewater reclamation process. Even though the TDS is much lower than seawater and most brackish water, reverse osmosis (RO), as the most popular desalination process, is applied. Energy consumption for the feedwater with a TDS 500 – 600 mg/L is 1.25 – 1.5 kWh per 1000 litters of water desalinated in OCWD (OCWD, 2018). That is the energy to power a 60 W bulb for 20 to 25 hours. This high energy consumption by RO under 80% recovery is the most energy-intensive module during the wastewater reclamation process. It is true that RO could play a unique role during seawater desalination with a 35,000 mg/L TDS, however, it is dominating the desalination operations in the entire range of TDS from 500 mg/L to 35,000 mg/L. Nearly every desalination plant with a feedwater TDS below 1500 mg/L is using RO in Texas, and they are operated typically below a 75% recovery rate (Texas water development board, 2010). Since the osmotic pressure in the brine waste highly depends on the recovery rate, RO faces a dilemma between recovery rate and energy consumption. Even though the high recovery rate could save more water from the limited water source and reduce brine discharge to minimize the waste disposal cost, most practices prefer operating under low recovery rate to save the energy. For municipal wastewater with TDS slightly higher than standard, an alternative low-energy desalination processes independent of recovery rate is needed. Ion exchange demineralization is commonly applied for low TDS brackish water desalination (Applebaum, 1968). It does not need high energy input to overcome osmotic pressure and the water recovery only depends on the regeneration efficiency. However, the frequent regeneration renders heavy chemicals consumption. Conventional ion exchange

demineralization utilizes mineral acid (i.e. HCl) and strong base (i.e. NaOH) for regeneration upon exhaustion. These two corrosive chemicals bring difficulties in a field practice and create hazardous waste. To take advantage of this low energy demand process, green-regeneration to eliminate the consumption of multiple corrosive chemicals and the production of hazardous waste is urgent to be explored.

Figure 1-1. Municipal wastewater plants with huge capacities and attractive features around the world that could serve as water sources.

Other common water sources such as groundwater are often brackish water with TDS less than 3000 mg/L, however, agricultural activities often render highly nitrate levels in the groundwater. Co-present fluoride due to regional geological condition also demands appropriate treatment processes to make the water sources usable.

1.1.1 Salinity

Salinity, or total dissolved solids (TDS), is critical during water supply. The United States Environmental Protection Agency (USEPA) has set up a recommended salinity level of 500mg/L for drinking water (USEPA Web, 2019). In the long term of human activities, there is a high consumption of low TDS water for potable and industrial applications and subsequent release of higher TDS wastewater back to the environment. This behavior is not sustainable in arid climates unless methods are used for water reuse or efficient treatments for non-potable water. Water desalination technology has been developed over many years to solve the water shortage issue. Seawater and many groundwater aquifers are not potable because of their high total dissolved solids (TDS). Seawater usually contains about 35,000 ppm of salt and brackish surface water or groundwater could have 1,000-10,000 ppm TDS (National Ground Water Association, 2010). However, the USEPA has established the National Secondary Drinking Water Regulations in which the TDS standard is 500 ppm (USEPA Web, 2019). Brackish water desalination becomes necessary in arid regions- novel, high-efficiency solutions are required for inland locations lacking waste brine disposal options.

Brackish water sources up to 3000μS/cm conductivity and 2000 ppm TDS are currently treated by RO plants in different locations. The California Department of Public Health (CDPH) has established a secondary maximum contaminant level (SMCL) drinking water standards for TDS in public water supplies. The recommended TDS SMCL is 500 mg/L, and the upper TDS SMCL is 1000 mg/L. A map of TDS in California's groundwater measured in 2007 is shown in Figure 1-2 (State water resources control board, 2010).

TDS in Groundwater, 2007
TDS concentrations using data from public supply wells (CDPH), environmental cleanup sites (SWRCB), Department of Water Resources (DWR), and the State Water Boards Groundwater Ambient Monitoring and Assessment (GAMA) Program. Red dots indicate wells where TDS concentrations are above short term public drinking water standards. Orange dots indicate wells where TDS concentrations are above upper limit public drinking water standards. Yellow dots indicate wells where TDS concentrations are above recommended public drinking water standards, and blue dots indicate wells below all public drinking water standards. Data source: GeoTracker GAMA.

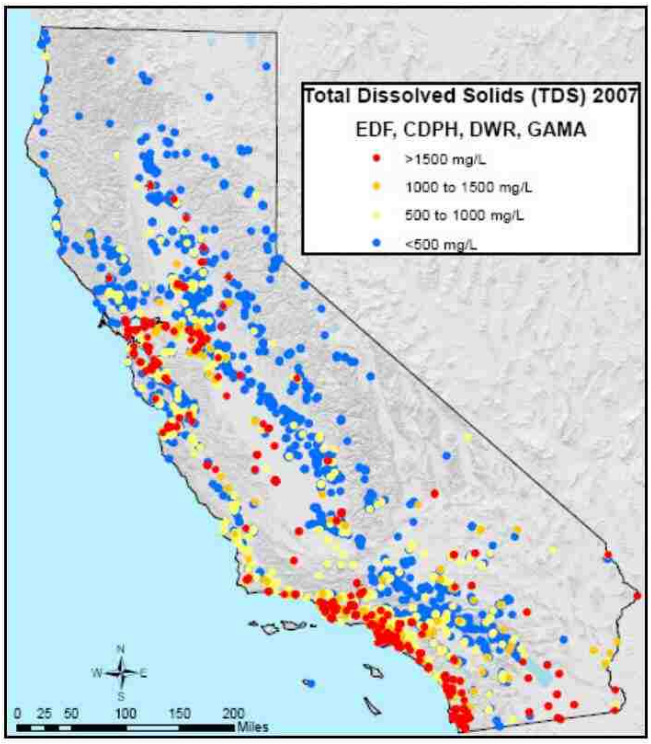

Figure 1-2. Groundwater map shows TDS levels across the state of California from publicly available data. Red, orange and Yellow dots indicate brackish water sources need to be desalinated to serve as potable water (State water resources control board, 2010).

Florida is the state that produces the highest volume of desalinated water in the U.S: 515 MGD across >140 facilities (Adamski and Knowles Jr., 2001). The most commonly used brackish water sources in Florida are Upper Florida Aquifer and Biscayne Aquifer (400-800 ppm TDS); seawater is avoided. An Upper Florida Aquifer TDS map is shown in Figure 1-3 (Adamski and Knowles Jr., 2001; Lai et al., 2009)

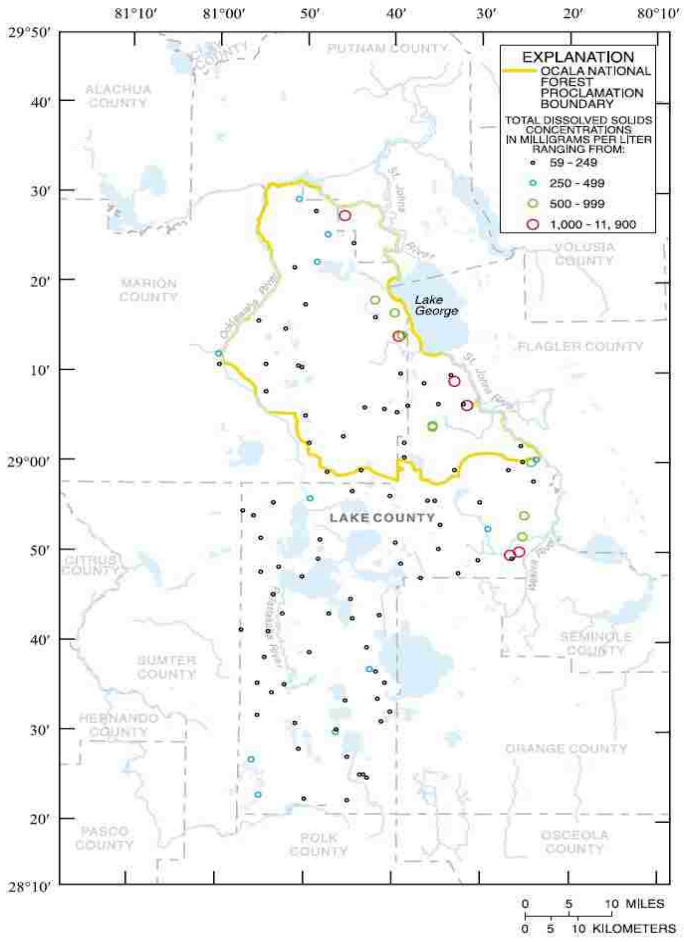

Figure 1-3. A map shows TDS in upper Florida aquifers. Green and red dots indicate the brackish water sources need to be desalinated to serve as potable water (Adamski and Knowles Jr., 2001).

In Texas, there are 46 desalination facilities reported by the Texas Water Development Board in 2010. Plant details reported are shown in Figure 1-4. Highlighted plants are the RO plants dealing with low TDS brackish water (less than 2000 ppm) (Texas water development board, 2010).

With many desalination facilities, from brackish water to seawater, A single energy intensive reverse osmosis process is universally applied and often operated under low recovery rate. Desalination will continue to be an important water challenge living along

with the demands of pure or low salt concentration water from human, yet the technology still needs to be developed and improved.

Desalination Plants	Process Type	Desal Prodution average (MGD)	Raw water TDS ppm	Membrane Recovery
City of Abilene (Hargesheimer Treatment Plant)	RO	1.2	1500	0.65 to 0.78
City of Beckville	RO	0.0082	1200	0.75
City of Brady	RO	0.5	1,200 - 1,600	0.75
City of Evant	RO	0.065	1100	0.8
City of Fort Stockton Osmosis/Desalination Facility	RO	3	1500	0.8
City of Kenedy	RO	0.413	1500	0.67
City of Robinson Reverse Osmosis Plant	RO	0.5	750	0.75
City of Seymour	RO	1	800	0.81
City of Tatum	RO	0.216	1200	0.75
Dell City	EDR	0.05	1466	0.75
DS Waters of America, LP	RO	0.09	470	0.75
River Oaks Ranch	RO	0.108	1500	0.7
Study Butte Terlingua Water System	RO	0.035	1425	0.75
Water Runner, Inc.	RO	1.5	790	0.95
Windermere Water System (Idle)	RO	0.5	900	No Data
[source]http://www2.twdb.texas.gov/apps/Desal/DesalPlants.aspx				

Figure 1-4. Desalination plants located in Texas with raw water TDS less than 1500 ppm. Highlighted RO plants could use ion exchange desalination technology.

1.1.2 Nitrate contamination

Application of excess ammonia fertilizer and consequent biological nitrification escalates the number of nitrate-contaminated groundwater sources. The crisis is the most pervasive in agriculture-intensive regions in the Midwest of the USA, Figure 1-5 (Wentz, 2011). World widely, nitrate contamination has been reported in the agricultural area in North China Plain (Su et al., 2013) and recently massive surface water remediation in the south of China by excessive onsite aeration in the high NH_4^+-N containing surface water could form a new nitrate contamination source during groundwater replenishment. Although the maximum contaminant level (MCL) for NO_3^- (10 mg/L as N) in drinking water has remained the same for over 40 years, the number of groundwater sources needing treatment has increased significantly.

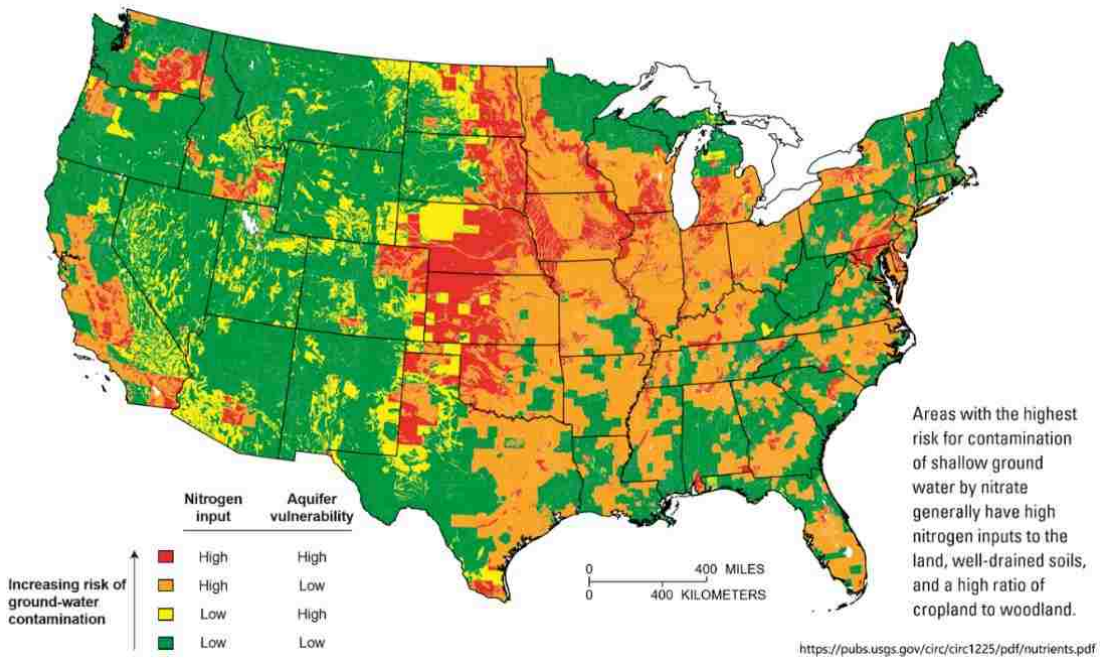

Figure 1-5. A map of areas that are at risk of nitrate contamination to shallow groundwater.

1.1.3 Trace contaminants

In addition to TDS issues and nitrate contamination with the water sources, natural contamination of various trace ions such as fluoride are also a major concern. These contaminations are regional but in large scale, and they are usually in trace amounts compared with other background ions, trace but toxic. For example, WHO has set a recommended limit of arsenic to 10 ppb, fluoride at 1.5 ppm (German, 2017). The global map in Figure 1-6 shows the fluorosis problems worldwide, where Fluoride could be more than 1.5 ppm. The ability to remove these ions, i.e. fluoride, from hundreds and thousands of ppm total dissolved solids in the background water, requires high selectivity during the treatment. Moreover, contaminants of these ions and high TDS or high nitrate could occur at the same complex water source, Figure 1-7 (Amini et al., 2008; German, 2017). Technologies to selectively remove trace contaminants and perform desalination and nitrate removal are in demand.

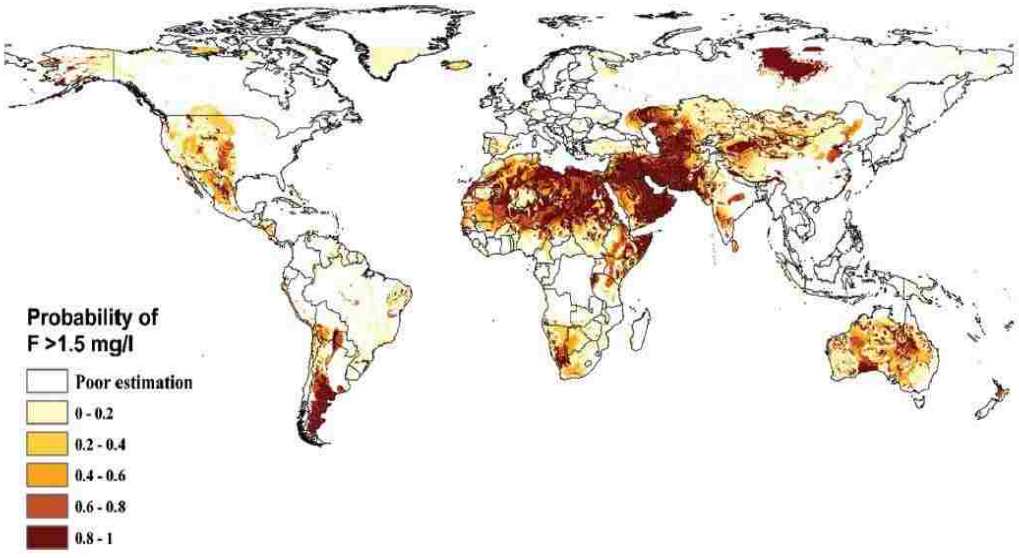

Figure 1-6. A map shows global fluorosis problems. (Amini et al., 2008)

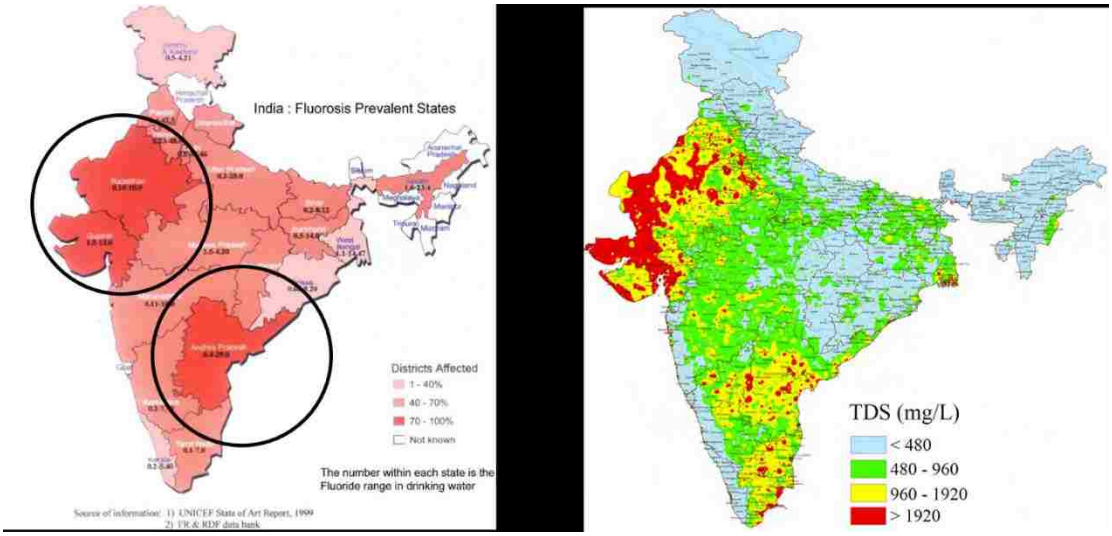

Figure 1-7. A map shows co-occurrence of high fluoride and high TDS. (German, 2017)

1.2 Challenges of water treatment technologies

1.2.1 Reverse osmosis (RO): recovery rate, energy consumption, selectivity

Reverse Osmosis is the most commonly used desalination process today. As seen from Figure 1-4, all the plants listed are installed with RO systems for brackish water desalination. However, there are many challenges for RO processes. One of the large concerns is the concentrate disposal. Brine concentrate is continuously produced during RO plant operation. Current disposal options are surface water or sewer discharge, land application, evaporation ponds and deep well injection based on plant condition and location (Smith and Sengupta, 2015a). But these practices are producing new issues such as re-contaminating water resources, reducing soil fertility, or high expenses. To reduce concentrate volume, we need to increase the recovery rate during operation. But, the energy requirement increases exponentially with recovery as shown in Figure 1-8 (Zhu et al., 2009). Some studies have been done to increase RO recovery rate from 80% to 90%, thus concentrate volume could reduce from 20% to 10%, or a 50% decrease in waste, which is significant (Smith and Sengupta, 2015b). However, energy costs would also increase significantly, and the overall sustainability is questionable.

A schematic of a typical RO system is shown in Figure 1-8 where Q_F, $Q_{B,}$ and Q_P are the flow rate of feed, brine and permeate water, respectively. C_F, $C_{B,}$ and C_P are the concentration of feed, brine and permeate water, respectively.

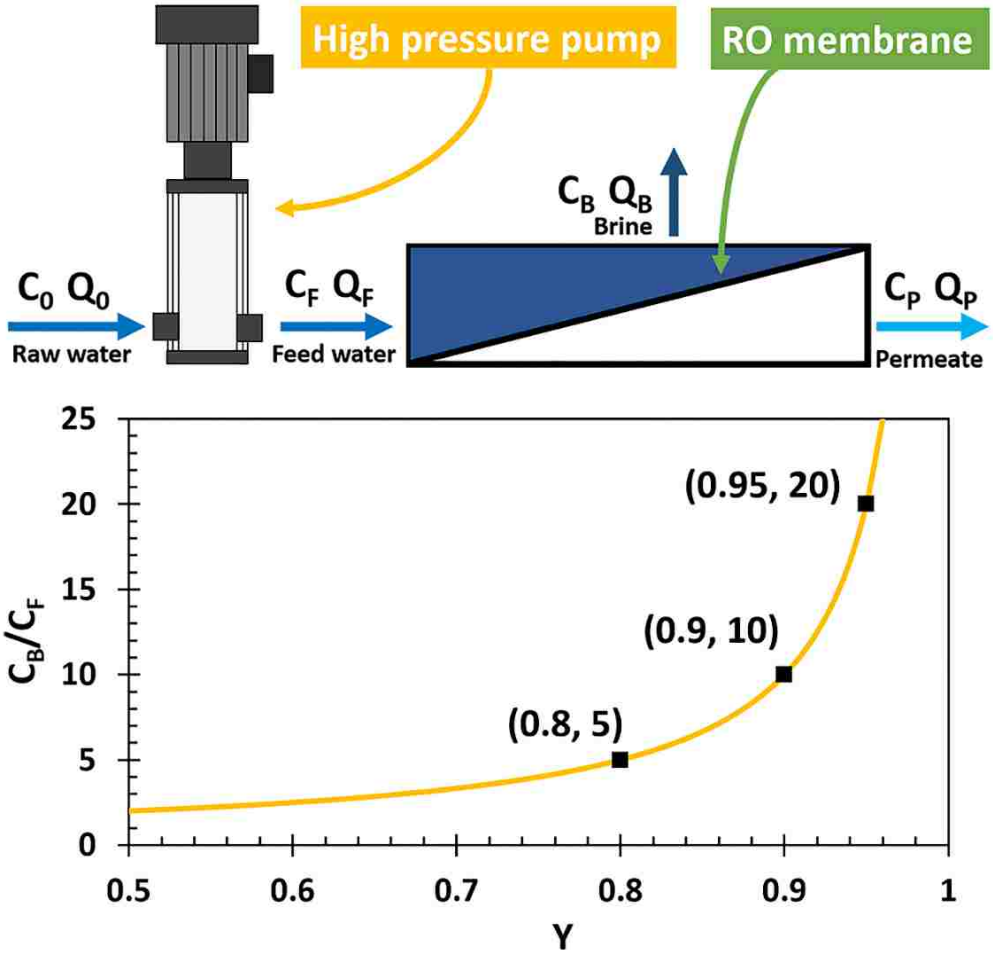

Figure 1-8 A schematic describes RO system and shows energy consumption increase rapidly with recovery rate.

The recovery or yield, Y, is defined as

$$Y = Q_P / Q_F \quad \text{Equation 1-1}$$

From the mass balance of dissolved solutes for the RO system,

$$Q_F C_F = Q_B C_B + Q_P C_P \quad \text{Equation 1-2}$$

Since $C_P \sim 0$

$$Q_F C_F = Q_B C_B \quad \text{Equation 1-3}$$

Also, for water

$$Q_F = Q_B + Q_P \quad \text{Equation 1-4}$$

Combing equations (1), (2) and (3),

$$C_B / C_F = 1/(1-Y) \quad \text{Equation 1-5}$$

Figure 1-8 shows how C_B is rapidly increasing beyond 70% recovery. The dilemma of RO on recovery rate and energy consumption is a huge challenge caused by the nature of the principle.

Besides the dilemma, RO performs non-selectivity and it tends to remove all the salts. With most of the researches ongoing trying to continuously increase the membrane permeability, it has been emphasized in a recent review (Werber et al., 2016) that RO processes need more selectivity toward target trace solutes than enhanced permeability.

1.2.2 Ion exchange demineralization: hazardous chemical consumption

Ion exchange naturally exists in nature. This phenomenon was first recognized scientifically by agriculture and soil chemists (SenGupta, 2017). The removal of ammonium ions from manure by cation exchanging soil is shown as follows: (SenGupta, 2017)

NH_4^+ (aq) + Na^+ (soil) ↔ NH_4^+ (soil) + Na^+ (aq) Equation 1-6

$2NH_4^+$ (aq) + Ca^{2+} (soil) ↔ $(NH_4^+)_2$ (soil) + Ca^{2+} (aq) Equation 1-7

Since then, Zeolite, naturally occurring aluminosilicates, is still being used as adsorbent or ion exchange material for selectively removing ammonium ions. Selectivity is the nature of ion exchangers and could be manipulated to handle which ion could be adsorbed and which one will be released. It is a fine art based on all the molecular chemistries and further we could apply this potential to remove trace contaminants selectively.

Ion exchange could also be applied to desalination. The most common two-bed process is to exchange cations with hydrogen ion (H^+), then followed by exchanging anions with the hydroxide ion (OH^-), finally forming H_2O. Salts were demineralized from the water, Figure 1-9.

$Na^+ + R\text{-}H^+ \leftrightarrow R\text{-}Na^+ + H^+$ Equation 1-8

$Cl^- + R\text{-}OH^- \leftrightarrow R\text{-}Cl^- + OH^-$ Equation 1-9

$H^+ + OH^- \leftrightarrow H_2O$ Equation 1-10

Overall, $Na^+ + R\text{-}H^+ + Cl^- + R\text{-}OH^- \leftrightarrow R\text{-}Na^+ + R\text{-}Cl^- + H_2O$ Equation 1-11

where, R denotes ion exchangers with matrix and functional groups.

Both cations and anions are finally being adsorbed on to the sites on the adsorbents, and the produced water comes from pre-loaded H^+ and OH^-, which follows the mass balance. Thus, it demands strong acid and strong base to regenerate the materials once exhausted,

providing the pre-loaded H^+ and OH^-. Hazardous chemical consumption and the disposal of waste acid and waste base form the challenges of such a process.

Novel ion exchange desalination processes aim to use ion exchange resins as a tool to produce low TDS water are also developed. Dr. Robert Kunin has proposed the use of ion exchange in desalination using carbon dioxide in 1964 (Kunin, 1964).

However, this process wasn't well applied at that time because there were no suitable materials to address the reaction kinetics issues during CO_2 regeneration (Greenleaf and SenGupta, 2009) to further increase the efficiency during such a process, also desalination technology was not as important as it is now. Even reverse osmosis technology had not been well developed and widely applied back then.

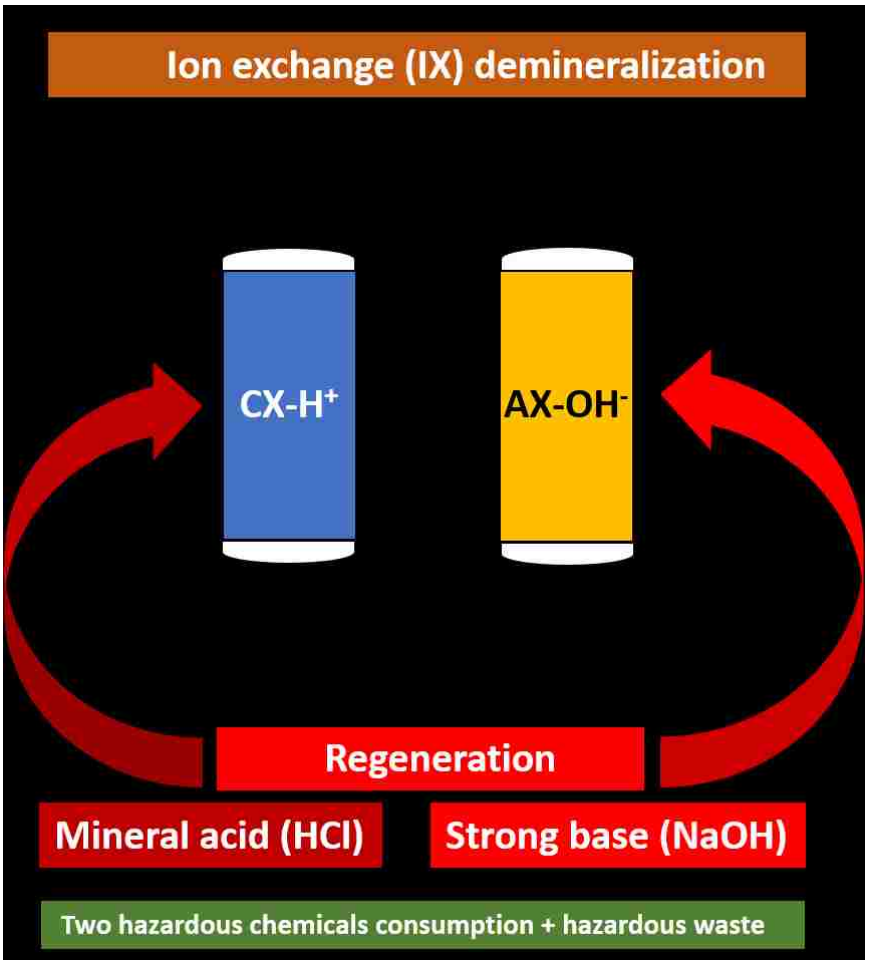

Figure 1-9. A schematic describes conventional ion exchange demineralization using two hazardous chemicals and producing hazardous waste.

1.2.3 Ion exchange nitrate removal: intensive brine consumption and brine waste

Anion exchange, with standard or nitrate-selective anion exchange resins, is the most universally practiced process for nitrate removal. In the presence of competing anions such as sulfate, nitrate selective resins (NSRs) have a higher capacity for nitrate from groundwater and do not succumb to chromatographic nitrate peaking (where effluent nitrate is greater than influent) (Habuda-Stanić et al., 2014; SenGupta, 2017). Resin capacity, nitrate affinity, and operating requirements are key considerations for process design. Upon exhaustion, the nitrate-loaded resins require intensive brine regeneration (10-15% NaCl) at daily frequency(Narasimhan and Agrawal, 2016), Figure 1-10. It is also the disposal of this brine-laden regenerant that poses maximum hardship during practice. Deep well injection is expensive, lacks local availability and faces restriction/bans in many states. Catalytic denitrification is a process yet to attain full confidence and maturity. Biological denitrification and regenerant recovery are not recommended for drinking water applications (Bergquist et al., 2016; Choe et al., 2015; Clifford and Liu, 1993; Guter, 1995; Narasimhan and Agrawal, 2016).

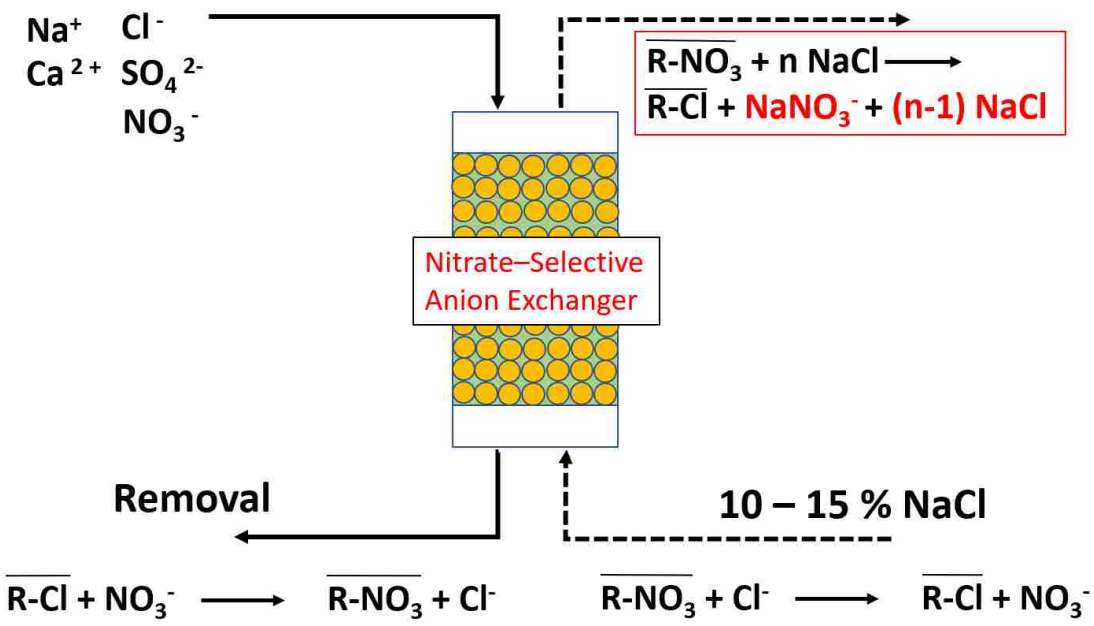

Figure 1-10 A schematic describes a traditional nitrate removal process.

1.3 Objectives

Based on water concerns and the challenges for current treatment technologies, there is a demand on the breakthrough of technology for desalination and nitrate reduction with selective trace ion removal, respectively or altogether, in an energy-saving way. The problems for current technologies are summarized as the following:

1. Reverse osmosis is very commonly applied for desalination, in a range from hundreds of TDS brackish water to seawater, but the energy consumption is intensive for the whole range of applications. The way to balance the recovery rate and energy consumption is a dilemma for RO. Higher recovery rate renders an exponential increase in energy consumption. There is no selectivity from RO, everything is being rejected.
2. Ion exchange processes exhibit selectivity and it could be manipulated to suit different applications in different ways with minor energy consumption. However, the demand for high concentration of brine or strong acid/base during regeneration renders high chemical consumption and waste disposal issues.

The objectives of this research are to develop a new process that could address and improve the challenges during the operations of desalination and nitrate reduction with trace ion removal. A new ion exchange process that could be sustained by carbon dioxide alone without waste disposal issues is discussed. It can perform desalination, nitrate removal and trace contaminant removal using a novel developed hybrid ion exchange resin loaded with metal oxide nanoparticles. It further could be integrated into other systems such as RO to reduce its energy consumption while keeping a high recovery rate. Carbon dioxide is the

only input to sustain the whole system, which would benefit carbon emission control and climate change.

CHAPTER 2 Concept of Hybrid Ion Exchange Process Driven by CO_2 (HIX-CO_2)

2.1 Carbon dioxide chemistry

Carbon dioxide is a unique gas that once it dissolves into water, forms both weak acid and a weak base, namely, carbonic acid and bicarbonate, which bicarbonate is often be referred to as alkalinity. Dissolution of carbon dioxide into water follows Henry's law with a constant $K_H = 10^{1.41}$. Once dissolved into water, it forms carbonic acid and followed by two-stage dissociation, forming bicarbonate and carbonate as following:

$CO_2\ (g) + H_2O \leftrightarrow H_2CO_3$ $pK_H = 1.41$ Equation 2-1

$H_2CO_3 \leftrightarrow H^+ + HCO_3^-$ $pK_{a1} = 6.38$ Equation 2-2

$HCO_3^- \leftrightarrow H^+ + CO_3^{2-}$ $pK_{a2} = 10.3$ Equation 2-3

The pC – pH diagram is shown in Figure 2-1. At pH lower than $pK_{a1} = 6.38$, the total concentration of carbon species from carbon dioxide merges with the concentration of carbonic acid. Carbonic acid is the dominant species at the lower pH range. While increasing the pH, the first stage of carbonic acid dissolution tends to move to the right of the Equation 2-2, resulting in an increasing concentration of bicarbonate. At pH between pK_{a1} and pK_{a2}, bicarbonate is the dominant species and the total carbon concentration merges with bicarbonate. Similarly, carbonate will dominant when pH is above $pK_{a2} = 10.3$. For most natural surface water bodies, the pH is usually around neutral, where most of the species is bicarbonate, i.e. the Yangtze river. As the second longest river in the world, Yangtze water quality is shown in Table 2-1. Yangtze river pH is 7.83, TDS is 193 ppm, in which, over half of it, 98 ppm is contributed by bicarbonate.

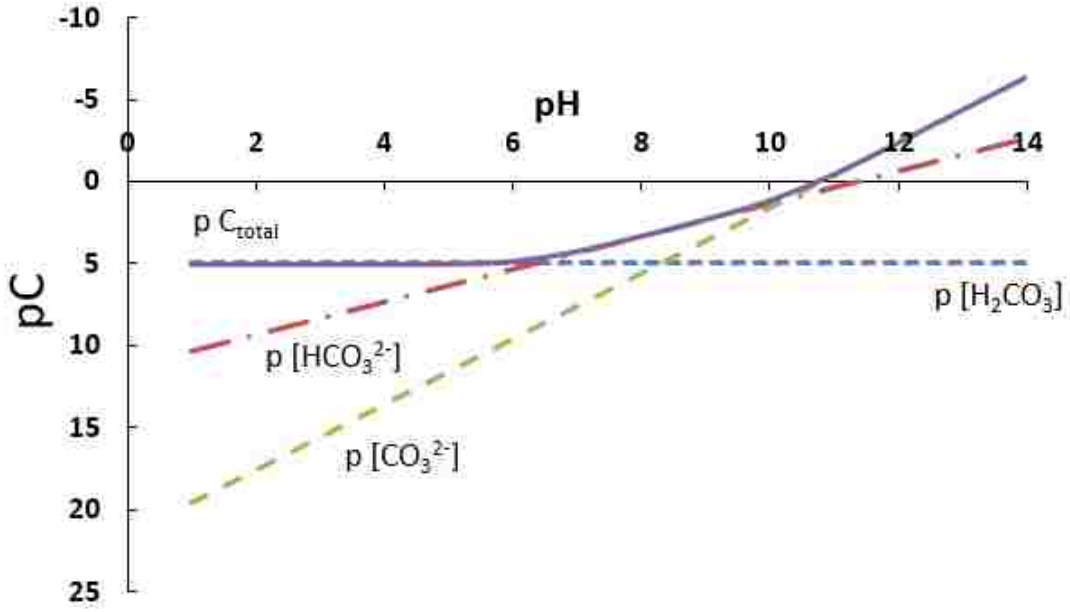

Figure 2-1. pC-pH diagram shows species from carbon dioxide dissolution under atmosphere pressure, where the carbon dioxide partial pressure is $10^{-3.5}$ atm.

Item	Concentration	Item	Concentration,
K^+, mg/L	2.48	Cl^-, mg/L	8.26
Na^+, mg/L	19.18	SO_4^{2-}, mg/L	55.12
Ca^{2+}, mg/L	32.14	NO_3^-, mg/L	6.39
Mg^{2+}, mg/L	6.49	F^-, mg/L	0.2
NH_4^+, mg/L	0.442	HCO_3^-, mg/L	97.69
Ba^{2+}, mg/L	0.0388	CO_3^{2-}, mg/L	0
Sr^{2+}, mg/L	0.1656	Conductivity, us/cm	278
pH	7.83	TDS, mg/L	193.3

Table 2-1. Table shows Yangtze river quality. Sampled 06/14/2016 from Yangtze river, Wuhu city, Anhui province, China.

The bicarbonate/carbonate system, often referred to as alkalinity, is an essential buffer for all the natural water sources. This ensures the water body keeps a consistent pH to ensure

the survival and prosperity of the global ecological system. It is closely relating to the partial pressure of carbon dioxide in the atmosphere.

Consider a pure water system such as distilled water, i.e. rain, at equilibrium with atmospheric carbon dioxide pressure. The electroneutrality of the aqueous phase exists as:

$$[H^+] = [HCO_3^-] + 2[CO_3^{2-}] + [OH^-] \quad \text{Equation 2-4}$$

Using $[H^+]$ to represents all the species on the right of the equation,

$$[H_2CO_3] = K_H P_{CO_2} \quad \text{Equation 2-5}$$

$$[HCO_3^-] = K_{a1} K_H P_{CO_2} / [H^+] \quad \text{Equation 2-6}$$

$$[CO_3^{2-}] = K_{a1} K_{a2} K_H P_{CO_2} / [H^+]^2 \quad \text{Equation 2-7}$$

$$[OH^-] = 10^{-14} / [H^+] \quad \text{Equation 2-8}$$

Overall,

$$[H^+] = K_{a1} K_H P_{CO_2} / [H^+] + 2 (K_{a1} K_{a2} K_H P_{CO_2} / [H^+]^2) + 10^{-14} / [H^+] \quad \text{Equation 2-9}$$

After iteration using $P_{CO2} = 10^{-3.5}$ atm, which is atmospheric carbon dioxide partial pressure,

$$pH = - \log([H^+]) \approx 5.6 \quad \text{Equation 2-10}$$

Which means, the pH of pure water system in equilibrium with atmospheric carbon dioxide partial pressure is around 5.6. That is the pH of clean normal rain. Rain with lower pH than 5.6 is typically called “acid rain”, and it is considered not clean due to likely contamination from acidic gas, such as SO_2 from coal combustion.

The atmospheric carbon dioxide partial pressure is not constant after the industrial revolution. As seen from the monitoring station in Hawaii, a scary level of 410 ppm of atmospheric CO_2 has been reached April 2018, Figure 2-2, and it still shows full speed on this tendency. Besides climate change, this tendency increases atmospheric carbon dioxide partial pressure and the pure water pH will decrease consequently as shown in Figure 2-4.

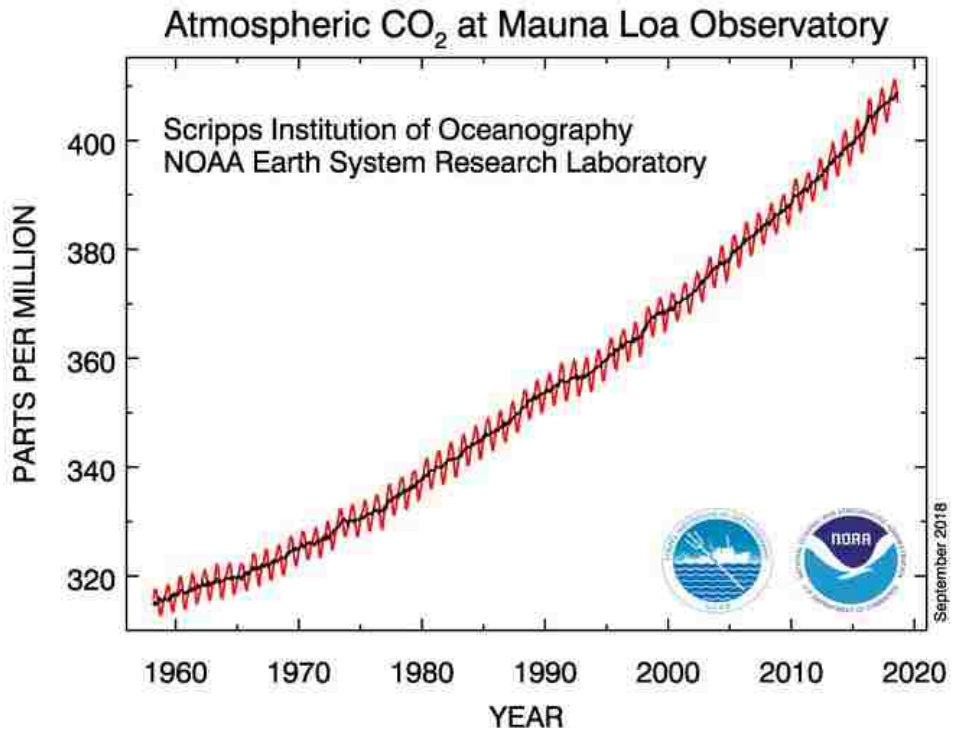

Figure 2-2. Atmospheric CO_2 level monitored at Mauna Loa Observation (NOAA, 2019).

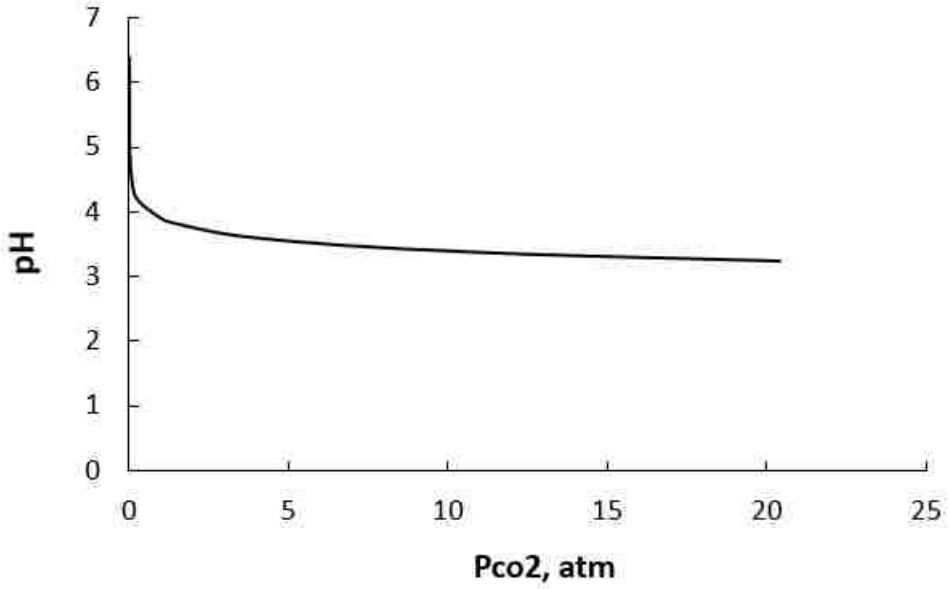

Figure 2-3. Equilibrium pH changes in pure water under increasing carbon dioxide pressure.

Besides pure water, it is worth pointing out the scenario of seawater pH changes under increasing atmospheric CO_2 partial pressure, as shown in Figure 2-4. Rising CO_2 concentration in the atmosphere also causes the pH drop in the ocean, namely, ocean acidification. Ocean acidification poses adverse impacts on ocean species such as pteropods, shellfish, and coral, even for a pH drop less than 0.5 (Orr et al., 2005). Chemical reactions happening in the ocean change the surface carbonate concentration and also saturation states of calcium carbonate minerals, which is biologically salient for ocean calcifying species such as pteropods, shellfish, and coral (Orr et al., 2005). Orr reported that pteropods cannot maintain shells in waters with undersaturated calcium carbonate. Evidence have been observed by Orr's group that pteropods living in Southern Ocean surface waters showed notable dissolution on their aragonite shells.

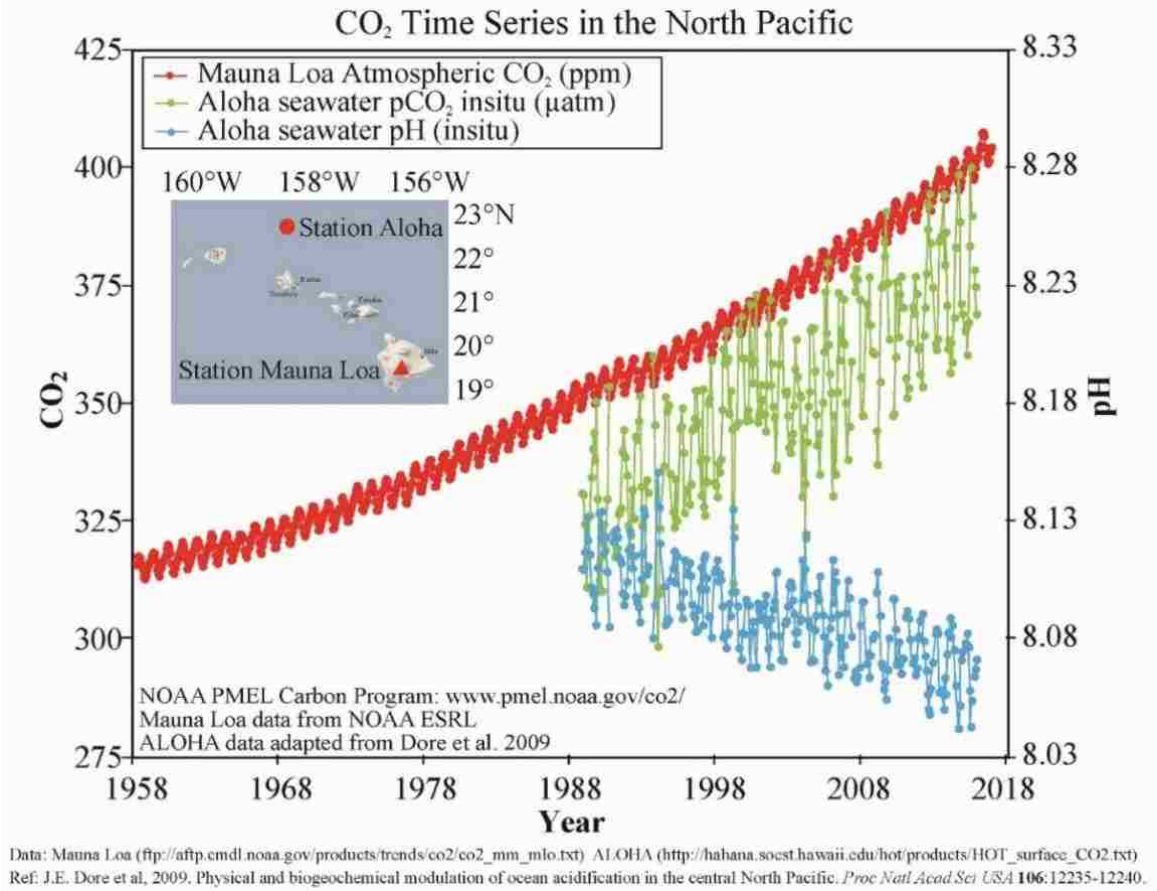

Figure 2-4. Ocean pH changes with atmospheric carbon dioxide concentration (NOAA, 2019).

Naturally, the atmospheric partial pressure of CO_2 should never increase to the level as shown in Figure 2-3, while the tendency stays true. So, by using pure carbon dioxide under high pressure in equilibrium with pure water, weak acid with pH close to 3 could be produced, and such a weak acid has the potential to generate alkalinity by changing the solution pH with base addition or hydrogen ion adsorption onto ion exchange materials. Therefore, carbon dioxide/carbonic acid is unique with its fundamental chemistry. That is the potential we can use it as the sole regenerant to regenerate both cation and anion exchangers.

2.2 CO_2 Driven Hybrid Ion Exchange Desalination (CHIX-Desal)

Upon dissolution in water, carbon dioxide or CO_2 produces carbonic acid (H_2CO_3) which can further dissociate, as shown below, into bicarbonate (HCO_3^-), often referred to as alkalinity due to its acid neutralizing capacity:

$$CO_2\ (g) + H_2O \leftrightarrow H_2CO_3 \quad pK_H = 1.41 \text{ at } 20^oC \qquad \text{Equation 2-11}$$

$$H_2CO_3 \leftrightarrow H^+ + HCO_3^- \quad pK_{a1} = 6.38 \text{ at } 20^oC \qquad \text{Equation 2-12}$$

Thus, in principle, CO_2 produces a unique opportunity to be used concurrently as both an acid (i.e., H_2CO_3) and a base (HCO_3^-) through process innovation. In a traditional demineralization process with ion exchange resins, a cation exchanger in H-form is followed by an anion exchanger in OH-form and the process warrants use of mineral acids (HCl or H_2SO_4) and alkali (NaOH) for regeneration. In the CHIX-Desal process, a recently developed hybrid anion exchanger with dispersed zirconium oxide nanoparticles (HAIX-NanoZr) possessing dual functional groups, is used (Padungthon et al., 2015; Sarkar et al., 2010; SenGupta, 2017; Sengupta and Padungthon, 2015). While covalently attached quaternary ammonia, functionalities provide anion exchange sites, zirconium oxide nanoparticles can selectively remove phosphate, a trace anion present in every municipal wastewater. Fluoride or arsenic, if present as contaminants in brackish groundwater, may also be selectively removed by HAIX-NanoZr.

For selective ion exchange and desorption, intraparticle diffusion is the critical rate-limiting step (Li and Sengupta, 2000; SenGupta, 2017). A shell-core weak-acid cation resin (SC-WAC) has functional groups residing primarily in the periphery and thus the intraparticle diffusion path length is relatively short. An innovative combination of SC-WAC and HAIX-NanoZr may offer a treatment synergy that can significantly reduce TDS

with minimal energy requirement while simultaneously removing and recovering phosphate from the wastewater if municipal wastewater is serving as the water source. Pressurized carbon dioxide (CO_2) is the only chemical needed to sustain the process. Contrary to traditional deionization, an anion exchanger precedes a cation exchanger in CHIX-Desal.

The schematic of a two-bed HIX-Desal process that can attain dissolved solids reduction and selective phosphate removal with CO_2 as the sole regenerant is illustrated in Figure 2-5.

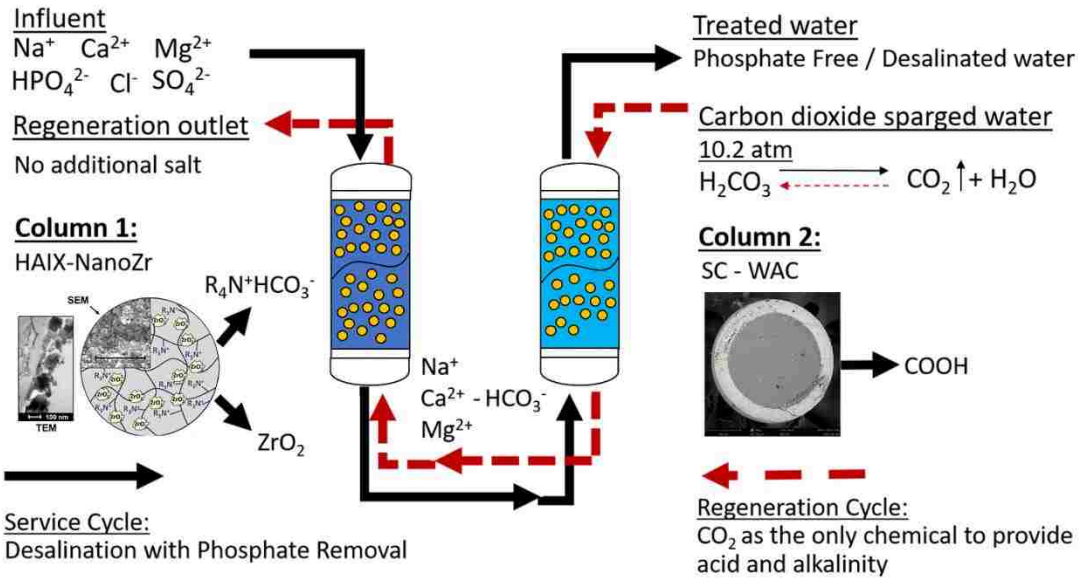

Figure 2-5 A schematic of a HIX-Desal process illustrating both desalination and CO_2 regeneration

Considering sulfate and calcium as the representative anion and cation present in secondary wastewater, the process- both service and CO_2-aided regeneration- is presented as follows:

Service cycle:

Column 1: Anion

$$2\overline{R^+HCO_3^-} + SO_4^{2-}\,(aq) + Ca^{2+}\,(aq) \rightarrow \overline{(R^+)_2SO_4^{2-}} + 2HCO_3^-\,(aq) + Ca^{2+}\,(aq)$$

Equation 2-13

Column 2: Cation

$$2\overline{RCOOH} + Ca^{2+}(aq) + 2HCO_3^-\,(aq) \rightarrow \overline{(RCOO^-)_2Ca^{2+}} + 2H_2O + 2CO_2\uparrow$$

Equation 2-14

Service overall:

$$2\overline{R^+HCO_3^-} + 2\overline{RCOOH} + SO_4^{2-} + Ca^{2+} \rightarrow \overline{(R^+)_2SO_4^{2-}} + \overline{(RCOO^-)_2Ca^{2+}} + 2H_2O + 2CO_2\uparrow$$

Equation 2-15

Regeneration cycle:

$$2CO_2\,(g) + 2H_2O \leftrightarrow 2H_2CO_3$$

Equation 2-16

Column 2: Cation

$$\overline{(RCOO^-)_2Ca^{2+}} + 2H_2CO_3 \leftrightarrow 2\overline{RCOOH} + Ca^{2+} + 2HCO_3^-$$

Equation 2-17

Column 1: Anion

$$\overline{(R^+)_2SO_4^{2-}} + 2HCO_3^- \leftrightarrow 2\overline{R^+HCO_3^-} + SO_4^{2-}$$

Equation 2-18

Regeneration overall:

$$\overline{(RCOO^-)_2Ca^{2+}} + \overline{(R^+)_2SO_4^{2-}} + 2CO_2\,(g) + 2H_2O \leftrightarrow 2\overline{RCOOH} + 2\overline{R^+HCO_3^-} + Ca^{2+} + SO_4^{2-}$$

Equation 2-19

2.3 CO_2 Driven Hybrid Ion Exchange Nitrate Removal (CHIX-N)

Chloride-form anion exchanger as universally applied for nitrate removal assures excessive chloride is presenting in the regenerant for an effective regeneration upon exhaustion as shown in equation 2-20.

$$\overline{R^+NO_3^-} + n(Na^+ + Cl^-) \leftrightarrow \overline{R^+Cl^-} + NO_3^- + (n-1)Cl^- + nNa^+ \quad \text{Equation 2-20}$$

To avoid brine (NaCl) input during regeneration and instead, innovatively use CO_2 the regenerant for both cation and anion exchanger, a bicarbonate form (HCO_3^-) nitrate selective resin (NSR) and a hydrogen form (H^+) cation exchanger are combined as a two-bed system, as shown in Figure 2-6. Carbon dioxide as the sole regenerant provides both acid (H_2CO_3) and base (HCO_3^-) needed for each exchanger upon its unique dissolution into water.

Again, NSR resins are doped with zirconium oxides nanoparticles for both selective nitrate removal and trace ligand removal, i.e. fluoride. Shell core weak acid cation (SC-WAC) resin assures a weak acid like carbonic acid could perform efficient regeneration (by loading hydrogen ion onto the resin) and consequently produce sufficient bicarbonate ions for the subsequent nitrate regeneration. The nitrate removal process and regeneration process are as follows:

Service cycle

$$\overline{R^+HCO_3^-} + NO_3^- + Na^+ \leftrightarrow \overline{R^+NO_3^-} + HCO_3^- + Na^+ \quad \text{Equation 2-21}$$

$$\overline{RCOOH} + Na^+ + HCO_3^- \leftrightarrow \overline{RCOONa} + H_2O + CO_2\uparrow \quad \text{Equation 2-22}$$

Overall

$$\overline{R^+HCO_3^-} + \overline{RCOOH} + NO_3^- + Na^+ \leftrightarrow \overline{R^+NO_3^-} + \overline{RCOONa} + H_2O + CO_2 \uparrow \quad \text{Equation 2-23}$$

Regeneration cycle

$$\overline{RCOONa} + H^+ + HCO_3^- \leftrightarrow \overline{RCOOH} + Na^+ + HCO_3^- \quad \text{Equation 2-24}$$

$$\overline{R^+NO_3^-} + HCO_3^- \leftrightarrow \overline{R^+HCO_3^-} + NO_3^- \quad \text{Equation 2-25}$$

Overall

$$\overline{R^+NO_3^-} + \overline{RCOONa} + H_2O + CO_2\,(g) \leftrightarrow \overline{R^+HCO_3^-} + \overline{RCOOH} + NO_3^- + Na^+ \quad \text{Equation 2-26}$$

Note that electrolytes, i.e. nitrate and sodium, are removed during the service cycle (**equation 2-23**) and desorbed from the ion exchanger during carbon dioxide regeneration (**equation 2-26**). It could be concluded from equations 2-24 and 2-25 that regeneration of the anion exchanger will only be successful when sufficient cation exchanger saturation and efficient cation regeneration happens in advance. Simultaneous electrolytes removal, namely partial desalination, is achieved as shown in equation 2-23 through carbonation chemistry and the following stripping of carbon dioxide. Fluoride is removed by zirconium oxide nanoparticles doped in the anion exchanger, which is independent of quaternary amine functional groups responsible for the nitrate removal.

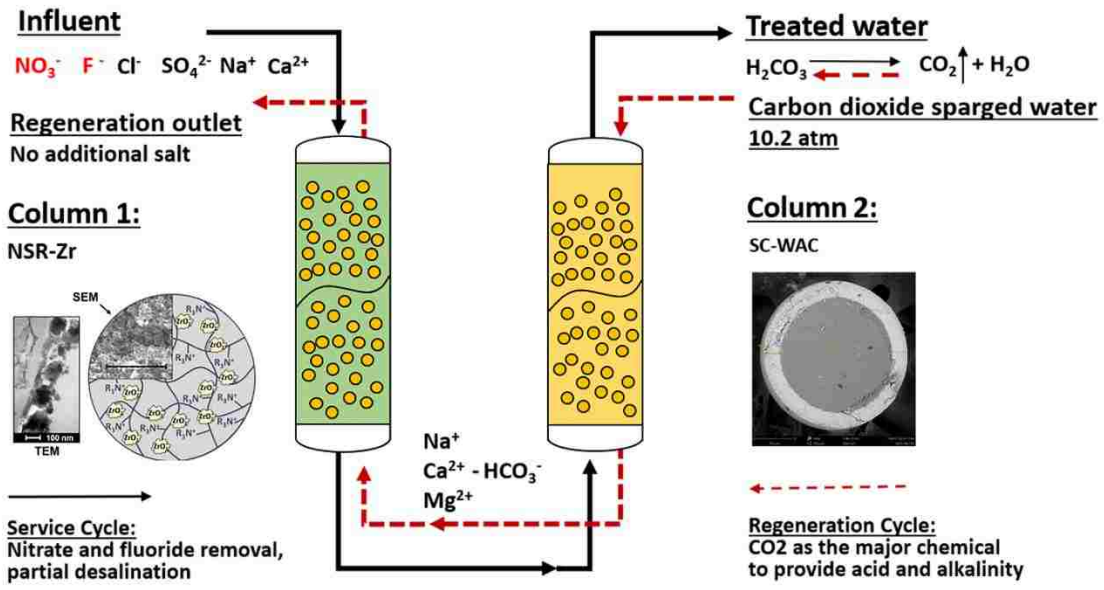

Figure 2-6. A schematic of the CHIX-N process illustrating both service cycle (nitrate/fluoride removal and partial desalination) and carbon dioxide regeneration.

2.4 Previous one-bed system regenerated by CO_2: CARIX challenges and intraparticle diffusion

Several applications have been studied by applying the fundamental chemistry of carbon dioxide. Carbon dioxide regenerated ion exchange (CARIX) is such an attempt to use carbon dioxide as the sole regenerate (Höll and Hagen, 1992; SenGupta, 1995). The process has been applied to full-scale plants (Höll, 1988). There are around 15 plants using this technology according to Veolia Waters (veolia, 2014). One type of the process only uses carbon dioxide as the weak acid source and uses a cation exchanger to remove hardness from the water. Another type is the full version to apply mixed bed resins of both cationic and anionic exchanger. However, the efficiency is very low. Even in pilot scale plant, it can only treat less than 50 bed volumes of water. Lab scale data is shown in Figure

2-7 (SenGupta, 1995). With a service cycle at such low capacities, it renders frequent regeneration and low efficiency.

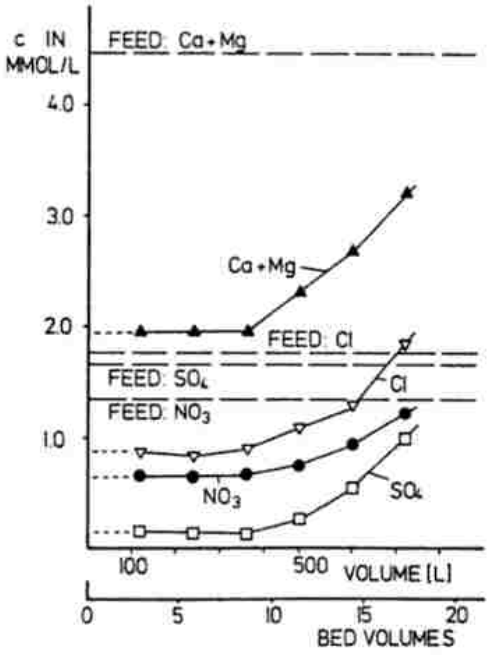

Figure 2-7. Effluent history of mixed bed CARIX process in the lab-scale experiment. Reproduced from book Ion exchange technology: Advances in pollution control (SenGupta, 1995)

The key reason hindering the improvement of efficiency is incomplete regeneration due to the weakness of carbonic acid. The efficiency of the proposed carbon dioxide regeneration process highly depends on hydrogen ion affinity over calcium and ion exchange kinetics. As probably every CARIX process applied, weak acid cation exchanger with weak acid carboxylate group exhibit a separation factor of H^+ over Ca^{2+} much higher than unity. This could improve efficiency by increasing the hydrogen ion affinity. However, with traditional sizes in the range of 500-1200 µm, weak acid cation exchange resin beads exhibit poor regeneration kinetics and the sorption of hydrogen ion is intra-particle diffusion controlled.

To validate the significance of the intra-particle diffusion path length, we could consider the behavior of a single bead during H^+ uptake. For the regeneration of gel-based weak-acid carboxylate group, H^+ uptake leads to a significant osmotic pressure drop where the H^+ and Ca^{2+} exchange happens, thus causing water expulsion from the gel phase. This initially happens at the outer periphery of the bead and loss of the water content decreases the overall interparticle diffusivity, which prevents the further regeneration of the inner core of the bead through the outer impervious shell. This renders most of the calcium ions remaining inside the exchanger after regeneration and then exhibit poor capacity during the service run.

To truly improve the efficiency and make carbon dioxide regeneration more convincing, intraparticle diffusion improvement is the key scientific challenge.

2.5 Selectively removal of trace ligand contaminant through inner sphere complexes

Ion exchange basically depends on the electrical charges of different ions, and their adsorption onto fixed opposite charges inside the adsorbent through coulombic interaction. However, due to the high concentration of background ions, namely, cations such as sodium, calcium and magnesium, anions such as chloride, sulfate, and nitrate, it is barely possible to selectively remove trace ions only through coulombic interactions. The principle for hybrid ion exchanger to selectively remove phosphate, arsenic, and fluoride is the formation of inner-sphere complexes through strong Lewis acids/bases interaction in addition to the coulombic interaction (Blaney et al., 2007). Lewis acids such as those metal oxides are strong electron acceptors, while trace ions such as phosphate, arsenic, and fluoride are strong electron donors, namely, Lewis bases. For the background ions such as chloride and sulfate being absent from such an interaction, they are hard to be adsorbed onto metal oxides by only forming outer sphere complexes through negligible coulombic interaction only. However, they have strong coulombic interactions with the ion exchanger itself since the ion exchanger has a high-density of fixed-charge carriers. This implies that hybrid ion exchange exhibits dual-functional sites. One is the pre-existing functional group responsible for ion exchange, such as quaternary amine, another is the loaded metal oxides nanoparticles. The two functional sites exhibit adsorption through different principles and barely affect each other. It is helpful to apply this into the two-bed desalination or nitrate removal system since the major exchange process by replacing anions with bicarbonate won't be affected and the extra metal oxide nanoparticles will selectively remove the trace contaminants. A schematic of how species of phosphate adsorbed onto zirconium oxides nanoparticles is shown in Figure 2-8.

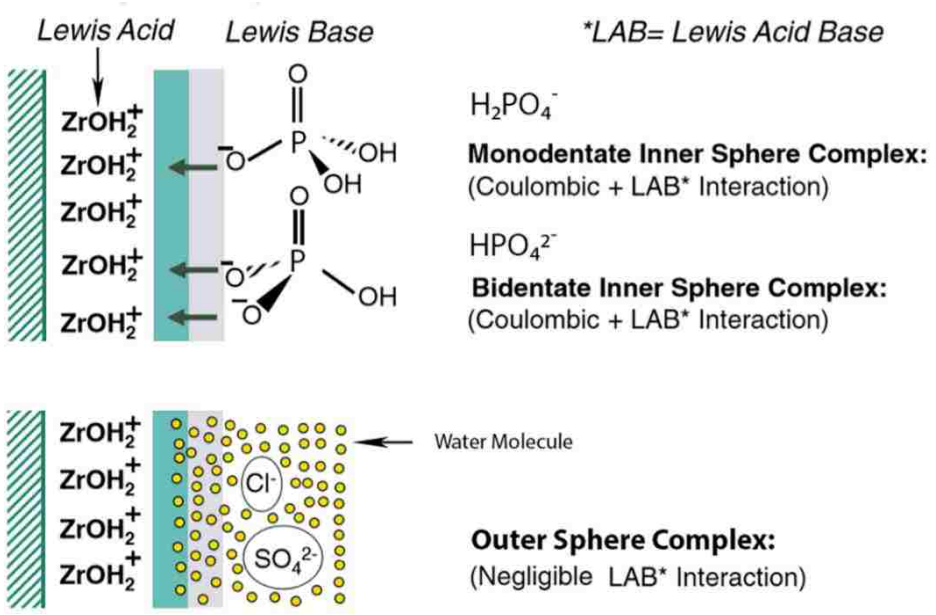

Figure 2-8. Mechanisms of arsenic and phosphate species adsorbed onto zirconium oxide nanoparticles.

CHAPTER 3 Experimental Setup, Materials and Methods

3.1 Bethlehem secondary wastewater

To validate the CHIX-Desal process with impaired brackish water, the influent wastewater was collected in a 20 L batch from the secondary effluent at the Bethlehem Wastewater Treatment Plant (Bethlehem, PA) (N 40 37.054, W 75 20.071). After collection, the influent batch was filtered through an 11 μm retention filter and then stored in a refrigerator.

The Bethlehem Wastewater Treatment Plant secondary wastewater composition is as follows: 2.4 mg/L phosphate as P, 130 mg/L Cl^-, 70 mg/L NO_3^-, 50 mg/L SO_4^{2-}, 100 mg/L HCO_3^-, TDS 484 mg/L, pH 7.44. By spiking with more electrolytes, such as NaCl, higher TDS of approximately 1200 mg/L has also been studied.

3.2 Lancaster nitrate contaminated groundwater

To validate the CHIX-N nitrate removal process, the influent groundwater was collected from the nitrate treatment facility of Northwestern Lancaster County Authority in Lancaster, PA (40°10'14.8"N 76°22'03.7"W). The site is surrounded by farms. The nitrate level in groundwater ranges from 6 ppm to 12 ppm as N. After collection, the groundwater was spiked with nitrate and fluoride (sodium salts) to approximately 15 ppm and 5.4 ppm, respectively.

The Lancaster nitrate contaminated groundwater composition is as follows: 64 mg/L NO_3^-, 5.4 mg/L F^-, 40 mg/L Cl^-, 60 mg/L SO_4^{2-}, 274 mg/L HCO_3^-, 90 mg/L Ca^{2+}, 70 mg/L Na^+, conductivity 791 μs/cm, pH 7

3.3 Experimental setup

High-pressure regeneration demands a solid system that can hold pressure without leakage. A stainless-steel experimental setup was manufactured by Swagelok at Allentown, PA, as shown in Figure 3-1. It includes a 10 L regeneration tank, which holds water under a high pressure of carbon dioxide. Carbon dioxide is provided by a high-pressure cylinder from Airgas. Two major columns are connected to the regeneration tank. Cation and anion exchangers are placed inside the columns, separately. A pump and a fraction collector were used to pump feedwater and collect the effluent, respectively. During the regeneration, the CO_2 pressure inside the regeneration tank provides the driving force for the flow. An extra backup column and regeneration tank are also included. The size of the resin columns is 300 mL.

A stainless-steel two-bed system with mini columns, 25mL, provided by Swagelok was also used in the lab for fast determination tests with smaller resin amount, Figure 3-2.

Usually, the 10L of water, or 50 bed volumes, is sufficient for regeneration of one cycle. Supply of water into the regeneration tank under high pressure during the process is not necessary. Another setup is integrated into the system when it is needed to pump more water into the regeneration tank during or between regeneration. For a continuously water supply into a pressurized tank without pressure building up inside the tank, the flow rate needs to be slow and balanced with the regenerant effluent flow rate. The regenerant flowrate for a 300mL column is relatively slow to keep a sufficient detention time. Thus, a bypass line from the outlet of the high-pressure pump is necessary to recirculate most of the water back into water storage tank when the pump flow rate is high, Figure 3-3.By controlling the valve on the bypass line, a point where the pump just could overcome the

pressure and pump water into the pressurized tank with minimum flow rate could be reached. There is a balance between carbon dioxide feed, water feed and carbonic acid output.

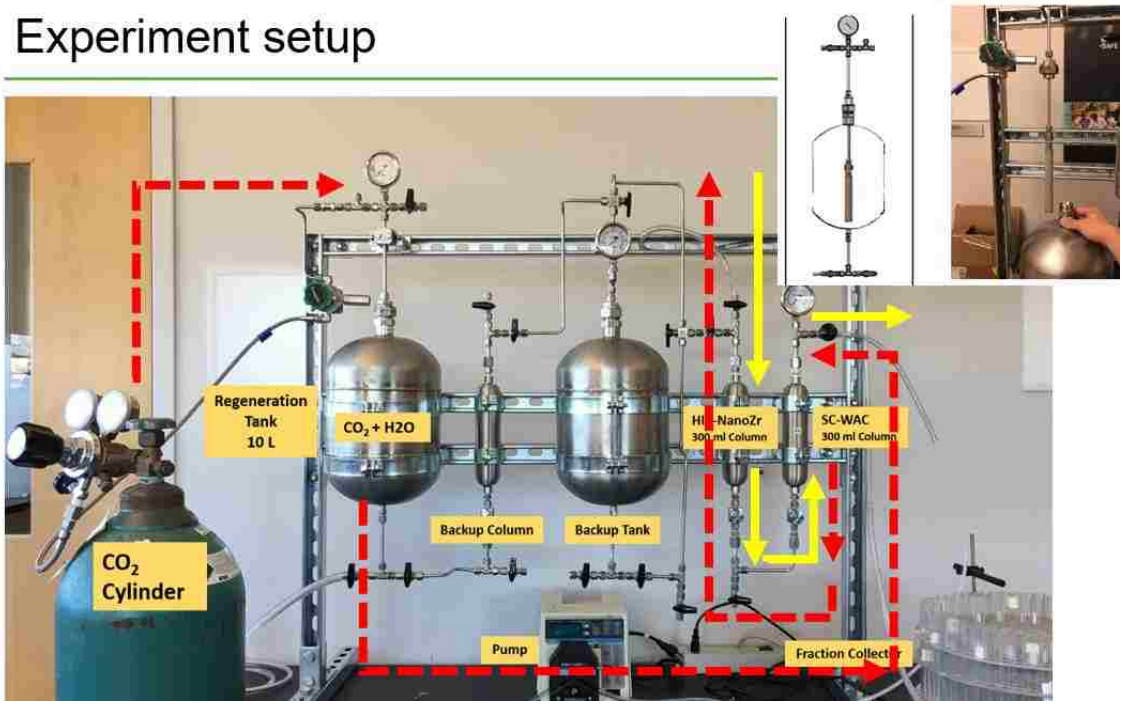

Figure 3-1. Two-bed carbon dioxide regeneration system.

Figure 3-2. Mini columns of carbon dioxide regeneration system.

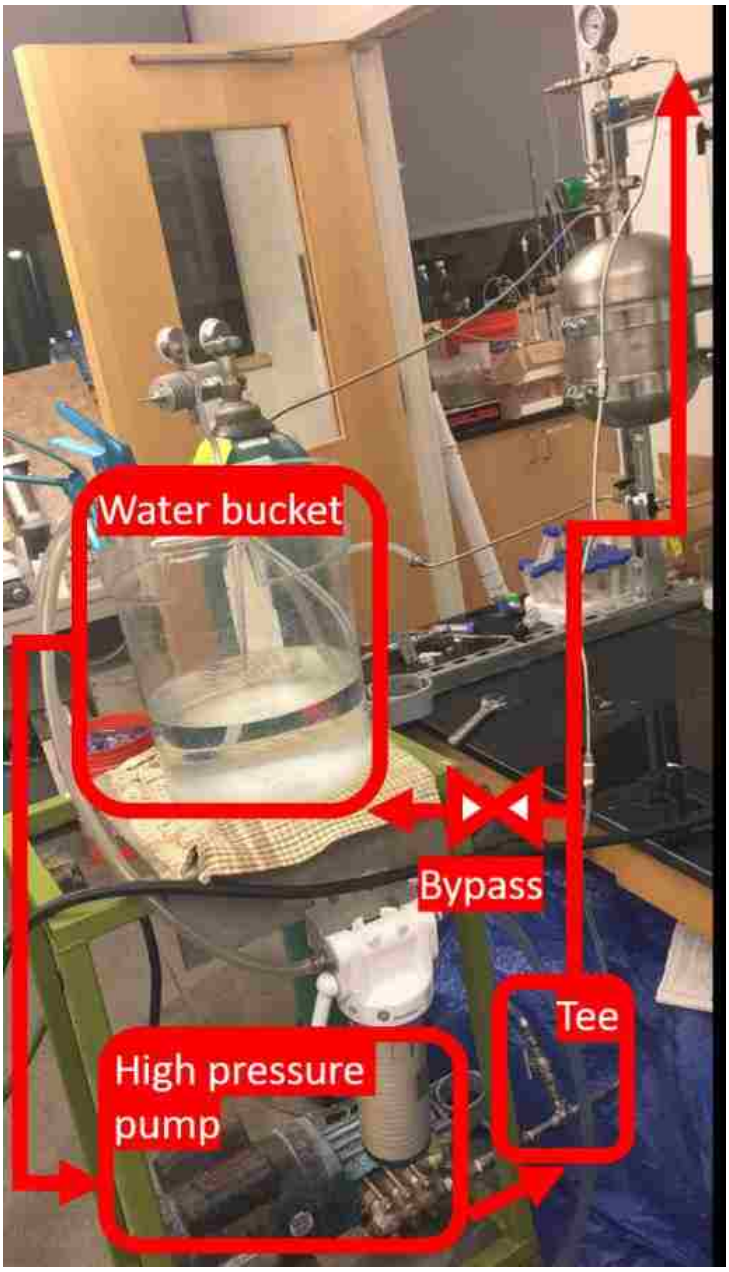

Figure 3-3. Continuous water supply system to pump water into pressurized regeneration tank at small flowrate.

Inside the regeneration tank, there is a diffuser with micropores connected to the carbon dioxide inlet tube to distribute carbon dioxide into microbubbles and improve the dissolving rate, Figure 3-4. This helps the aqueous phase reach equilibrium with the partial pressure quickly.

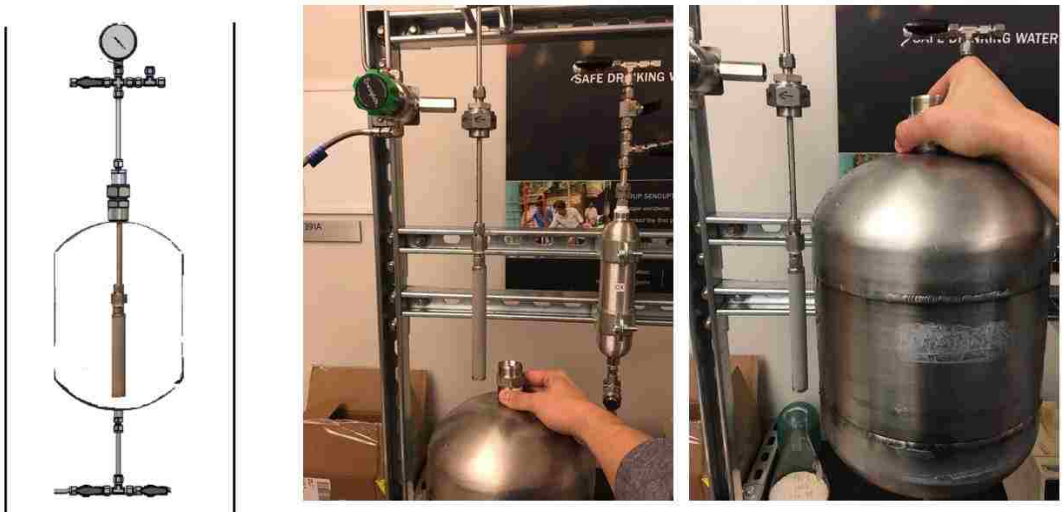

Figure 3-4. carbon dioxide diffuser system for the regeneration tank.

3.4 Materials

Intraparticle diffusion kinetics could be improved by shortening the intraparticle diffusion path length. Experiments have been done by John Greenleaf (Greenleaf et al., 2006) and Surapol Padungthon (Padungthon et al., 2011) on improving the carbon dioxide regeneration efficiency by using ion exchange fibers. Similarly, ion exchange powders and shell core ion exchange resins can also improve the intraparticle diffusion kinetics by shortening the intraparticle diffusion path length.

3.4.1 Ion exchange fibers

Ion exchange fibers are long thin fibers with fixed functional groups. Weak acid cation exchange fibers have carboxylic functional groups and are capable of performing cation exchange, as shown in Figure 3-5.

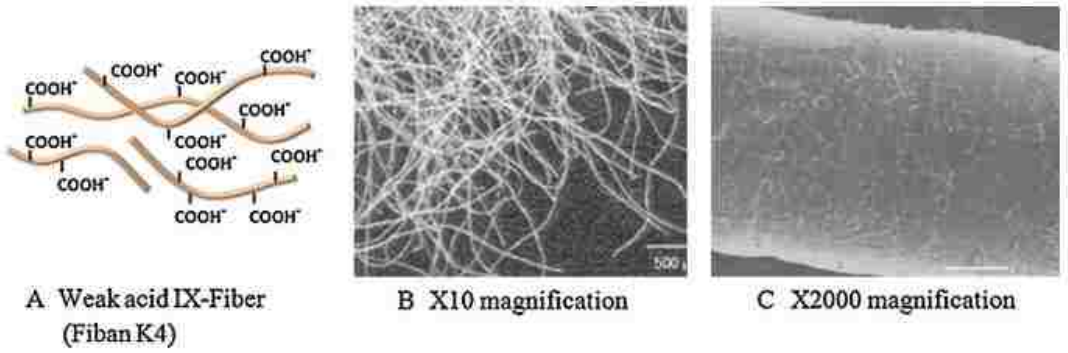

Figure 3-5. (A) Weak acid cation exchange fibers with carboxylate functional groups (B) Virgin fiber materials photographed at x10 magnification. (C) SEM photograph of a single fiber (x2000) (Padungthon et al., 2011)

With the cylindrical shape and only 10 – 50 μm diameters, the intraparticle diffusion path length has been significantly reduced and is much shorter than a spherical resin beads with diameters 500 – 1200 μm. From Padungthon's comparison test in Figure 3-6, it clearly shows the improvement in carbon dioxide regeneration by using fibers rather than large

resins beads. Currently, Veolia is applying fibers on its environmental-friendly CARIX process for softening. However, the reason fibers are not being commonly used are their difficulties of being applied to fixed bed columns. The hydraulic properties are not as good as uniformed settled resin columns. Moreover, the capacity is lower than weak acid cation exchange resins and not conveniently commercially available.

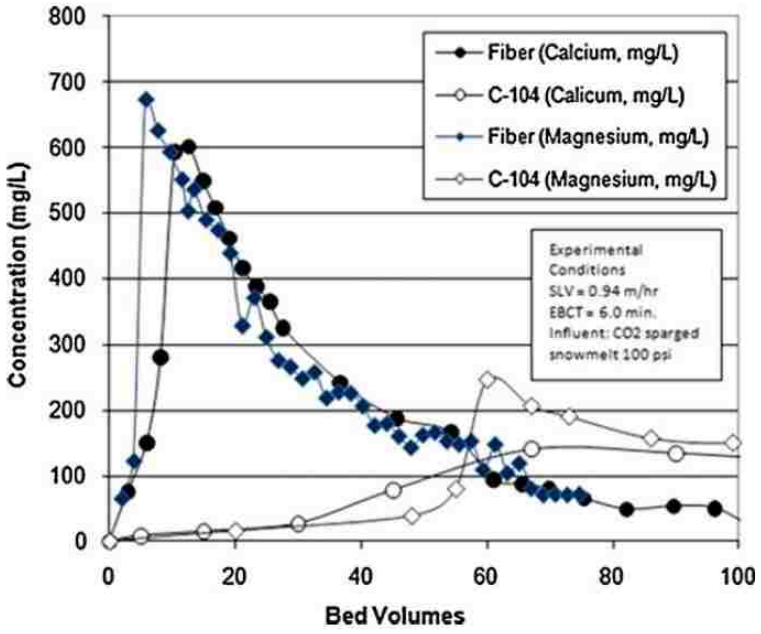

Figure 3-6. Regeneration comparison between virgin weak acid fibers and resins loaded with divalent cations using carbon dioxide under 100 psi. (Padungthon et al., 2011)

3.4.2 Ion exchange powder

By shortening the intraparticle diffusion path length even further from fibers, ion exchange powder is produced by cutting the fibers into fine powders. The intraparticle diffusion kinetics are highly improved, but even more difficult to apply the powder into a fix-bed column. The fine powders will stick together, Figure 3-7, which renders poor permeability and huge hydraulic head lose. But the regeneration completed within 6 bed volumes indicates their faster exchange kinetics than ion exchange fibers, whichneed 20 bed volumes of regeneration for saturated monovalent ions, Figure 3-8.

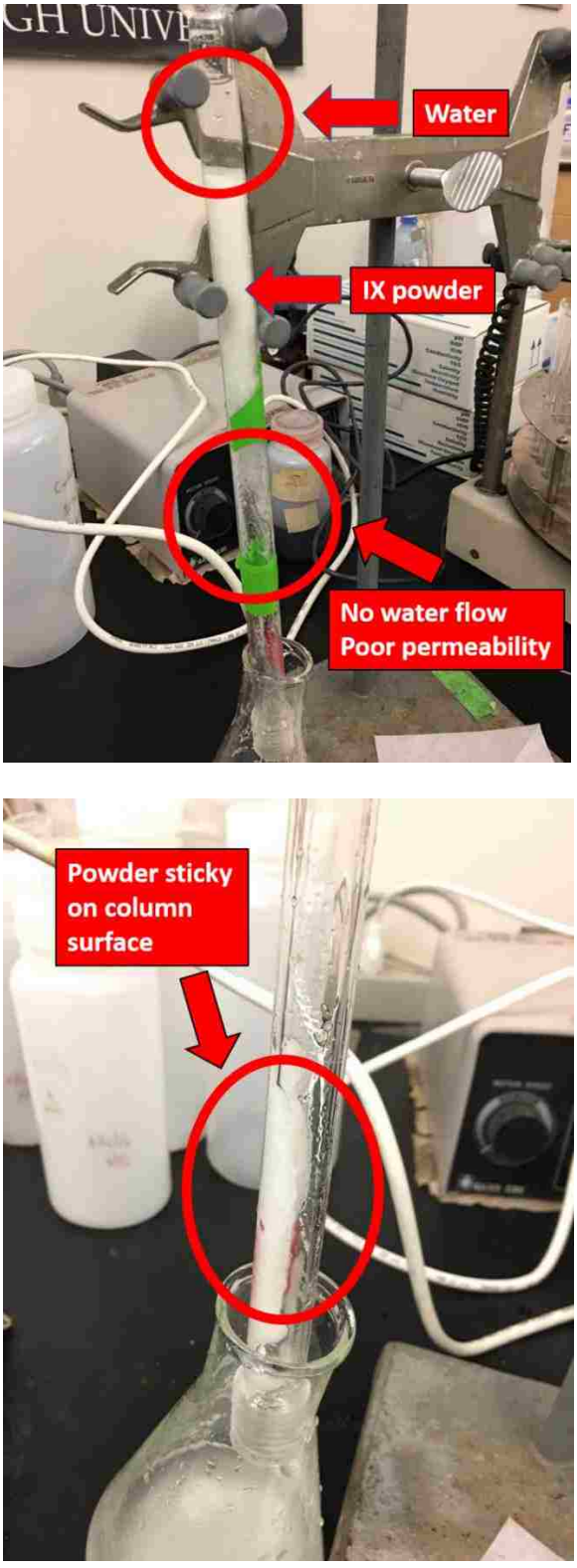

Figure 3-7. Ion exchange powder applied in fixed bed column.

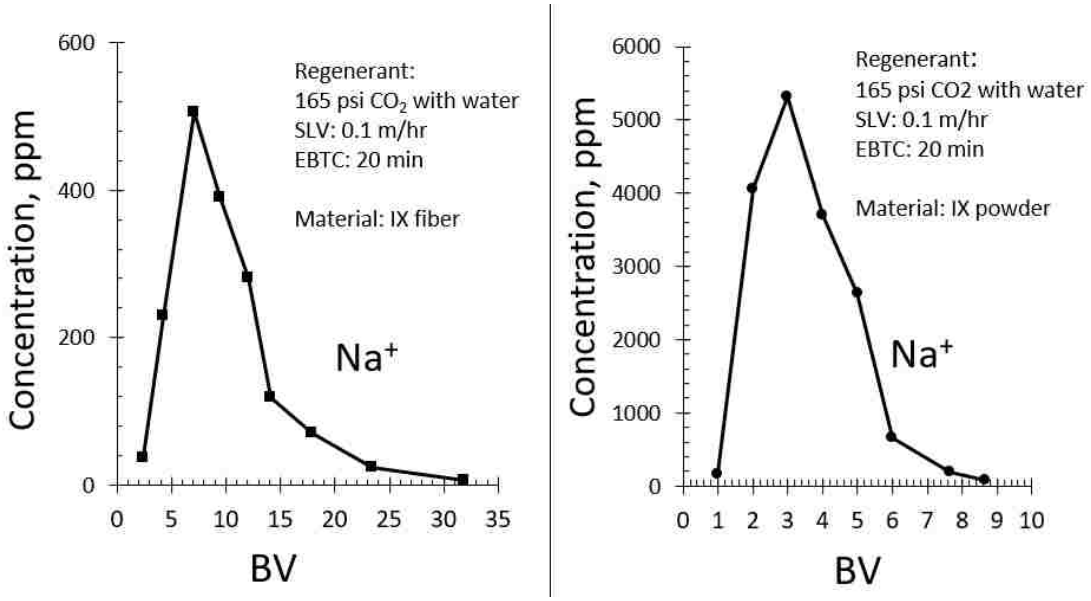

Figure 3-8. Regeneration of ion exchange fiber (left) and powders (right) loaded with sodium using carbon dioxide under 165 psi.

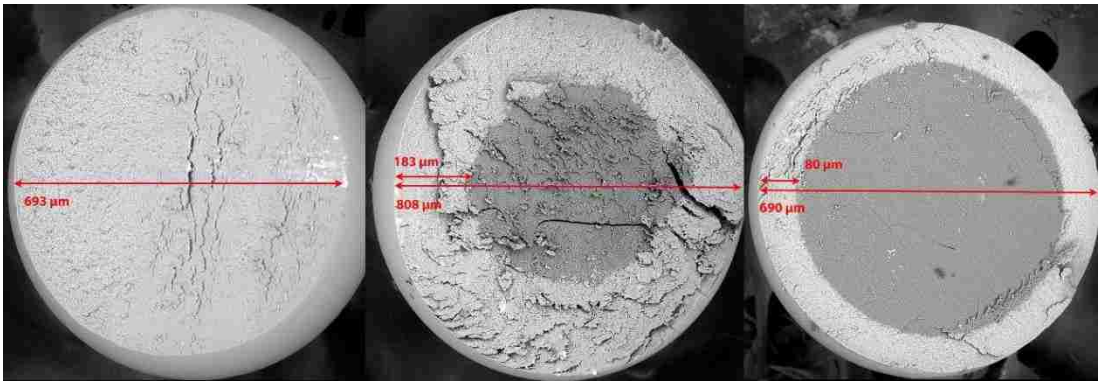

Figure 3-9. SEM photograph of C104 (left), SSTC104 (middle) and SCWAC-100 (SSTWAC-100) (right) after treated with copper.

3.4.3 Shell core ion exchange resin

To get the best material suited for carbon dioxide regeneration, intraparticle diffusion kinetics, hydraulic properties, and convenience for a typical column application are the demands that need to be balanced. Compared with ion exchange fibers and powders, which only perform better kinetics, shell core ion exchange resins are more balanced on these properties. With a spherical shape in the form of commonly used beads style, they could easily be applied in the fixed-bed column without any hydraulic issues. Traditional ion exchange resin beads as used in the CARIX processes could not perform satisfactory regeneration efficiency due to the long intra-particle diffusion path length, with particle diameter ranges 500 – 1200 μm. Shell core ion exchange resin, such as commercially available Purolite SSTC104, was manufactured to increase generic regeneration efficiency issues. The resin beads are partially functionalized on the periphery. Even though the diameter is similar with traditional resin beads, the functional groups only exist on the periphery of the resin surface with a depth around 200 μm. This makes saturated ions stays on the periphery of the beads, and hydrogen ion does not need to go to the deep core to replace ions, which improves the kinetics significantly. However, the commercially available SSTC104 only perform around 50% recovery rate during the lab test with 150 psi carbon dioxide regeneration. It is better than 30% which performed by traditional bead C104, but it is still not satisfactory.

Finally, a specially manufactured shell-core resin SCWAC was obtained upon special request from Purolite. It was specially designed for our carbon dioxide regeneration process with functional groups even more shallow on the periphery of the resin, with depth only around 100 μm. The functional group distribution of three resins is shown in Figure 3-9.

With saturated calcium on the resin, regeneration recovery rate further improved to nearly 80% by SCWAC. The data are shown in results and discussion section.

3.5 Analytical methods

3.5.1 Conductivity and pH

Conductivity was measured using a handheld accumet conductivity meter, Model # AP75. pH was measured using Accumet XL15 pH meter from Fisher Scientific.

3.5.2 Cations

Cations such sodium, calcium, and magnesium were measured by Perkin Elmer Flame Atomic Absorption Spectrometer (AAnalyst 200).

3.5.3 Anions

Ion chromatography was used to determine the anion concentration, such as chloride, nitrate, and sulfate. Dionex ICS-1000 Ion Chromatograph with chromatography column AS14 and conductivity detector is equipped.

Chloride was analyzed also by argentometric titration method. Samples were diluted to 100 mL and placed into 250 mL Erlenmeyer flask. Sample pH was adjusted to between 7 and 10 using 2% NaOH with the addition of 1 mL 5% K_2CrO_4 indicator. Pretreated samples were titrated against standardized 0.0141 N $AgNO_3$ while stirring on a stir plate. Chloride precipitates with Ag^+ will form the dark red precipitate Ag_2CrO_4 and solution will change color from yellow to pinkish.

Sulfate was also determined through sulfate testing kit available from the Hach Company (SulfaVer 4 Method #8051). An aliquot of 10 mL is placed in a glass sample cell and one

pillow of powdered $BaCl_2$ is added. The cell is then swirled to dissolve $BaCl_2$, and sulfate will precipitate as $BaSO_4$. After 5 minutes of reaction time, the sample is analyzed using Hach Spectrometer, Model DR 5000. Sample absorbance of the sample is directly correlated to mg/L of SO_4^{2-}.

3.5.4 Scanning electron microscopy

Photographs of ion exchange resins were performed using a Phenom XL desktop SEM. Samples were prepared by slicing individual ion exchange beads with razor blades and mounted onto metal sample holders using double-sided carbon tape.

3.5.5 Fixed column runs

All the experiments without the requirements of high-pressure carbon dioxide regeneration were conducted using fixed-bed column runs as shown in Figure 3-10. Epoxy coated glass column or a PVC assembled column was used with a constant flow pump and fraction collector. The amount of material or resin volume used is called one bed volume (BV). Superficial liquid velocity (SLV) and empty bed contact time (EBCT) were recorded for each run. The volume of water passed through the bed was also recorded and divided by the material volume, noted as "BVs of water treated". Results were plotted as the concentration of concern indicator (y-axis) versus bed volume of water treated by the bed (x-axis).

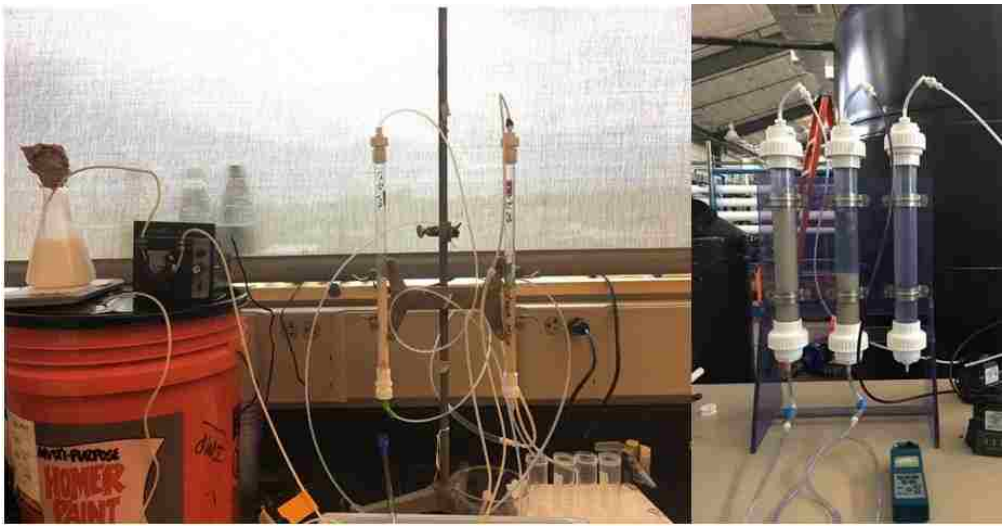

Figure 3-10. Setup used for fixed bed column runs.

3.6 Hybrid Ion Exchanger (HAIX-NanoZr and NSR-Zr) and trace ion removal

A hydrated metal oxide such as hydrated zirconium oxide has been observed to have strong affinity for some trace ligand contaminants (Dou et al., 2012). However, the fine particles of these metal oxide are hard to apply in a fixed bed column since they are almost impermeable as nanoparticles. Hybrid ion exchangers by impregnating metal oxide nanoparticles into ion exchange resin have been developed to utilize the selectivity of metal oxides on trace contaminants. A hybrid anion exchanger (HAIX-NanoFe) doped with hydrated ferric oxide (HFO) was invented to selectively remove arsenic at ppb levels (Cumbal and Sengupta, 2005). A different hybrid anion exchanger (HAIX-NanoZr) loaded with zirconium oxide was also developed to selectivity remove trace fluoride from groundwater (Padungthon et al., 2015), and the parent anion exchanger could be a nitrate selective resin to form NSR-Zr. These materials now have been developed and used on sites in India and worldwide for years to provide safe drinking water free of arsenic and fluoride (German, 2017). Besides the water concern of desalination and nitrate

contamination as discussed in the previous section, powerful materials that could selectively remove trace contaminants are also available now. By integrating these innovative hybrid ion exchangers with nanoparticles, i.e. HAIX-NanoZr or NSR-Zr, the new process is capable of providing softened, desalinated nitrate-reduced and trace contaminant free water sustained by only carbon dioxide.

3.6.1 Donnan membrane effect

There are two types of ion exchanger that both could be doped with metal oxides, namely, cation exchange resin and anion exchange resin. Cation exchange resin with either carboxylic (weak) or sulfonic (strong) functional groups have fixed negative charges and could perform cation exchange, while an anion exchange resin does the opposite, with amine groups showing fixed positive charges to perform anion exchange. It has been observed that hybrid cation exchange resin and anion exchange resin have significantly different performance during trace ion removal such as arsenic, specifically, arsenite and arsenate, Figure 3-12 (Cumbal and Sengupta, 2005).

Parent Oxyacids	pK_a Values	Predominant Dissolved Species at pH 6.0	Predominant Dissolved Species at pH 8.0	Sorption Interaction
As(V): H_3AsO_4	pK_{a1} = 2.2 pK_{a2} = 6.98 pK_{a3} = 11.6	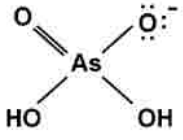	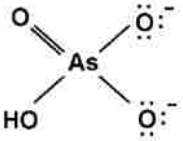	As(V) species or arsenates can undergo Coulombic (ion exchange) as well as Lewis acid-base interaction
As(III): $HAsO_2$	pK_{a1} = 9.2	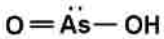	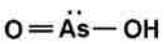	As(III) species or arsenites can undergo only Lewis acid-base interaction

Table 3-1. Arsenic species. Oxyacids and Conjugate Anions of As (V) and As (III) and H_2AsO_4. (Cumbal and Sengupta, 2005)

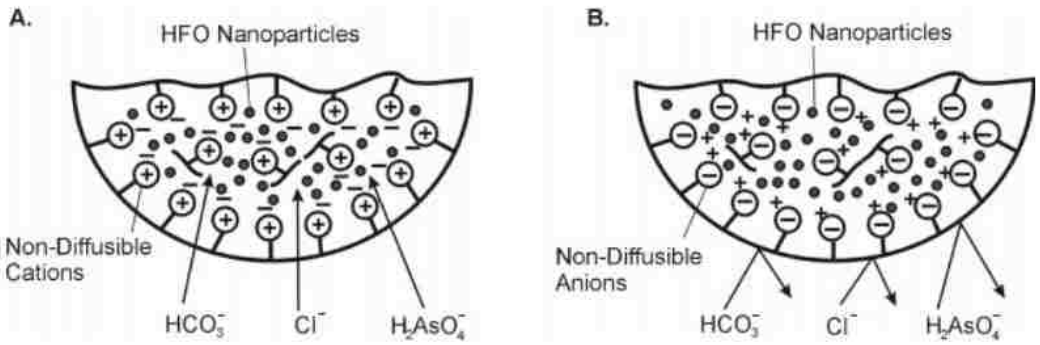

Figure 3-11. Schematic illustrating the Donnan membrane effect (A) enhanced permeation of anions into the hybrid sorbent in the presence of non-diffusible cations (anion exchanger) and (B) exclusion of anions from the hybrid sorbent in the presence of non-diffusible anions (cation exchanger).

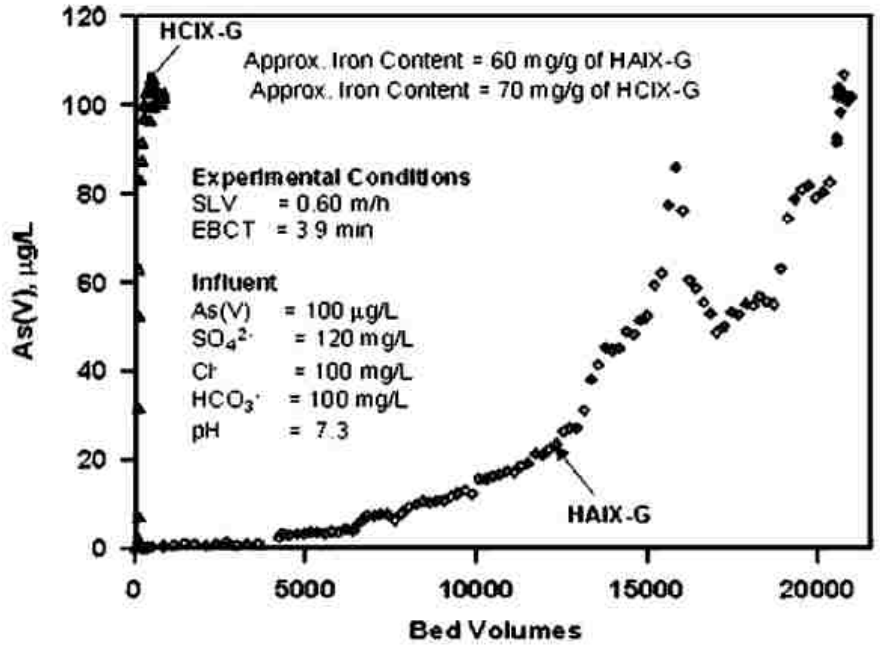

Figure 3-12. As (V) effluent history comparison by using HCIX and HAIX (Cumbal and Sengupta, 2005).

This could be explained by the Donnan membrane effect, as illustrated in Figure 3-11. It is shown in Table 3-1 that arsenate species in water have two negative charges in a neutral pH environment, thus, it will be expelled by the resin with a high density of negative charges, namely a cation exchange resin. By this exclusive effect, arsenate is hard to get into the resin and won't interact with the ferric oxide nanoparticles. The total removal effect will be poor by using a hybrid cation exchange resin (HCIX). However, while the resin holds fixed positive charges, more arsenate will be accumulated inside the resin and more will be absorbed by the metal oxides through Lewis acid-base interactions. This effect plays a significant role if considering removal of trace ions with charges in the aqueous phase.

3.6.2 pH effect

Since charges of the species are important, it is salient to note that metal oxides surface also have pKa values. Zirconium oxides have two pKa values, pH 6 and pH 7.8 as shown in Figure 3-13 (German, 2017). This indicates that most of the metal oxide sites will be negatively charged under pH greater than 6 and negatively charged above pH 7.8. In the range of pH 6 to 7.8, the sites are positive and negative balanced. Charges of both metal oxides surface and ions will affect the adsorption and desorption process significantly. The capacity decreases while pH is increased above pH 4. This is because the positively charged metal oxide surface area decreased, and when the metal oxide surface is negatively charged, they start to desorb the fluoride ions, which are also negatively charged. By manipulating the pH, a high capacity for fluoride removal and efficient regeneration thus could be performed.

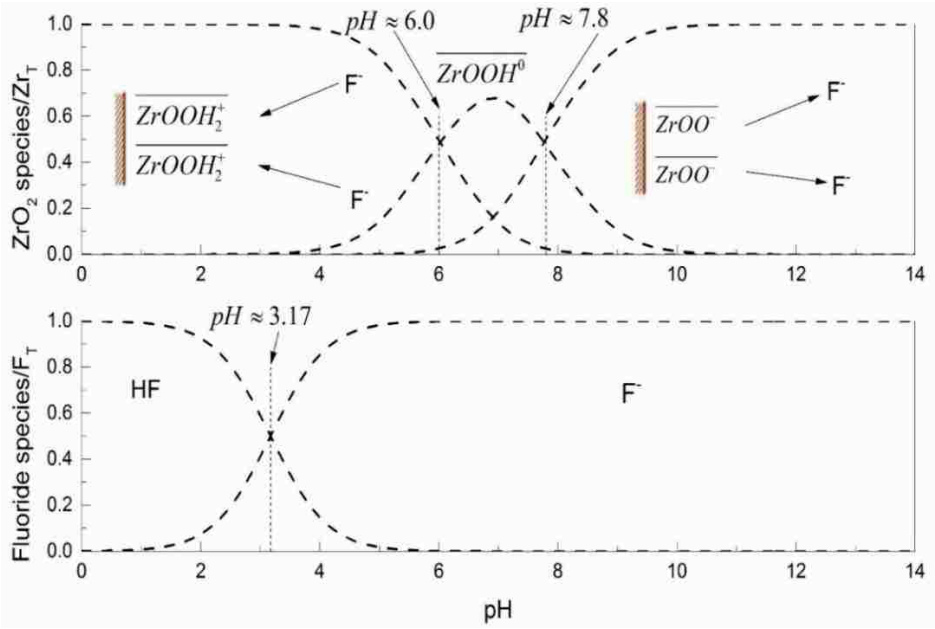

Figure 3-13. Distribution of surface functional groups of hydrated zirconium oxide particles with pH; pC-pH diagram of fluoride (German, 2017).

3.6.3 Synthesis of hybrid ion exchanger with hydrated zirconium nanoparticles

Synthesis of HAIX-NanoZr or NSR-Zr is performed in the lab by the following procedure:

1) Produce a 15% (w/v) ZrO_2 solution (using waste zirconium oxide) with either 10% sulfuric acid or 20% H_2SO_4 with methanol at a 50:50 ratio (note: methanol decreases the dielectric constant)
2) Mix anion exchange resin beads (or nitrate selective resin beads) in Zr solution for 15 hrs
3) Decant and dry the resin
4) Mix dry resin with an equal volume of 5% NaOH.

The synthesis process needs to ensure the high zirconium content inside the resin, and the content will directly determine the capacity of the exchanger.

CHAPTER 4 Results and Discussion: CO_2 Driven Hybrid Ion Exchange Desalination Process (CHIX-Desal)

4.1 TDS reduction and regenerability for multiple cycles

Results of three consecutive cycles of operation with the filtered secondary wastewater from Bethlehem, PA with a TDS of approximately 500 mg/L are in Figure 4-1A. Note that for three consecutive cycles, with the proposed process using CO_2 as the sole regenerant, more than 50% TDS removal was consistently achieved for well over 200 bed volumes. Equally important, as shown in Figure 4-2, individual species of interest, namely, calcium and sulfate, often responsible for membrane fouling and equipment scaling, were removed efficiently.

The elution curves for two consecutive regeneration cycles using CO_2 are presented in Figure 4-1B**;** regeneration efficiency was consistent and the three consecutive service cycle runs have nearly identical effluent histories with the same TDS reduction as shown in Figure 4-1A. Figure 4-3 provides sulfate and calcium elution profiles during CO_2 regeneration.

The results of three consecutive service runs for a synthetic feed water with a TDS of 1250 mg/L with CO_2 regeneration in between are included in Figure 4-4**.** Note that nearly 50% reduction in TDS was achieved for almost 200-bed volumes with the near-complete removal of sulfate and calcium. No bacterial growth was observed in the columns during the multiple cycles of desalination and CO_2 regeneration.

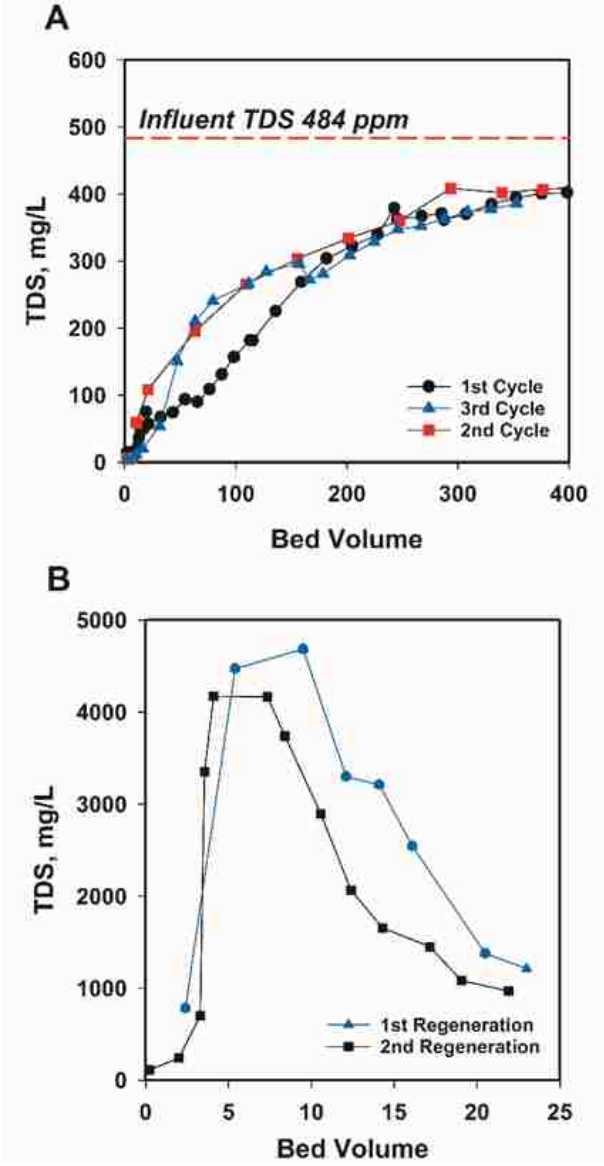

Figure 4-1. A) TDS removal or desalination over three consecutive service cycles using Bethlehem secondary wastewater. Influent composition and operation condition: 2.4 mg/L phosphate as P, 130 mg/L Cl^-, 70 mg/L NO_3^-, 50 mg/L SO_4^{2-}, 100 mg/L HCO_3^-, TDS 484 mg/L, pH 7.44, SLV 0.41 m/hr, EBCT 4.65 min; B) TDS elution during CO_2 regeneration of both columns. Regenerant and operation condition: CO_2 sparged water under 150 psi CO_2 partial pressure, EBCT 30 min. (EBCT= Empty bed contact time)

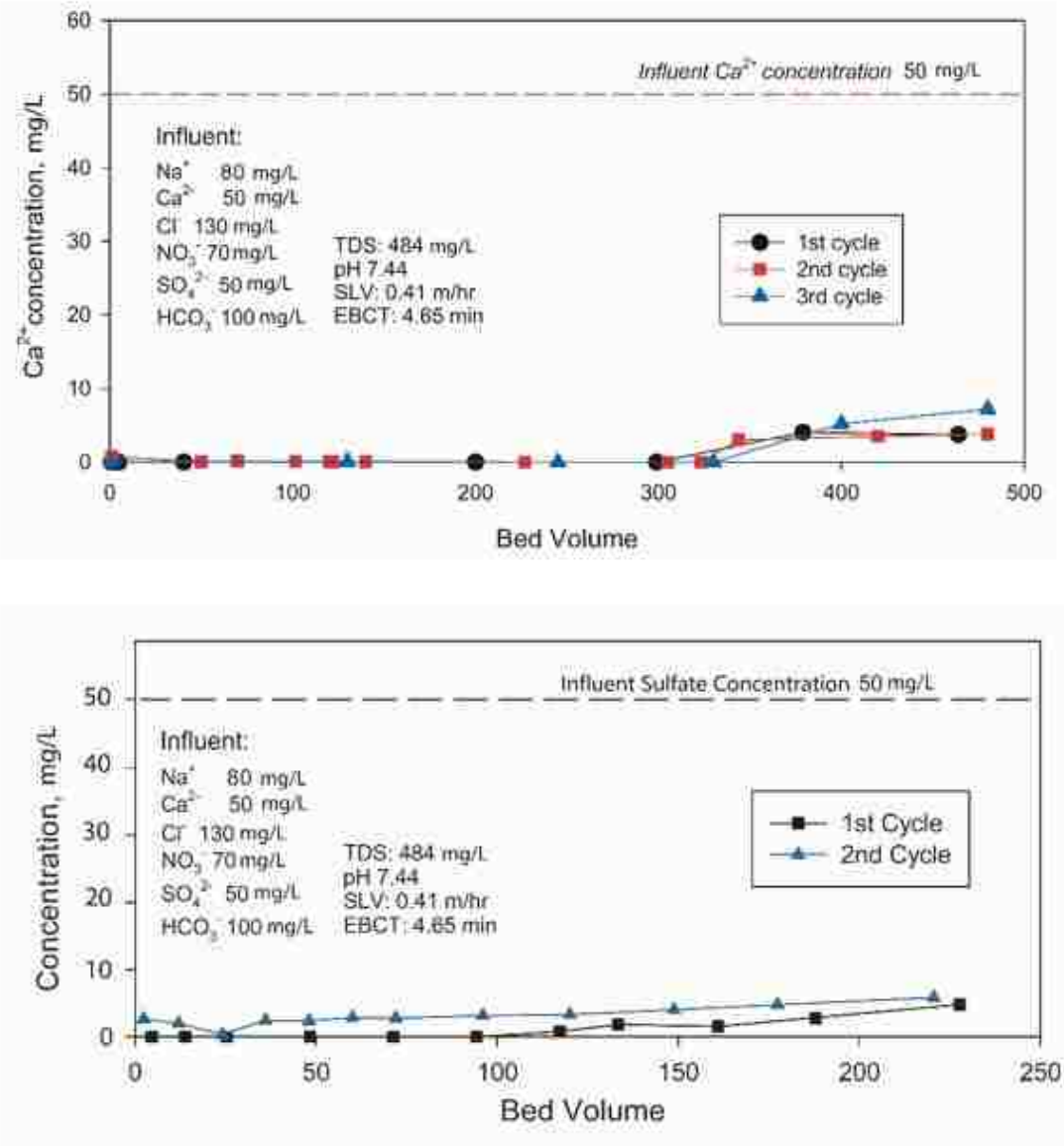

Figure 4-2. Calcium (top) and sulfate (bottom) effluent during the HIX-Desal service cycle. Note: calcium and sulfate were selectively removed to low concentrations (less than 10 mg/L) for the duration of the operation.

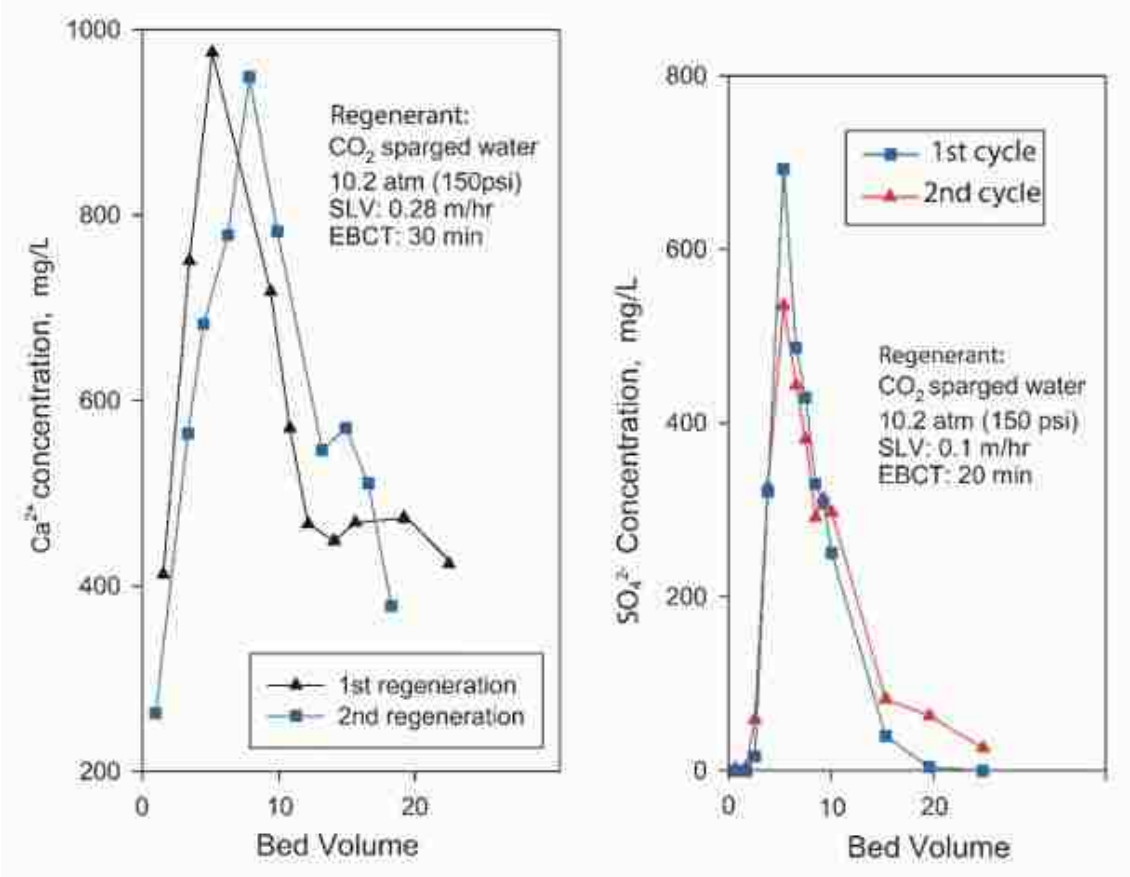

Figure 4-3. Calcium (Left) and sulfate (right) elution profiles during CO_2 regeneration of HIX-Desal. Note consistent regeneration performance during both cycles.

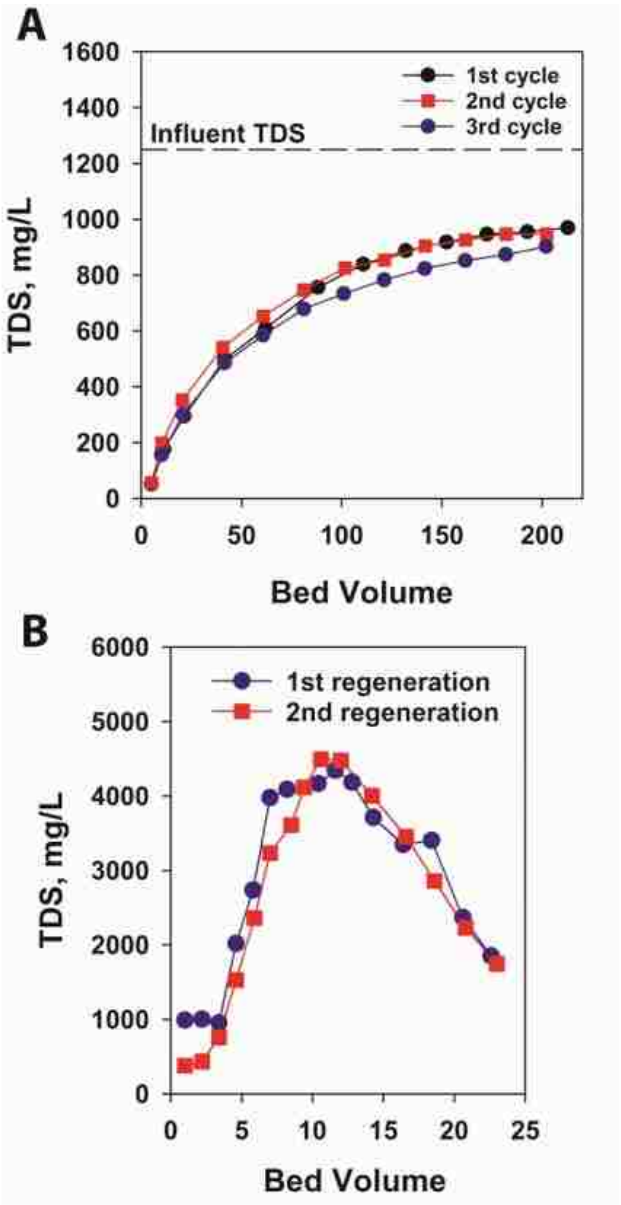

Figure 4-4. (A) Desalination performance over three consecutive service cycles using Bethlehem secondary wastewater. Influent composition and operation conditions: 100 mg/L Ca^{2+}, 300 mg/L Na^{+}, 62 mg/L NO_3^{-}, 200 mg/L Cl^{-}, 80 mg/L SO_4^{2-}, balanced HCO_3^{-}, 2.4 mg/L P, TDS 1250 mg/L, pH 7, SLV 1.4 m/h, EBCT 3.3 min. (B) TDS elution during CO_2 regeneration. Regenerant and operation conditions: CO_2 sparged water under 150 psi CO_2 partial pressure, EBCT 30 min. (EBCT= Empty bed contact time).

4.2 Phosphate recovery

Two successive phosphate effluent histories for the Bethlehem plant wastewater are shown in Figure 4-5**;** note that phosphate removal is very efficient and continues for a much longer duration: over 1000 bed volumes. Phosphate is sorbed onto ligand exchange sites of HZrO nanoparticles and not amenable to desorption during CO_2 regeneration. Thus, HAIX-NanoZr may intermittently be regenerated with KOH to recover nearly 95% of the phosphorus as potassium phosphate (K_2HPO_4), Figure 4-5, a potentially high-value fertilizer without generating any secondary waste stream. In contrast to previous phosphate recovery studies from wastewater, the HIX-Desal process achieves concurrent salinity reduction or hardness removal during the process (Blaney et al., 2007; Greenleaf et al., 2006; Sendrowski and Boyer, 2013; Sengupta and Pandit, 2011)

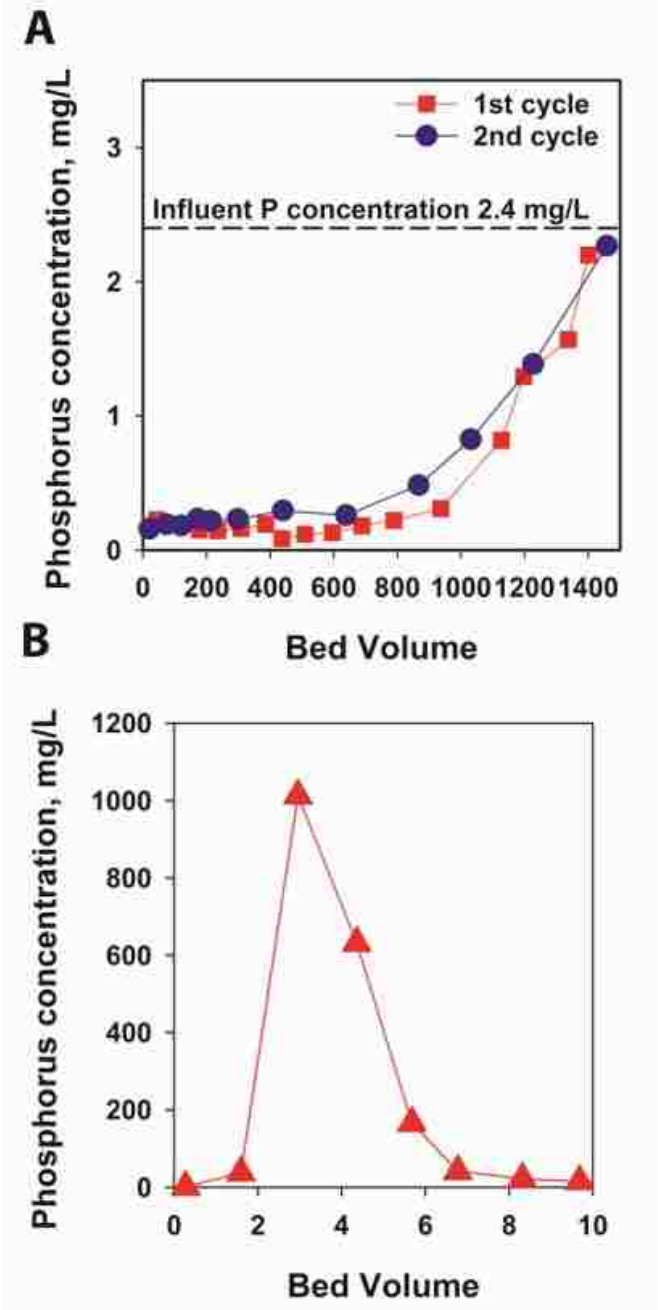

Figure 4-5. (A) Selectively removal of phosphate. Influent composition and operation conditions: 100 mg/L Ca^{2+}, 300 mg/L Na^{+}, 62 mg/L NO_3^{-}, 200 mg/L Cl^{-}, 80 mg/L SO_4^{2-}, balanced HCO_3^{-}, 2.4 mg/L P, TDS 1250 mg/L, pH 7, SLV 1.4 m/h, EBCT 3.3 min. (B) Elution of phosphate with 2% KOH.

To further reinforce the underlying sorption mechanism of phosphate from other commonly present bulk anions such as sulfate and chloride, slices of both exhausted and parent HAIX-NanoZr were characterized in by SEM-EDX mapping Figure 4-6, which shows i) Zr (purple) in the parent exchanger; ii) phosphorus in the exhausted bead; and iii) sulfur and chloride in the exhausted bead. Note that the presence of Zr in the parent resin and P in the exhausted resin merge with each other implying phosphate is adsorbed almost solely by zirconium oxide nanoparticles. On the contrary, sulfate, and chloride are distributed throughout the bead, thus confirming that quaternary ammonium groups of the parent anion exchanger are the primary sorption sites for sulfate and chloride anions.

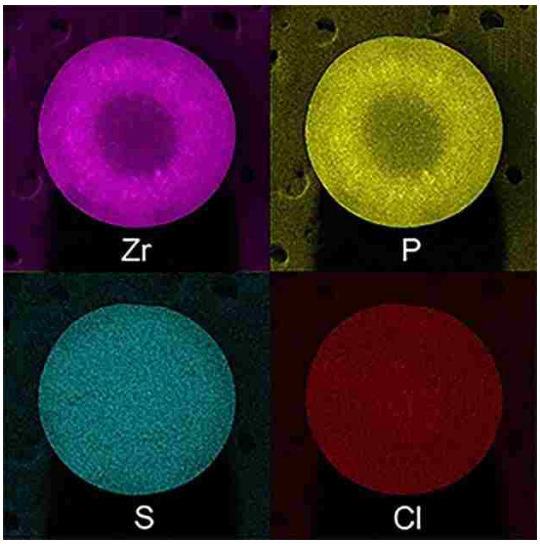

Figure 4-6. SEM-EDX mapping of Zr, P, S and Cl.

4.3 Thermodynamics

The two-bed softening, and the desalination process is favorable based on a thermodynamics view. The heart of the process is an exchange of anion with bicarbonate and subsequent exchanging of cations with hydrogen ions, followed by carbonic acid formation and stripping of carbon dioxide out from the system. So, it is mainly the following reactions driving the process,

$HCO_3^- + H^+ \leftrightarrow H_2CO_3 \qquad K_{a1} = 10^{6.38}$ Equation 4-1

$H_2CO_3 \leftrightarrow H_2O + CO_2\,(g) \qquad K_H = 10^{1.41}$ Equation 4-2

Overall: $HCO_3^- + H^+ \leftrightarrow H_2O + CO_2\,(g)\ K_{overall} = 10^{7.79}$ Equation 4-3

$\Delta G^o = -RT \ln K_{overall} = -43.72$ KJ/mol Equation 4-4

As seen from the overall free energy, the overall process is thermodynamically favorable. However, the reverse reaction during regeneration is not. It requires the input of energy to drive the process. In application, the energy comes from the compression of carbon dioxide to form high partial pressure above the aqueous phase. Since high pressure carbon dioxide is available for many applications and carbon dioxide emission sources are common, this won't hinder the application of such a process.

4.4 CO_2 consumption

Carbon dioxide is the only chemical needed to sustain the whole system, thus, the consumption of carbon dioxide is monitored during the test. The carbon dioxide high-pressure cylinder was placed on an electrical balance to monitor the weight loss during regeneration. Carbon dioxide is in liquid form inside the 800-psi cylinder. The weight loses determines the total carbon dioxide consumption and the weight loss based on time could show the consumption rate, while the weight loss based on the volume of regenerant used shows the concentration of carbon dioxide in the regenerant. Carbon dioxide consumption in kilograms and the regenerant volume data are shown in Figure 4-7. The slope of the trending line shows the concentration of carbon dioxide in the regenerant. Under 150 psi test, the carbon dioxide concentration was determined as 0.0475 kg per liter of regenerant during the regeneration. It corresponds to around 1 mol/L carbon dioxide. Consider the carbon dioxide chemistry in a closed system of consistent 10.2 atm partial pressure, the pH of the regenerant will be increased from around 3 to around 6.6 during the depletion of hydrogen ion in the cation exchanger column. From carbon dioxide chemistry pC – pH diagram from Figure 4-8, we can read that by increasing the pH from around 3.4, which is the original pH under 10.2 atm, the total carbon dioxide dissolved in the water will increase. At pH 3.4, the total concentration is 0.32 mol/L, while at pH around 6.6, the total concentration is close to 1 mol/L. That agrees with what we monitored during the test. This indicates that the consumption highly depends on the pH changes in the closed system. There will be higher carbon dioxide concentration with higher pH inside. Obviously, there will be higher bicarbonate concentration after the cation exchanger and then better overall regeneration.

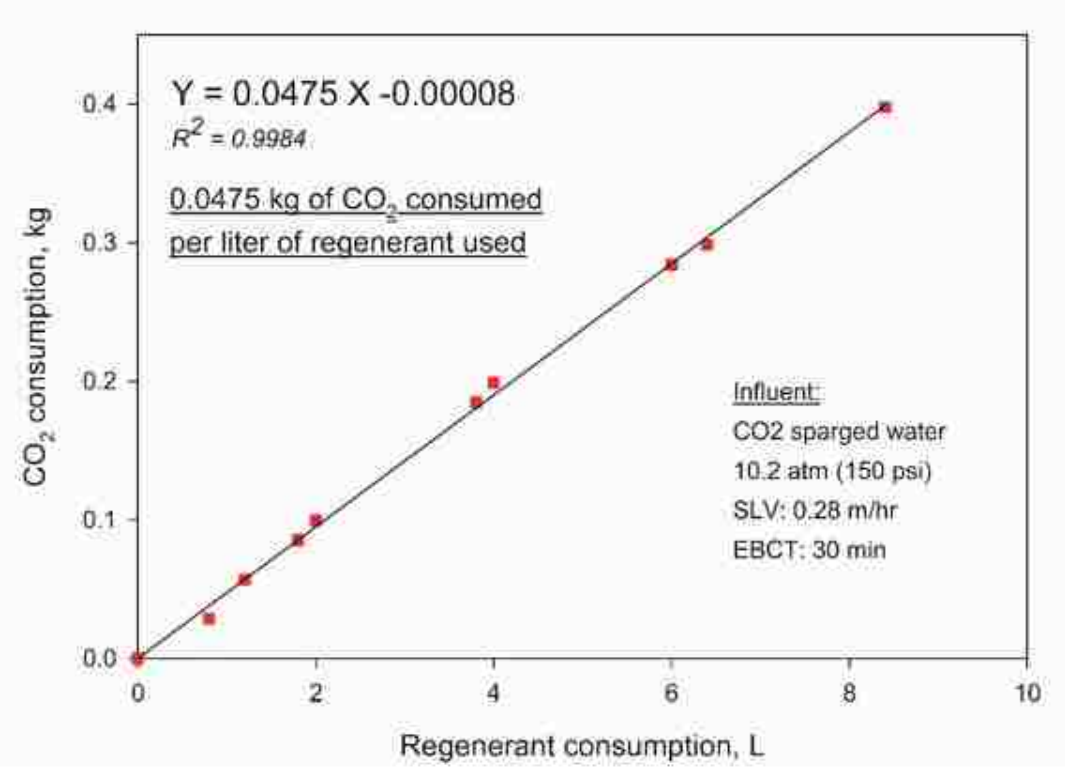

Figure 4-7. Carbon dioxide consumption during regeneration.

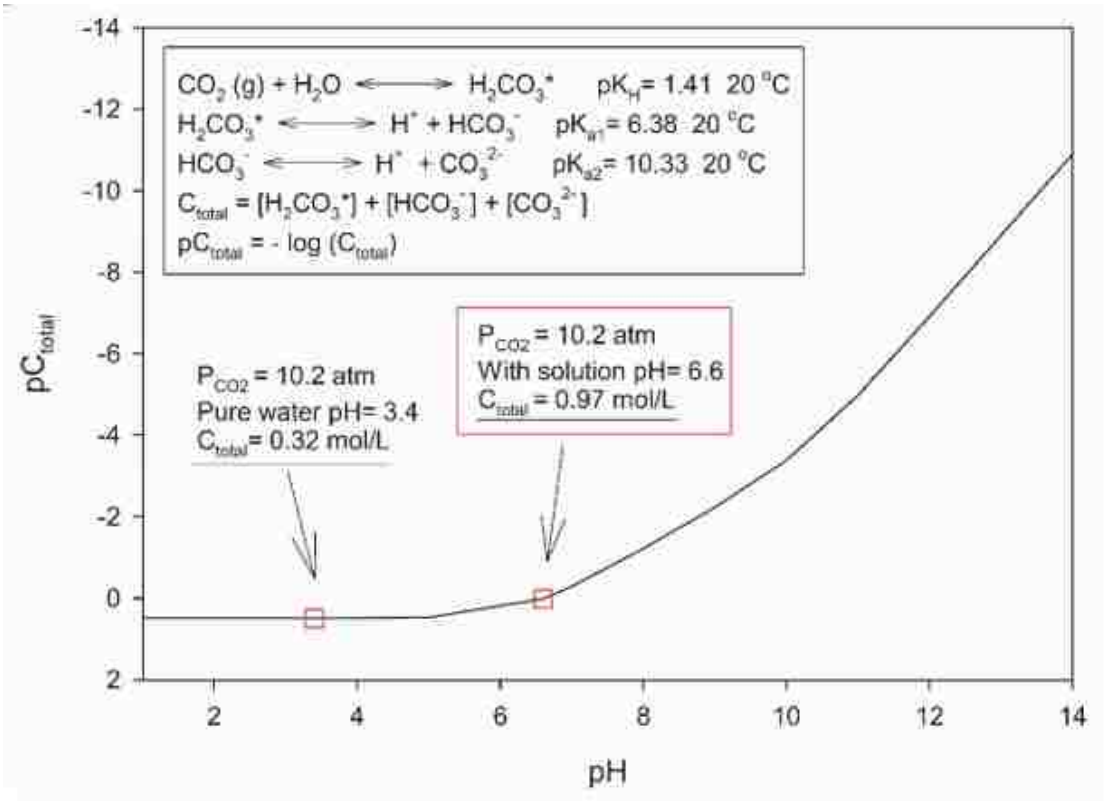

Figure 4-8. Total carbon dioxide concentration changes under 10.2 atm partial pressure.

4.5 CO_2 pressure

As discussed in the carbon dioxide chemistry section, the partial pressure of carbon dioxide affects the pure water system pH significantly. It also decides the total carbon dioxide dissolved in the aqueous phase. The pC – pH diagram of carbon dioxide under three different partial pressures is plotted in Figure 4-9. From atmospheric carbon dioxide partial pressure to 10.2 atm, the total carbon dioxide concentration increased by 4 orders of magnitude.

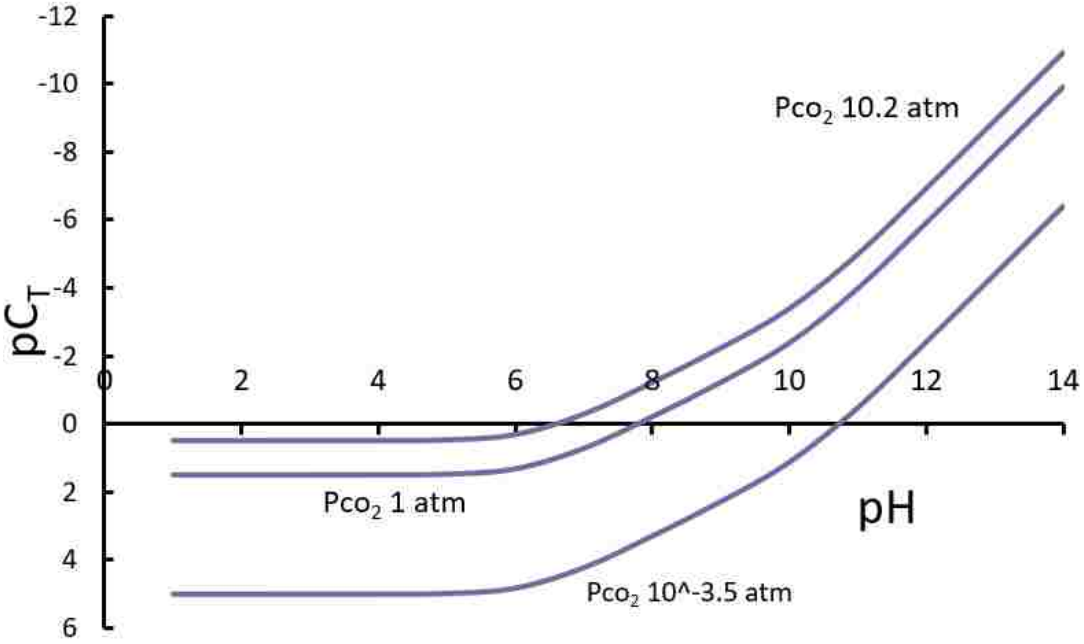

Figure 4-9. Total carbon dioxide concentration at different partial pressure.

Based on the experience during traditional mineral acid regenerated softening processes, or any other ion exchange process requiring regeneration, the counterpart ion concentration in the regenerant needs to be significantly higher than stoichiometry to achieve efficient regeneration. Hydrogen ion (H^+) serving as the counterpart ion is mainly provided by the carbonate system depicted in the first stage of carbonic acid dissolution. Furthermore, it is associated to the Henry's Law constricted reaction, thus, higher carbon dioxide partial pressure directly determines the aqueous hydrogen ion concentration and play a significant role in regeneration efficiency, calcium peak concentration and recovery are distinctively higher under high partial pressure.

To theoretically understand the partial pressure influence, we can consider the overall equilibrium expression ($K_{overall}$) governing regeneration as shown in equation 2-17 and be rewritten as follows

$$K_{overall} = \frac{[(\overline{RCOOH})]^2[C_a^{2+}][HCO_3^-]^2}{[(\overline{RCOO)_2Ca}]P_{Co_2}^2} \quad \text{Equation 4-5}$$

Considering the individual equilibrium constants for equations 2-1 to 2-2, $K_{overall}$ can be rewritten as

$$K_{overall} = K_H^2 K_{a1}^2 K_{IX} \quad \text{Equation 4-6}$$

where K_H, K_{a1}, and K_{IX} are Henry's constant for carbon dioxide dissolution in water, the first dissociation constant of carbonic acid, and the equilibrium constant for the ion exchange between hydrogen and calcium ion respectively. Equations 4-5 and 4-6 can be rewritten as

$$[C_a^{2+}][HCO_3^-]^2 = K_H^2 K_{a1}^2 K_{IX} \frac{[\overline{(RCOO)_2 C_a}]}{[\overline{(RCOOH)}]^2} P_{Co_2}^2 \quad \text{Equation 4-7}$$

Under the condition of electroneutrality considering ideality,

$$2[C_a^{2+}] \approx [HCO_3^-] \quad \text{Equation 4-8}$$

and for any given percentage regeneration efficiency, the calcium and hydrogen loading on the resin is constant, equation 4-7 can be simplified as

$$[C_a^{2+}] = \text{constant} P_{Co_2}^{2/3} \quad \text{Equation 4-9}$$

Converting to log form

$$\log[C_a^{2+}] = 0.67 \log P_{CO2} + \log \text{constant} \quad \text{Equation 4-10}$$

Equations 4-9 depicts enhancement of calcium concentration with an increase in carbon dioxide partial pressure, and they are linear under log-scale as demonstrated in equation 4-10. Three experimental data points of calcium concentration versus corresponding partial pressure during regeneration runs showed in Figure 4-10 were fitted in log-log form as shown in Figure 4-11**.** The fitting for the $\log Ca^{2+}$- $\log P_{CO2}$ line, under some assumptions including ideality, has a slope of 0.65, which is very close to the predicted value of 0.67 in equation 4-10.

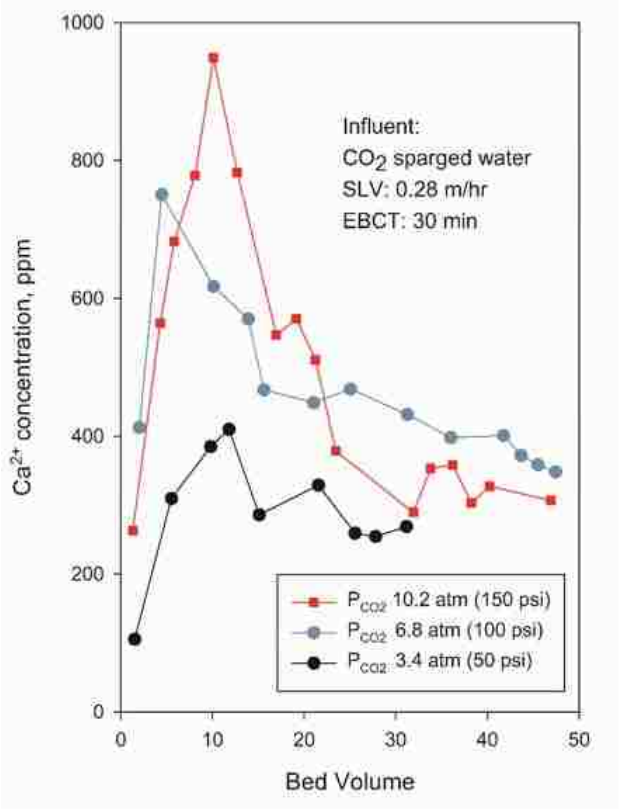

Figure 4-10. Regeneration of calcium-saturated cation exchanger under different partial pressure.

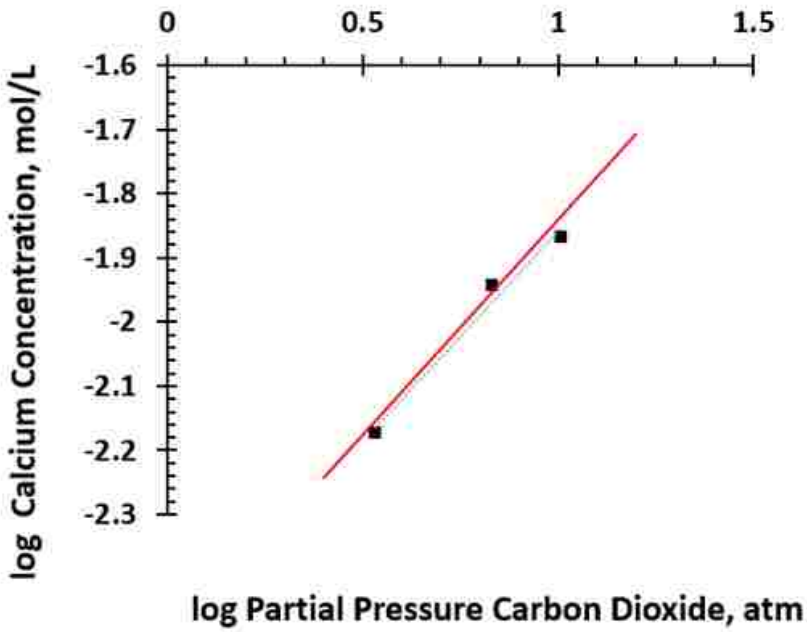

Figure 4-11. Log scale of calcium concentration under different carbon dioxide pressure. Red line is slope = 0.67 based on equation 4-10, while blue dot line is the trend line based on experimental data

4.6 Anion exchanger: role to permanent hardness removal

As discussed in previous sections, the possibilities to separate two columns and use carbon dioxide as sole regenerant to regenerate both cation and anion exchanger highly depends on the application of SCWAC-100. The requirement on the anion exchange kinetics during regeneration is not as critical as on cation exchange. However, the anion exchanger does play a significant role during the service cycle. From the desalination reactions, the key role of the anion exchanger is to exchange anions with bicarbonate, then most of the cations will be associated with bicarbonate rather than strong acid counter-ions, such as chloride. This is essential due to the weak acid cation exchanger have a strong affinity for hydrogen ion as proved and applied during regeneration, however, this ability renders that it can only exchange cations associated with weak acid counter-ions, such as bicarbonate. For example, if the weak acid cation exchanger is in hydrogen form, it won't remove sodium and calcium associated with chloride. Calcium associated with chloride, namely, permanent hardness, will not be removed in such a scenario. For natural water bodies, where it contains bicarbonate, calcium is associated with bicarbonate, namely, temporary hardness, could be removed without concern. However, there will be permanent hardness also. Thus, the anion exchanger in bicarbonate form in front is very salient for the softening process. Otherwise, the softening will be partial and incomplete for water sources containing bicarbonate, and non-softening if the water source is absent with bicarbonate when the weak acid cation exchanger is in the hydrogen ion form. The significance could be extended to consider the effect on partial desalination, too. If there is no anion exchanger in front, the partial desalination effect will be highly diminished depending on the percentage of alkalinity in the source water. So, the anion exchanger is essential for the whole service cycle of

softening and desalination, and it could be regenerated by utilizing the weak base chemistry from carbon dioxide.

Based on the above discussion, the anion exchanger material is an important source to introduce alkalinity into the solution. The demand on the anion exchanger material is its capacity. It is true that anion exchanger will always have lower capacity than cation exchanger. Tests have been done to compare different anion exchange resins in Figure 4-12. The testing process starting with weak acid cation exchanger to remove the original alkalinity first, then anion exchanger introduces alkalinity into a solution based on its capacity. Finally, the last weak acid cation exchanger column removes all the alkalinity and conducts the desalination and softening. The total bed volume treated reflects the capacity of the anion exchanger. Eventually, Purolite A600E was chosen. Even the kinetics of the anion exchanger during regeneration are not essential, it is worth mentioning that a shallow shell version of A600E resin is also commercially available.

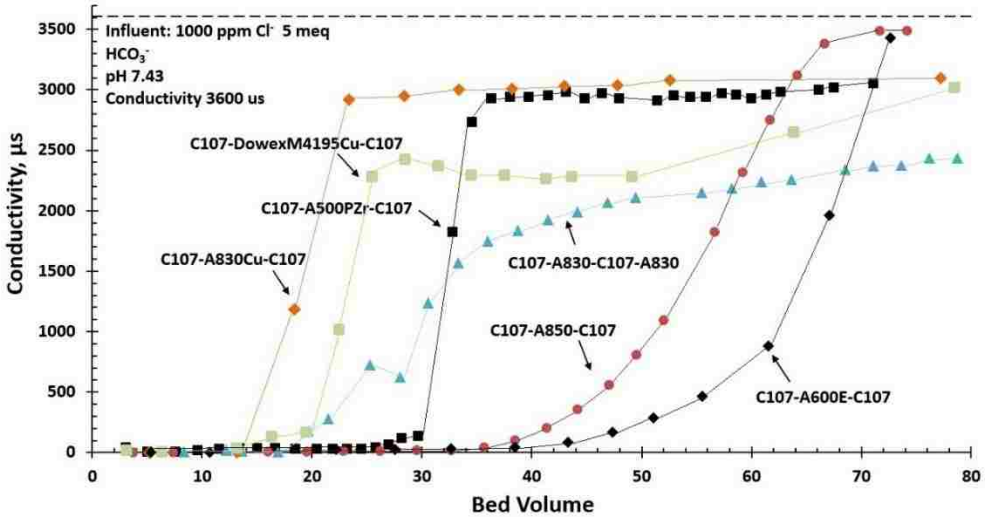

Figure 4-12. Performance comparison of different anion exchange resins.

4.7 Exchanger position: CX-AX vs. AX-CX

Based on the discussion of the importance of the anion exchanger, it is not hard to notice the importance of the position of the anion exchanger. During normal ion exchange demineralization applications, it is often that the cation exchanger precedes the anion exchanger. However, in the new two-bed system application the anion exchanger precedes the cation exchanger. This is due to the importance of bicarbonate existence on the weak acid cation exchanger. The comparison of two set-ups on the desalination effect is shown in Figure 4-13. With a synthetic feed water containing no alkalinity, almost no desalination is achieved in a set-up where cation exchanger precedes anion exchanger. However, a set-up with the anion exchanger preceding cation exchanger exhibits partial desalination. This is another distinctive part of the novel two-bed system.

Experimental data as shown in Figure 4-13 show clearly different performance by two opposite column sequences, that is i) the hydrogen-form cation exchanger (SCWAC) precedes the bicarbonate-form anion exchanger (CX-AX) and ii) the reverse (AX-CX). With influent only containing 500 mg/L $MgSO_4$, desalination only happens with the AX-CX setup as shown in Figure 4-13 . Individual species analysis as shown in Figure 4-13 and the part C further indicates that anion exchange is the same with different setup, however, cation exchange only happens when the bicarbonate-form anion exchanger precedes the cation exchanger.

Understandably, such a unique sequence could not fit into a conventional process since an OH- -form anion exchanger renders calcium precipitation, thus both column performance will be hindered. However, it becomes critical for the HIX-Desal process. SC-WAC resins as weak acid cation exchangers containing functional groups, namely, carboxylic groups

(-COOH), exhibit strong affinity for hydrogen ions. Such a strong affinity benefits the weak acid regeneration, however, results in that it can only exchange cations associated with weak base anions, such as bicarbonate. A natural salt such as sodium chloride, or magnesium sulfate could not be subject to efficient cation exchange in contact with a weak acid cation exchanger. That indicates a reaction as shown in equation 4-11 is unlikely to happen from left to right since the released hydrogen ion will tend to be adsorbed back to the resin by carboxylic groups, while the reaction could happen efficiently from right to the left. However, with the HCO_3^- - form anion exchanger prior to the WAC exchanger, released bicarbonate associating with cations could render the reaction as shown in equation 4-12 to happen. Note that carbon dioxide generated in equation 4-12 resulted in the desalination effect.

$$2\overline{RCOOH} + Mg^{2+}\,(aq) + SO_4^{2-}\,(aq) \leftarrow \overline{(RCOO^-)_2Mg^{2+}} + 2H^+ + SO_4^{2-} \qquad \text{Equation 4-11}$$

$$2\overline{RCOOH} + Mg^{2+}\,(aq) + 2HCO_3^-\,(aq) \rightarrow \overline{RCOO^-Na^+} + H_2O + CO_2\uparrow \qquad \text{Equation 4-12}$$

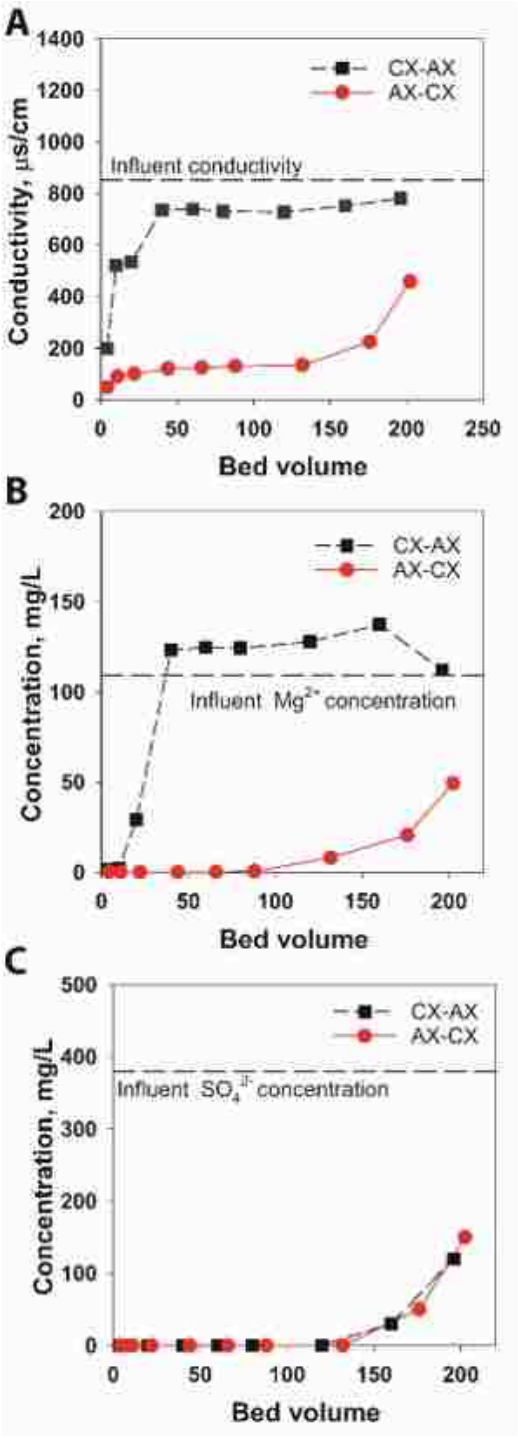

Figure 4-13. Desalination effect comparison for a different set-up, CX-AX, and AX-CX. Influent: 500ppm $MgSO_4$.

4.8 Strong acid cation vs. weak acid cation

The choice of a weak acid cation exchange resin is due to its high affinity for hydrogen ions. This is salient during weak acid regeneration. However, this is not the only reason. It is also important to notice that, compared with strong acid cation exchange resins, weak acid cation exchange resins exhibit higher calcium absorption capacity and higher affinity for calcium. It is the advantage of the carboxylic acid group over the sulfonic acid group. This renders a much longer service cycle by using weak acid cation exchange resins during softening. For the same feed water, a strong acid resin, Purolite C145, only runs for 400 bed volumes, while a weak acid resin such as Pruolite C104, made around 800 bed volumes as shown in Figure 4-14.

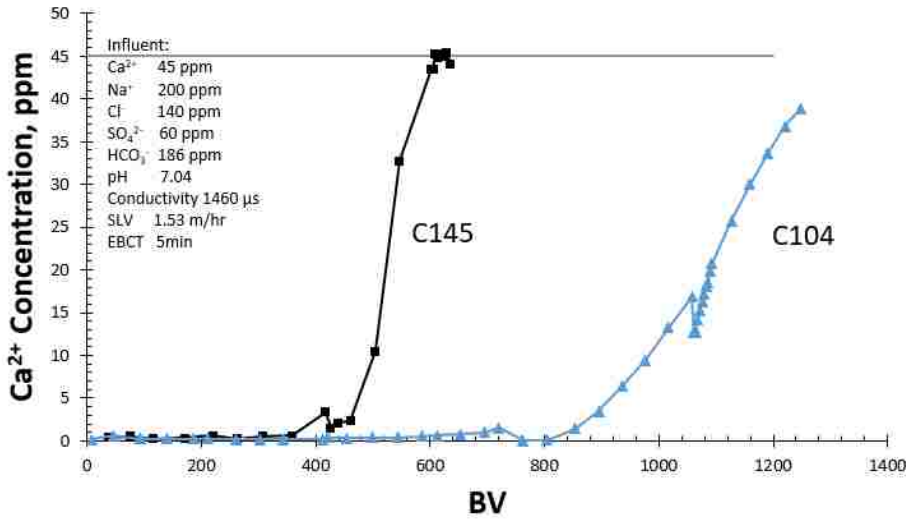

Figure 4-14. Comparison of calcium removal capacity between strong and weak acid cation exchange resin. C145: Strong acid cation exchange resin. C104: Weak acid cation exchange resin.

4.9 Interruption test and capacity of SCWAC100

As described at the beginning of this chapter, SCWAC-100 is the heart to make such a process successful. The key is that it provides faster kinetics. The kinetics could be demonstrated by an interruption test during a column run.

As shown in Figure 4-15, SCWAC-100 exhibits much lower concentration drops after an interruption test. This is due to its shorter intraparticle diffusion path length and corresponding fast kinetics. Though the capacity is slightly lower than its parent resin, it is the best choice for a carbon dioxide driven process.

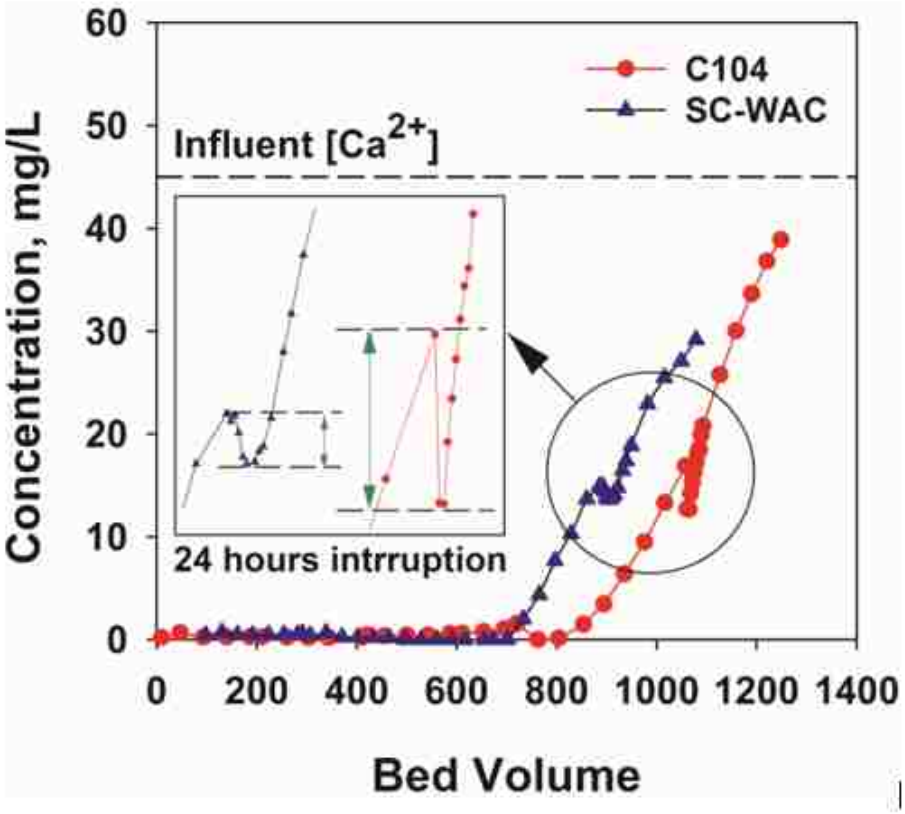

Figure 4-15. Interruption test of SCWAC-100 and C104.

4.10 Regeneration comparison between SCWAC and conventional resin

After saturation with calcium, regeneration performance under the same conditions are shown in Figure 4-16 and Figure 4-17. With 10.2 atm CO_2 partial pressure, SC-WAC resin exhibit efficient calcium elution within 20 bed volumes of regeneration. For the same bed volume of regeneration, approximate 80% calcium on the resin phase is eluted out, while it is only around 30% for a conventional weak acid cation exchange resin.

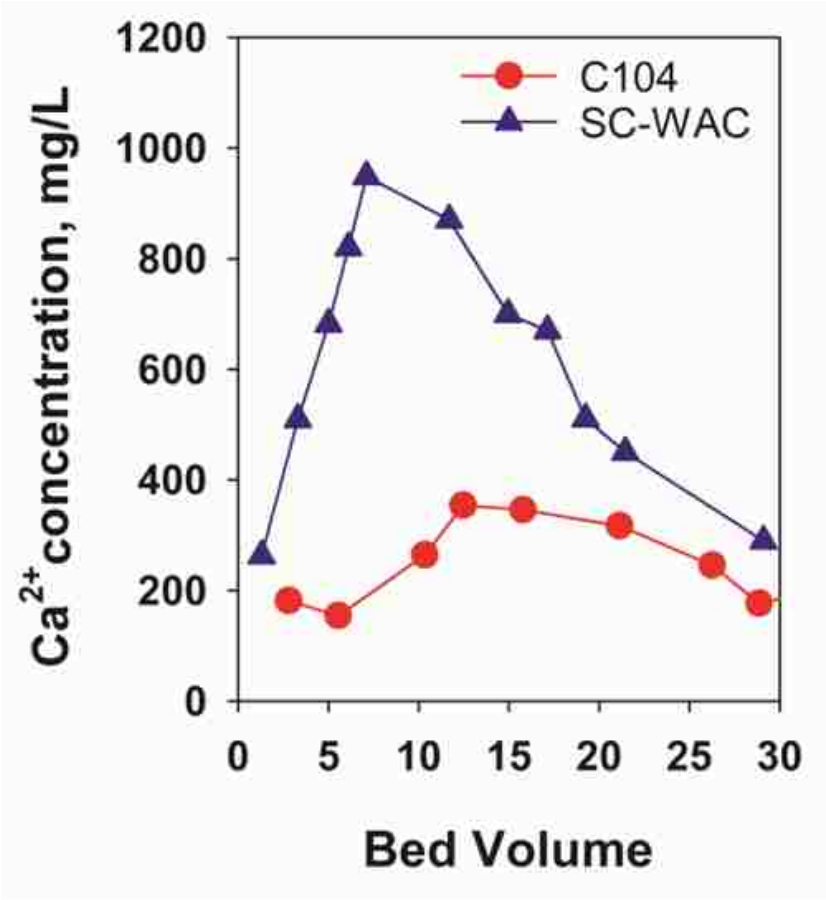

Figure 4-16. Regeneration comparison under identical 10.2 atm CO_2 pressure.

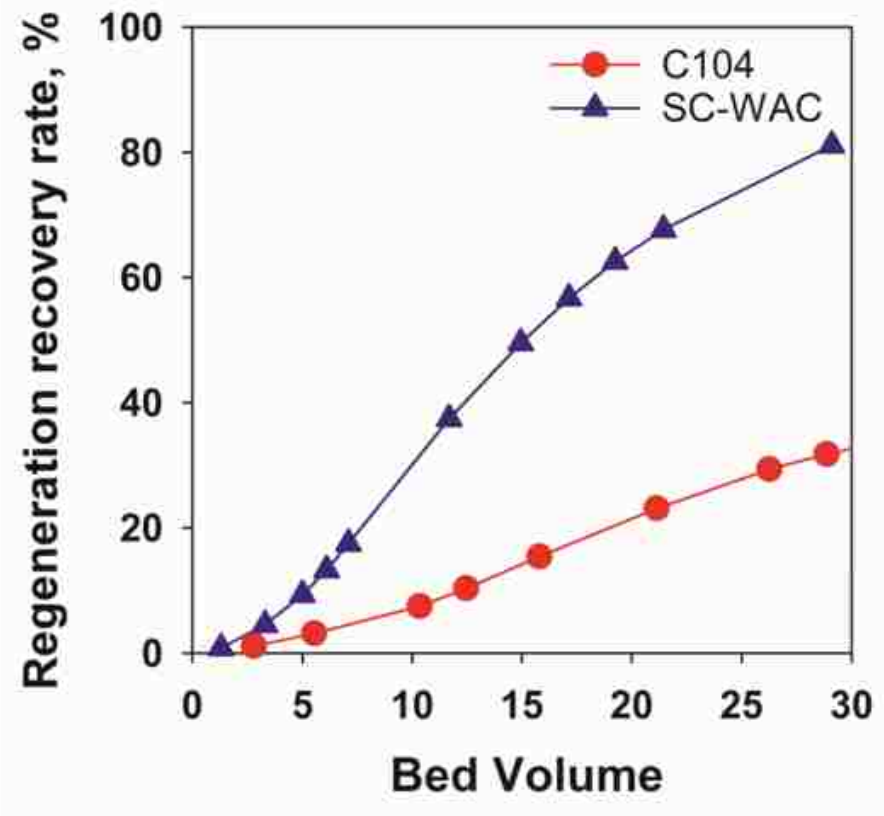

Figure 4-17. Regeneration recovery rate comparison versus regeneration bed volumes.

CHAPTER 5 Results and Discussion: CO_2 Driven Nitrate Removal Process (CHIX-N)

5.1 Nitrate removal during successive fixed-bed column runs

Hybrid nitrate selective resins were used to remove nitrate from groundwater in Lancaster. Three consecutive cycles of nitrate removal results are plotted in Figure 5-1. With spiked 62 ppm of nitrate in the groundwater, which is higher than the contaminated site, the process consistently ran 200 bed volumes before the influent nitrate level was reached. Maximum contaminant level (MCL) for nitrate was reached after 120 bed volumes. During the successive nitrate removal runs, regenerations were operated under 10.2 atm (150psi) carbon dioxide partial pressure. Twenty bed volumes of carbon dioxide sparged water was performed. Compared to using 16% brine as the regenerant in the Lancaster facility, intensive chemical consumption was eliminated. Approximately 20 ppm nitrate leakage was observed at the beginning of the service cycle.

5.2 Simultaneous Fluoride Removal and Partial desalination

NSR-Zr resins have two functional groups, namely, quaternary amine groups and zirconium oxide sites. Original amine groups on the nitrate selective resins perform nitrate removal, while zirconium nanoparticles independently remove fluoride. With groundwater spiked with approximately 5 ppm fluoride, fluoride effluent history as shown in Figure 5-2. Figure 5-3 shows the conductivity plot of the effluent during the service cycles. Approximately 50% TDS reduction has been consistently observed for the total 200 bed volumes run. This is because the conversion of salts into carbonic acid and then carbon dioxide is generated and escaped from the liquid phase.

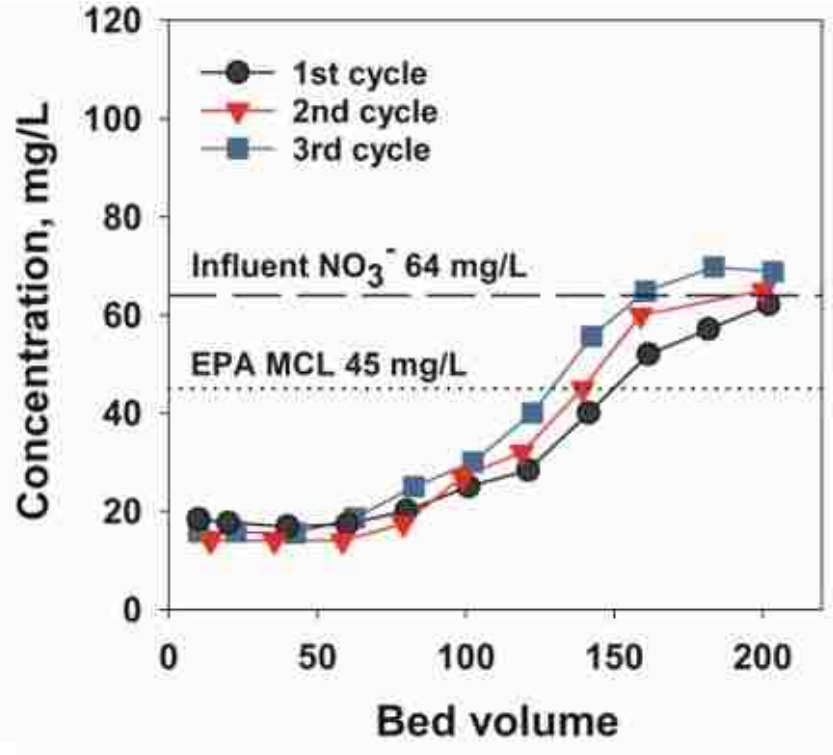

Figure 5-1. Nitrate removal over three consecutive service cycles using Lancaster nitrate-contaminated groundwater. Influent composition and operation conditions: 64 mg/L NO_3^-, 5.4 mg/L F^-, 40 mg/L Cl^-, 60 mg/L SO_4^{2-}, 274 mg/L HCO_3^-, 90 mg/L Ca^{2+}, 70 mg/L Na^+, conductivity 791 µs/cm, pH 7, SLV 1.4 m/h, EBCT 3.3 min.

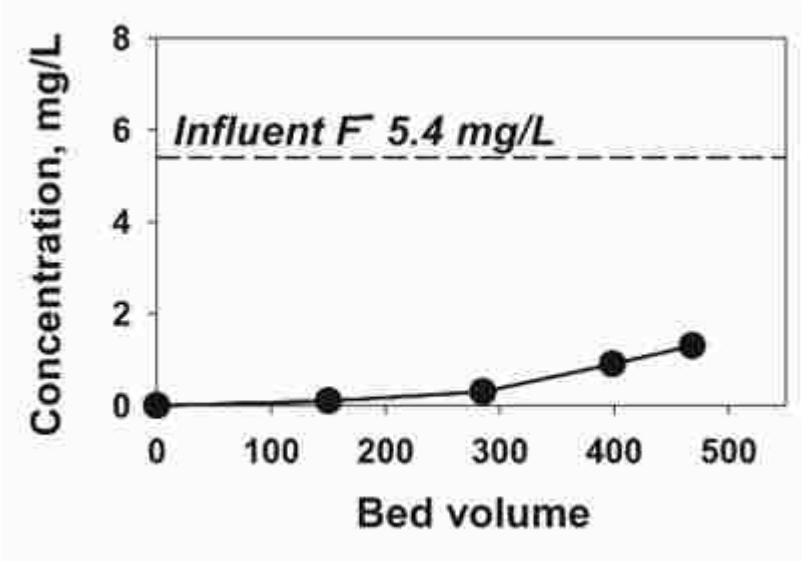

Figure 5-2. Fluoride removal. Influent composition and operation conditions: 64 mg/L NO_3^-, 5.4 mg/L F^-, 40 mg/L Cl^-, 60 mg/L SO_4^{2-}, 274 mg/L HCO_3^-, 90 mg/L Ca^{2+}, 70 mg/L Na^+, conductivity 791 µs/cm, pH 7, SLV 1.4 m/h, EBCT 3.3 min.

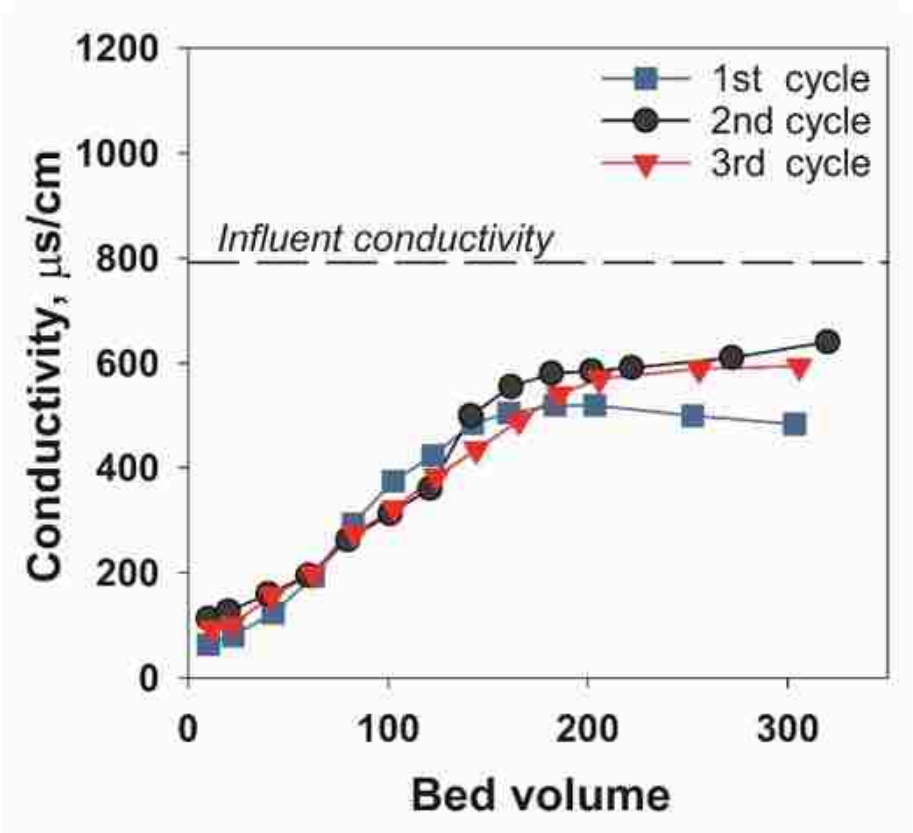

Figure 5-3. Simultaneous partial desalination during nitrate removal with CHIX-N process.

5.3 Fluoride removal characterization

In an attempt to reconcile the experimental results with the underlying scientific hypothesis, slices of both exhausted and regenerated HAIX-NanoZr were characterized in Figure 5-4 by SEM-EDX mapping which shows i) Zr (purple) in the parent exchanger; ii) fluoride in the exhausted bead, and iii) sulfur in the exhausted bead iv) chloride in the exhausted bead. Note that the presence of Zr in the parent resin and F in the exhausted resin merge with each other implying fluoride are adsorbed almost solely by zirconium oxide nanoparticles. On the contrary, sulfate, and chloride distributed throughout the bead, thus confirming that quaternary ammonium groups of the parent anion exchanger are the primary sorption sites for sulfate and chloride anions. Nitrate is the same as the sulfate and chloride, however, due to nitrogen noise coming from the background ammonium groups, nitrate mapping is not shown in the SEM image.

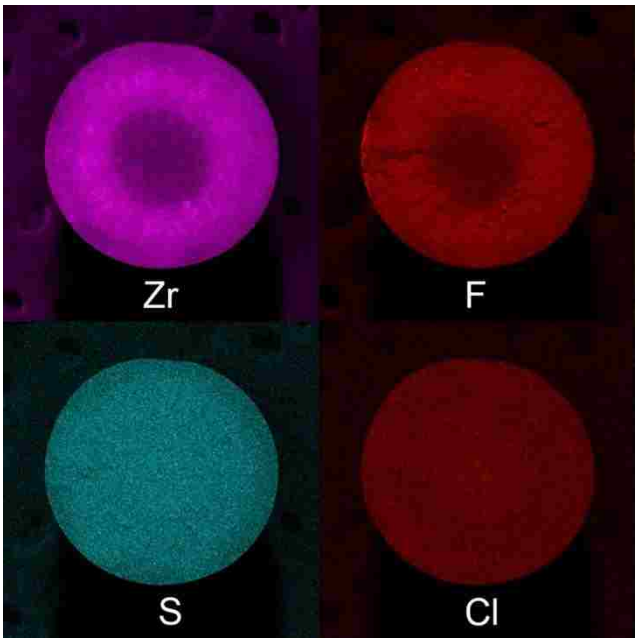

Figure 5-4. SEM-EDX spectroscopy indicating removal of fluoride by zirconium oxide present in HAIX-NanoZr, without impacting anion exchange capacity, i.e., nitrate capacity.

5.4 Comparison with 12% brine regeneration

Successive runs as shown in Figure 5-1 demonstrate the nitrate removal cycles are sustained by using carbon dioxide to replace the brine demand. The operation in the Lancaster facility used 16% NaCl to perform the regeneration, and the waste was diluted four times by slow rinse and fast rinse water. The final regeneration waste still contained 4% of NaCl. Compared to this traditional operation, the proposed process doesn't generate a high concentration of brine waste. Final regeneration waste could be even more diluted after combination. This causes minor difficulties for waste disposal. A comparison of operation (treatment and regeneration) between the proposed process and typical 12% NaCl regeneration was performed in Figure 5-5 and Figure 5-6.

A 50% regeneration recovery rate has been achieved through 10.2 atm carbon dioxide regeneration, and 20 bed volumes of around 2000 µS/cm regeneration waste have been produced. While there is more than 90 % of regeneration recovery rate for 2 bed volumes of 12% NaCl regeneration, the regeneration waste is produced with more than 100000 µS/cm in conductivity. Due to the lower efficiency, the capacity after carbon dioxide regeneration cycles are only about half of the NaCl regeneration, however, the regeneration waste is considered much easier for disposal. In addition to that, the proposed process achieves simultaneous fluoride removal and partial desalination, Figure 5-7 which brine regeneration cycle does not. The partial desalination of the proposed process primarily results from carbon dioxide formation during the service cycle. Due to the use of weak acid resins, only cations associated with bicarbonate could be removed. Groundwater usually contains a high concentration of calcium and bicarbonate, thus most of the calcium could be removed by such processes. Additionally, more bicarbonate ions are introduced to the

flow due to the use of the anion exchange resin in bicarbonate form first. Thus, TDS reduction could be consistently achieved even if the bicarbonate level is low in the raw water. For a larger scale application, stripping and recovery of the carbon dioxide from the effluent could be applied.

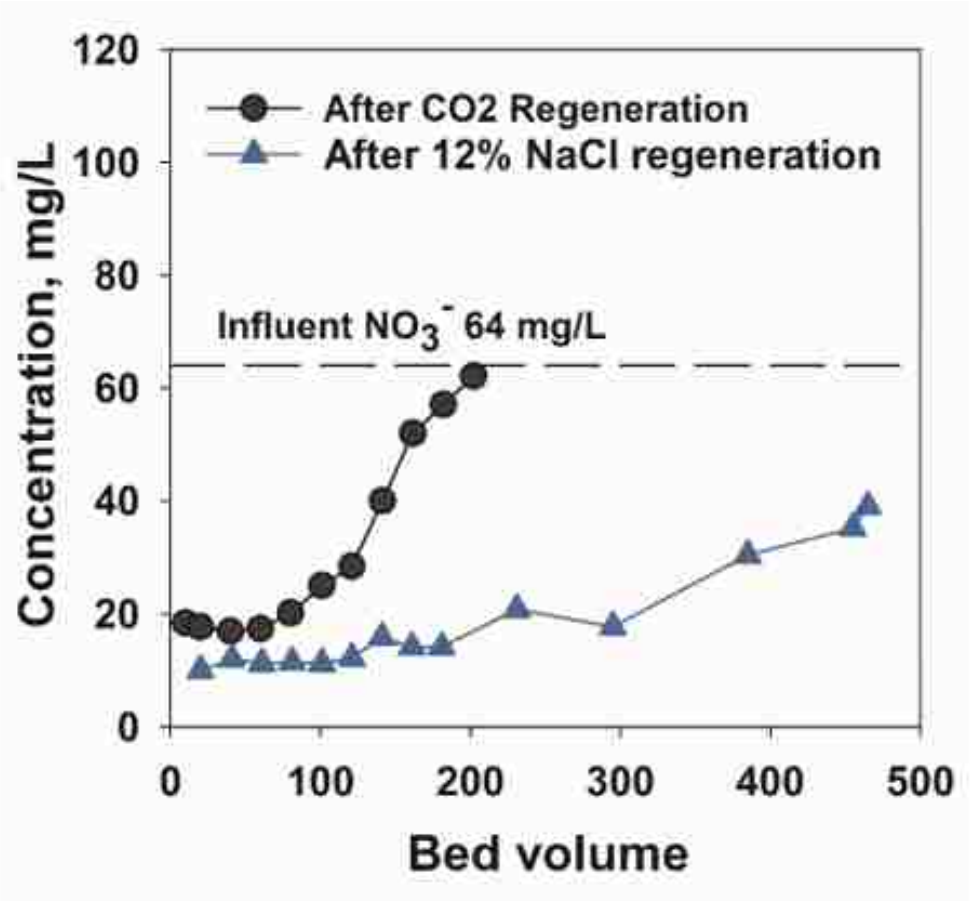

Figure 5-5. Comparison of treatment between proposed carbon dioxide sustained process and typical 12% NaCl regeneration cycles. Influent composition and operation conditions: 64 mg/L NO_3^-, 5.4 mg/L F^-, 40 mg/L Cl^-, 60 mg/L SO_4^{2-}, 274 mg/L HCO_3^-, 90 mg/L Ca^{2+}, 70 mg/L Na^+, conductivity 791 µs/cm, pH 7, SLV 1.4 m/h, EBCT 3.3 min.

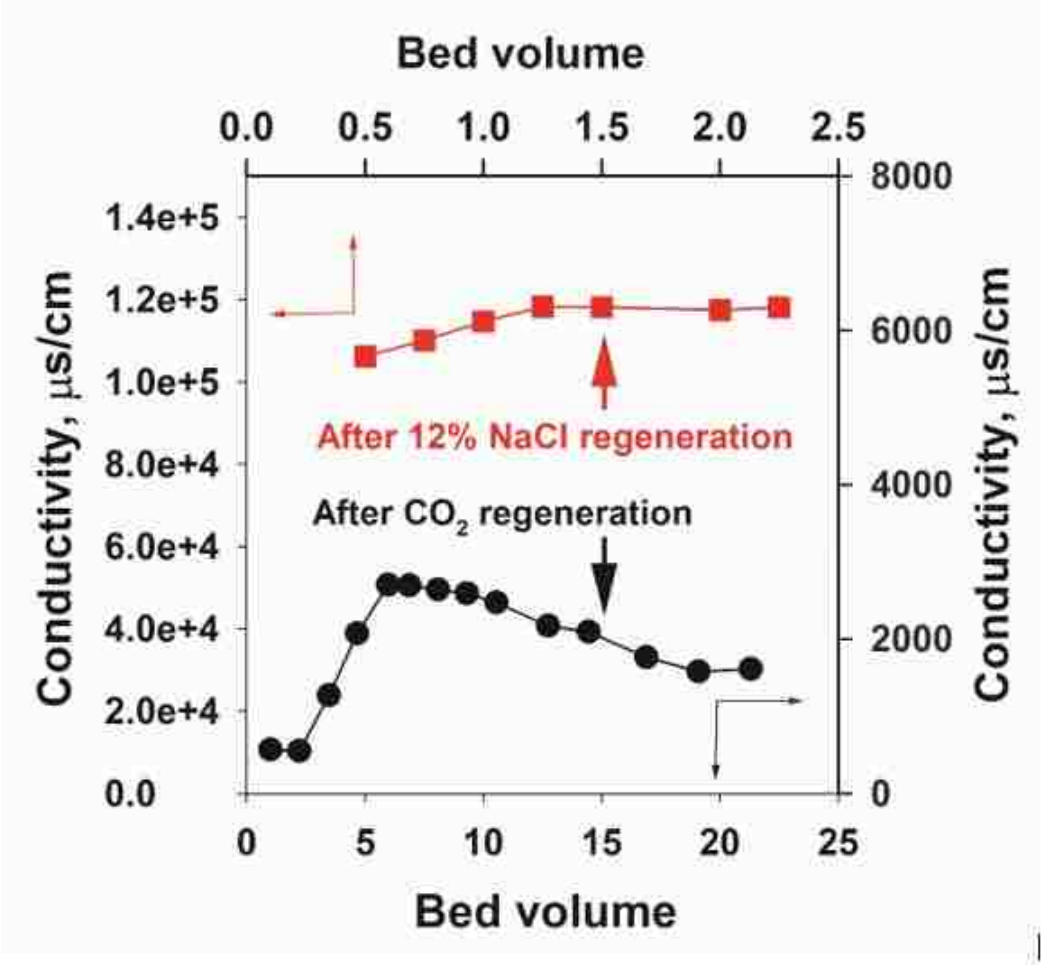

Figure 5-6. Comparison of regeneration between proposed carbon dioxide sustained process and typical 12% NaCl regeneration cycles. Influent composition and operation conditions: 64 mg/L NO_3^-, 5.4 mg/L F^-, 40 mg/L Cl^-, 60 mg/L SO_4^{2-}, 274 mg/L HCO_3^-, 90 mg/L Ca^{2+}, 70 mg/L Na^+, conductivity 791 µs/cm, pH 7, SLV 1.4 m/h, EBCT 3.3 min.

Nitrate selective resins have strong affinity for nitrate, which makes complete regeneration a non cost-effective process during practical operation. Partial regeneration is commonly applied for most of the nitrate remove facilities. Nitrate leakage is well accepted for leakage levels under the MCL. As with the traditional partial regeneration, use of carbon dioxide also causes nitrate leakage as shown in Figure 5-1. A comparison between pilot nitrate test data using 12 % NaCl regeneration in the literature and carbon dioxide sustained process is shown in Figure 5-8. Nitrate leakage amounts are close except the capacity for CO_2 process is lower. A technical report for Purolite A520E is also shown in Figure 5-9, with a nitrate leakage curve based on brine regeneration is released by Purolite.

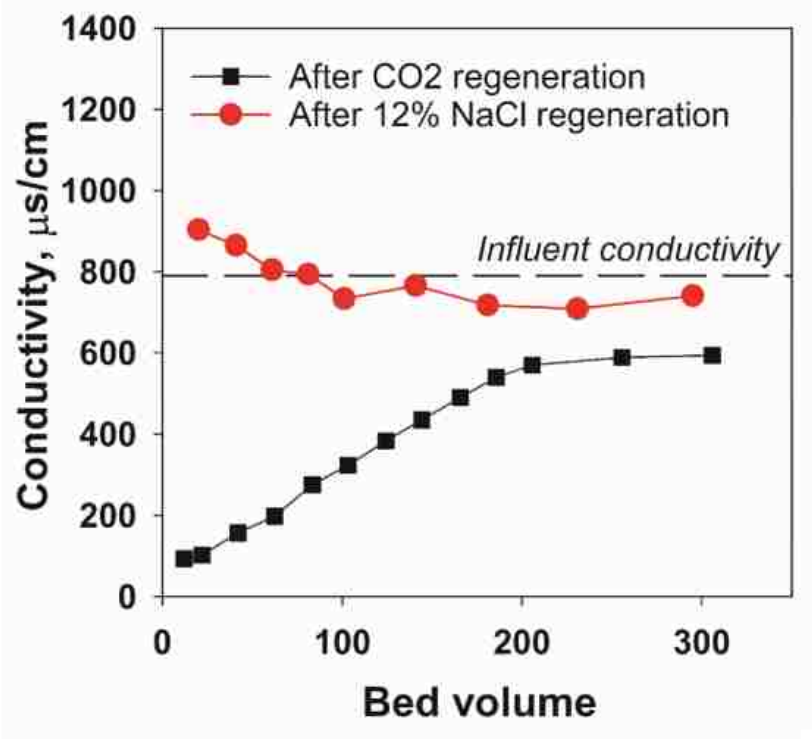

Figure 5-7. Comparison of desalination effect between proposed carbon dioxide sustained process and typical 12% NaCl regeneration cycles.

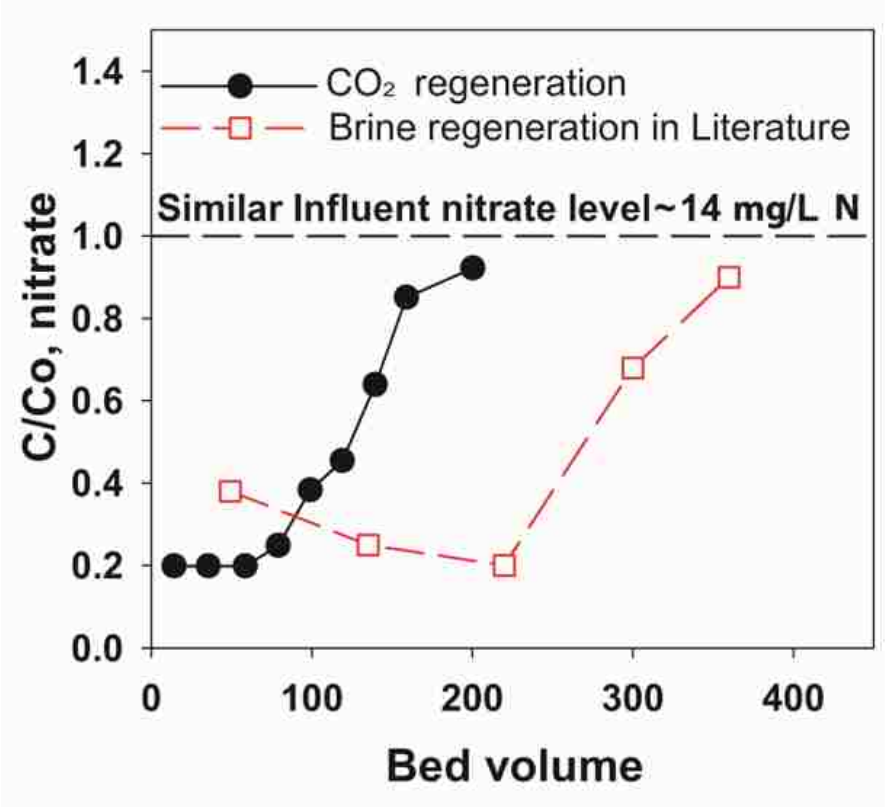

Figure 5-8. Treatment and leakage comparison between CHIX-N and literature pilot test.

PUROLITE A-520E, COUNTER-FLOW REGENERATION

Fig. 5 OPERATING CAPACITY

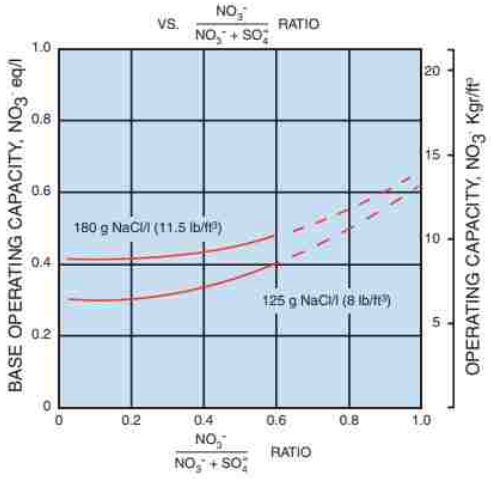

Fig. 6 NITRATE LEAKAGE

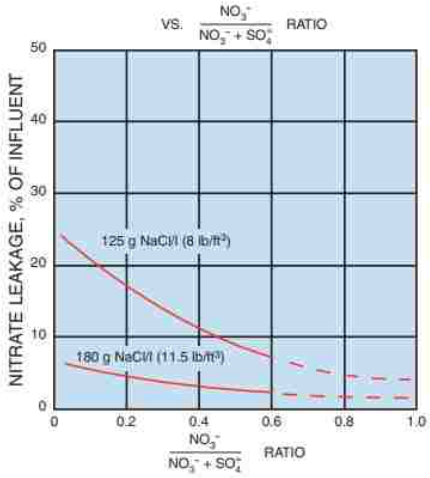

Presupposing that the objective of the nitrate removal treatment is to obtain potable water of a quality which meets the World Health Organization (WHO) limit, where the nitrate/(nitrate + sulphate) ratio is higher than 0.6, a nitrate selective resin is not necessary. A standard strong base resin can give higher throughputs as a result of its higher total capacity. It will be seen that up to the ratio of 0.6 the curves in Figs. 3 - 6 are continuous to show where **Purolite A-520E** is the recommended resin. The discontinuous curves are given so that comparisons may be made with alternative resins. Where lower leakages than the WHO limit are required, for example in the processing of certain foods, **Purolite A-520E** will often give a superior performance to the standard resins even where nitrate/(nitrate + sulphate) ratios are higher than 0.6. One particular advantage here is that there is no slug of highly concentrated nitrate at breakthrough as is found with standard resins, hence the possibility to excessively contaminate the food product by overrunning the bed is avoided.

https://www.cefns.nau.edu/capstone/projects/CENE/2014/NitrateTreatabilityOptimization/Appendicies/Appendix%202%20Engineering%20Bulletin.pdf

Figure 5-9. Comparison of nitrate leakage and capacity between proposed carbon dioxide sustained process and pilot test data from literature and A520E resin leakage curve reported by Purolite.

5.5 Running length prediction after brine regeneration

It is possible to predicate the water output of a nitrate selective resin, such as A520E. The following shows the prediction of running length for normal A520E operation after brine regeneration. For an influent composition used in the experiment as shown in Table 5-1. x is the molar fraction of species i.

Anions	mg/L	meq/L	x,i
NO3-	64	1.03	0.13
Cl-	40	1.12	0.14
SO42-	60	1.25	0.15
HCO3-	274	4.49	0.56
sum		7.90	

Table 5-1. Influent composition of anion for nitrate removal test.

With A520E nitrate selective resin, capacity Q = 0.9 eq/L, the separation factor of chloride, sulfate and bicarbonate corresponding to nitrate is shown in Table 5-2.

Separation factor	Value
$\alpha\ Cl^-/NO_3^-$	0.25
$\alpha\ SO_4^{2-}/NO_3^-$	0.0001
$\alpha\ HCO_3^-/NO_3^-$	0.125

Table 5-2. Separation factor or selective for different species onto nitrate. (SenGupta, 1995)

The fraction of nitrate on the resin after equilibrium could be calculated through equation 5-1

$$Yn = \frac{Xn}{Xn+\alpha\{c/n\}Xc+\alpha\{s/n\}Xs+\alpha\{h/n\}Xh} \quad \text{Equation 5-1}$$

where, Yn = fraction of nitrate on resin phase, Y_{NO3-};

Xn = fraction of nitrate in aqueous phase, X_{NO3-};

Xc = fraction of chloride in aqueous phase, X_{Cl-};

Xs= fraction of sulfate in aqueous phase, $X_{SO4\ 2-}$

Xh = fraction of bicarbonate in aqueous phase, X_{HCO3-};

$\alpha\ \{c/n\} = \alpha\ Cl^-/NO_3^-$;

$\alpha\ \{s/n\} = \alpha\ SO_4^{2-}/NO_3^-$;

$\alpha\ \{h/n\} = \alpha\ HCO_3^-/NO_3^-$;

Plug in all the parameters, Yn = 0.55

Running length could be predicated as Q*Yn / T*Xn = 480 BVs, which is similar to the run shown in Figure 5-1 after brine regeneration.

5.6 Nitrate leakage prediction

For an incomplete regeneration, i.e. 50% regeneration, the fraction of nitrate on the resin is

$Y_{NO3-} = 0.275$ after regeneration.

For a counter-current regeneration, consider the beginning of the effluent history, where there is only bicarbonate without any other species, the aqueous phase is in equilibrium with the resins near the outlet, where $Y_{NO3-} = 0.275$

The binary system is shown in the following equation,

$$\overline{R^+NO_3^-} + HCO_3^- \leftrightarrow \overline{R^+HCO_3^-} + NO_3^-$$

Consider the activity coefficient is 1 for ideal water solution,

$$K_{HCO3-/NO3-} = \frac{[R-HCO_3^-]\,[NO_3^-]}{[R-NO_3^-]\,[HCO_3^-]}$$

Divided by resin capacity Q, and aqueous total concentration T, the fraction of each species could be integrated into the above equation as the following,

$$K_{HCO3-/NO3-} = \frac{\{Y_{HCO_3^-}\}\{X_{NO_3^-}\}}{\{Y_{NO_3^-}\}\{X_{HCO_3^-}\}}$$

$$K_{HCO3-/NO3-} = \frac{\{1-Y_{NO_3^-}\}\{X_{NO_3^-}\}}{\{Y_{NO_3^-}\}\{1-X_{NO_3^-}\}}$$

where, $K_{HCO3-/NO3-} = 0.125$

$Y_{NO3-} = 0.275$,

Through iteration,

$X_{NO3-} = 0.045$

Nitrate leakage is $[NO_3^-]$ = 22 mg/L, which is close to what is observed.

It is worth noting that, even with an 80% regeneration, where $Y_{NO3-} = 0.1$, the nitrate leakage is still around 6.7 mg/L, and for 90% regeneration, the leakage is around 3.2 mg/L.

Regeneration percentage versus nitrate leakage is summarized in Table 5-3 and Figure 5-10. Note that a regeneration percentage beyond 20% has the potential to bring the nitrate leakage below the MCL 45 mg/L as NO_3^-.

Regeneration percentage, %	Y_{NO3-}	Nitrate leakage, mg/L
0	0.55	65
10	0.495	53.5
20	0.44	43.8
30	0.385	35.5
40	0.33	28.4
50	0.275	22.2
60	0.22	16.68
70	0.165	11.8
80	0.11	7.45
90	0.055	3.5
100	0	0

Table 5-3. Regeneration percentage versus nitrate leakage.

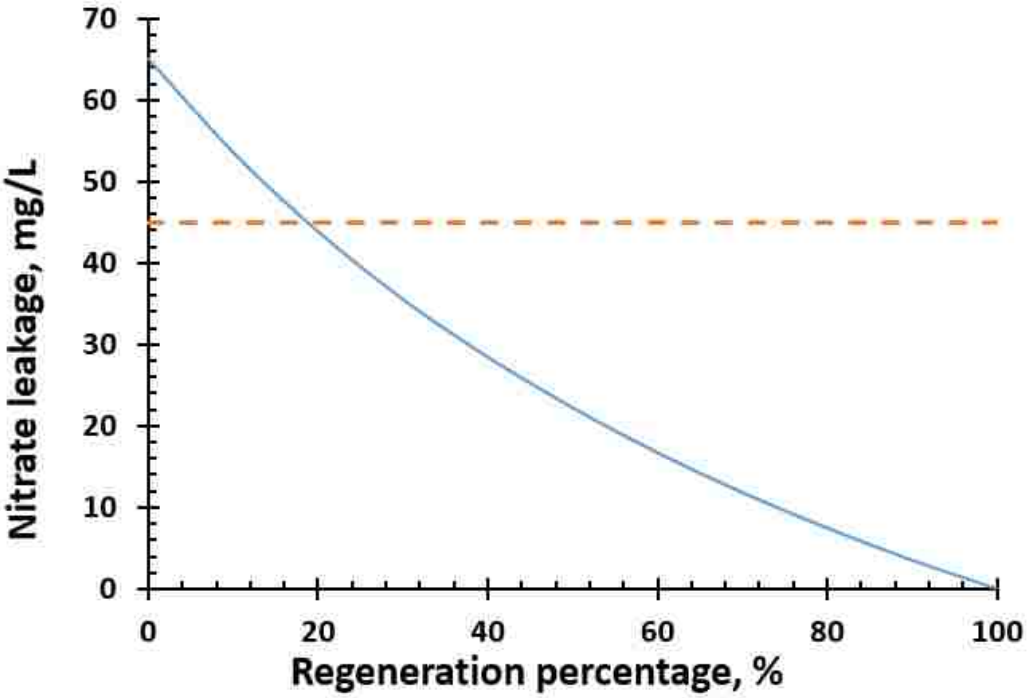

Figure 5-10. Regeneration percentage versus nitrate leakage

CHAPTER 6 Sustainable Hybrid Ion Exchange Pretreatment for Reverse Osmosis

6.1 Inorganic fouling for RO membrane

As discussed in Chapter one, reverse osmosis is the most commonly applied desalination processes. For a 60% recovery rate, concentration in the concentrate is 2.5 times higher than the influent. Similarly, for a 90% recovery rate, the concentrate concentration becomes 10 times higher. Typically, the concentration on the surface of the membrane will be even higher than the bulk solution (Smith and Sengupta, 2015), such a phenomenon is called concentration polarization. This poses a very high risk that precipitates such as $CaCO_3$, $CaSO_4$, silica or phosphate will precipitate on the membrane surface causing membrane scaling and fouling. In field reverse osmosis systems, anti-scaling chemicals are often added to prevent scaling and fouling, however, it does not always work (Gabelich et al., 2007). This is a big challenge associated with the recovery rate and energy consumption. Recovery rate will drop down and energy consumption will increase when scaling and fouling happens. Research on using ion exchange as pretreatment have been explored to reduce the sulfate concentration (Smith and Sengupta, 2015b). Applications of cation exchangers to remove calcium before reverse osmosis system also have been used in some fields. However, none of them are targeting on removing multi-ions simultaneously.

The proposed HIX-Desal process sustained by carbon dioxide and integrated with the hybrid ion exchanger could meet the demand for anti-scaling pretreatment for reverse osmosis, Figure 6-1. As is shown in previous sections, both calcium and sulfate could be efficiently removed through cation and anion exchangers and be regenerated efficiently

through carbon dioxide. Phosphate could also be selectively removed by nanoparticle sites doped in the anion exchanger.

In addition to the inorganic ions removal, partial desalination during the pretreatment will be highly beneficial to the RO system. The concentration of the feed water into RO will be 50% reduced and that will reduce the concentrate concentration at the same recovery rate and consequently osmosis pressure drops. Lower energy consumption could be expected or higher recovery rate. Higher recovery rate definitely reduces the waste volume. Moreover, this system might be sustained by the carbon dioxide from the industrial factory itself. The overall effect will be helping industries reduce water treatment cost, and reduce energy consumption, waste discharge volume, and carbon emission.

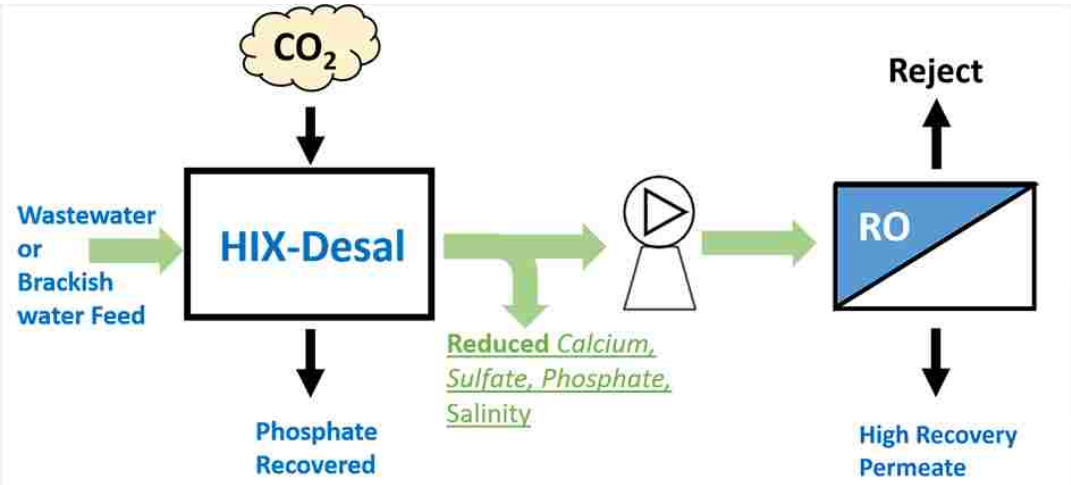

Figure 6-1. A schematic of HIX-Desal pretreatment system for RO.

6.2 Silica removal

The ability to selectively remove silica by HAIX-NanoZr have also been studied. The ability to remove of silica highly increases its attractiveness as a multi-ions removal anti-scaling system.

HIX-NanoZr silica removal efficiency was tested at the US Bureau of Reclamation (USBR) Brackish Groundwater National Desalination Research Facility (BGNDRF, Alamogordo, NM). under three different conditions at two different empty bed contact times (EBCTs) to see water chemistry impacts on silica removal performance: baseline groundwater, low pH, and high TDS (Figure 6-2). Groundwater from Well #2 at BGNDRF was used for silica removal testing, Table 6-1. Sodium metasilicate was added to the feed tank with Well #2 groundwater to increase the silica to 90 mg/L as SiO_2; HCl and/or NaOH was added to the feed water to adjust the pH.

Constituent	**Value**
pH	7.2
Conductivity	6440 µS/cm
Alkalinity	245 mg/L as $CaCO_3$
Calcium	500 mg/L as Ca^{2+}
Chloride	520 mg/L
Hardness, Total	2550 mg/L as $CaCO_3$
Magnesium	315 mg/L
Phosphate	0.85 mg/L as PO4
Sodium	650 mg/L
Silica	20 mg/L as SiO_2
Sulfate	3200 mg/L

Table 6-1. BGNDRF Well #2 water chemistry prior to dosing sodium metasilicate.

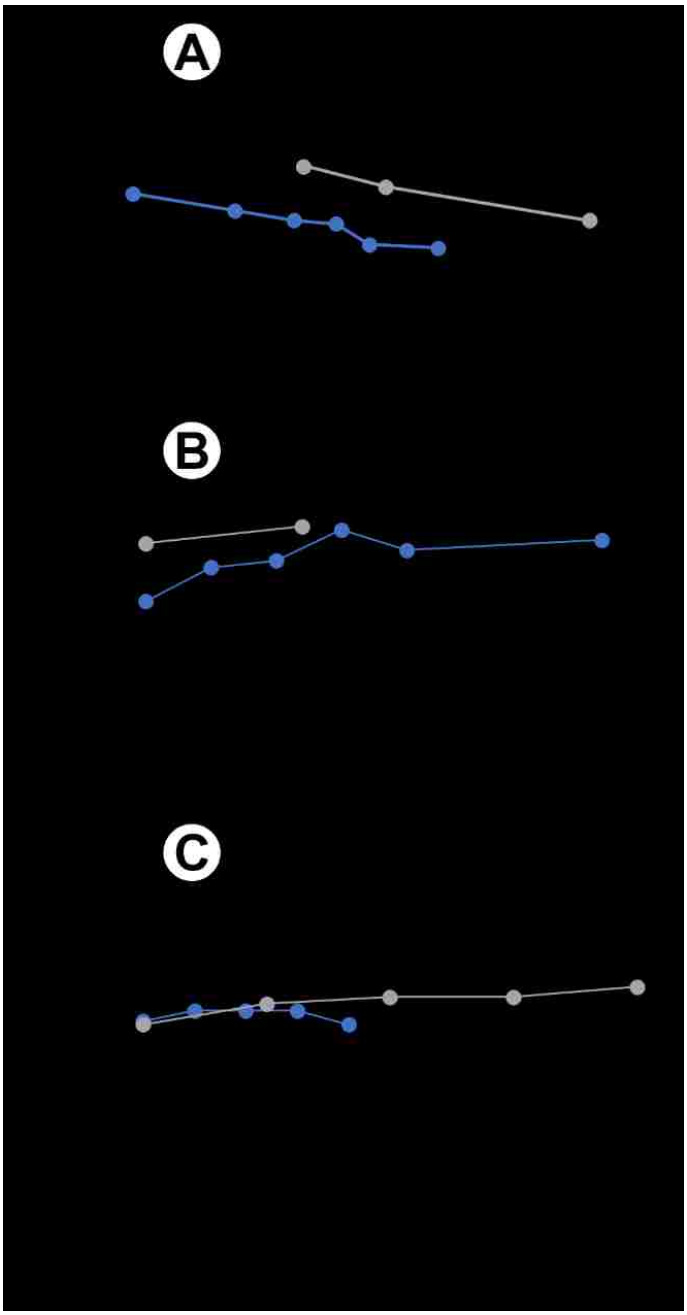

Figure 6-2. Silica removal by HIX-NanoZr at two different empty bed contact times (EBCTs) and three different water chemistries: A) BGNDRF Well #2 spiked sodium silicate; B) Feed A at pH 5; C) Feed A with 6,500 µS/cm NaCl addition.

Unlike traditional ion exchange processes, the shape of the effluent curve for silica removal demonstrates the unique underlying processes: there was neither a traditional gradual nor sharp breakthrough curve. The effluent silica decreased over the run length in Figure 6-2. Conventional ion exchange materials and processes are kinetically fast and are not impacted by changes in EBCT. For silica removal by HIX-NanoZr, increasing EBCT had a significant impact on removal efficiency in Figure 6-2. The specific surface interactions at the nanoparticle surface-water interface should be further studied to optimize silica capacity of HIX-NanoZr across different operating conditions.

Figure 6-3. Pilot test in BNGDRF, Alamogordo, NM.

CHAPTER 7 Conclusions and Future Studies

7.1 Conclusions

Throughout the discussion, we have understood the challenges during water treatment in regard to desalination, nitrate reduction and trace ligand contaminant removal, especially, using ion exchange. This study innovatively introduced carbon dioxide into the ion exchange regeneration process and addressed the challenge of efficiency and kinetics for such a practice. By using a modified cation exchanger and hybrid anion exchanger, the proposed carbon dioxide driven hybrid ion exchange processes (HIX-CO_2) could

- achieve desalination without intensive energy consumption
- achieve nitrate reduction with multiple treatment purposes
- achieve efficient softening with both temporary hardness and permeant hardness
- conduct selective trace contaminant removal such as phosphate, fluoride, etc.
- eliminate brine, strong acid, and strong base consumption while performing the abovementioned functions
- produce treated water without intensive brine or hazardous regenerant waste disposal
- provide a new way to combine carbon emission with large scale water treatment practices to prompt carbon dioxide recycle and reuse.
- resourcing the impaired water discharge and carbon emission, relieve water shortages and help mitigate climate change.

Specific scientific contributions from this study are i) addressing the intraparticle diffusion kinetics during carbon dioxide regeneration and its significance on regeneration efficiency, being the novel use and test with the shell core weak acid

cation exchange resin (SCWAC) validate the improvement on ion diffusion kinetics by shortening the functional group distribution depth. This is the premise for efficient regeneration on the cation exchanger and the following separately positioned anion exchanger; ii) the validation of the critical role of CO_2 pressure in such a regeneration practice. Higher CO_2 partial pressure renders higher dissolved inorganic carbon concentration in the aqueous phase, specifically, more hydrogen ions, and consequently more bicarbonate ions upon increasing pH. The improvement on the regeneration efficiency has been observed and aligned with theoretical modeling prediction. iii) the necessary and novel application of the unique column sequence, being an anion exchanger precedes a cation exchanger, which is opposite from the conventional two-bed ion exchange demineralization process. Such a setup is validated and follows the underlying scientific principle that the weak acid cation exchanger carries high hydrogen ion affinity and could not perform cation exchange with neutral salt. iv) the development of a process that is able to address multiple concerns in the nexus of water, energy, nutrient recovery, and CO_2 mitigation.

7.2 Future work

While the processes and applications have been developed and tested in the lab, future work remains on

- Efficient carbon dioxide recovery and reuse to minimize carbon dioxide consumption
- Or efficient carbon dioxide capture process to recover carbon dioxide directly from the source to reduce the cost
- A pilot test to move toward to field applications

Reference

Adamski, J.C., Knowles Jr., L., 2001. Ground-Water Quality of the Surficial Aquifer System and the Upper Floridan Aquifer, Ocala National Forest and Lake County [WWW Document]. URL https://pubs.er.usgs.gov/publication/wri014008

Amini, M., Mueller, K., Abbaspour, K.C., Rosenberg, T., Afyuni, M., Møller, K.N., Sarr, M., Johnson, C.A., 2008. Statistical Modeling of Global Geogenic Fluoride Contamination in Groundwaters. Environ. Sci. Technol. 42, 3662–3668. https://doi.org/10.1021/es071958y

Applebaum, S.B., 1968. Demineralization by ion exchange. Elsevier.

Bergquist, A.M., Choe, J.K., Strathmann, T.J., Werth, C.J., 2016. Evaluation of a hybrid ion exchange-catalyst treatment technology for nitrate removal from drinking water. Water Res. 96, 177–187. https://doi.org/10.1016/j.watres.2016.03.054

Blaney, L.M., Cinar, S., SenGupta, A.K., 2007. Hybrid anion exchanger for trace phosphate removal from water and wastewater. Water Res. 41, 1603–1613. https://doi.org/10.1016/j.watres.2007.01.008

Choe, J.K., Bergquist, A.M., Jeong, S., Guest, J.S., Werth, C.J., Strathmann, T.J., 2015. Performance and life cycle environmental benefits of recycling spent ion exchange brines by catalytic treatment of nitrate. Water Res. 80, 267–280. https://doi.org/https://doi.org/10.1016/j.watres.2015.05.007

Clifford, D., Liu, X., 1993. Biological denitrification of spent regenerant brine using a sequencing batch reactor. Water Res. 27, 1477–1484. https://doi.org/https://doi.org/10.1016/0043-1354(93)90028-G

Cumbal, L., Sengupta, A.K., 2005. Arsenic removal using polymer-supported hydrated Fe(III) oxide (HFO) nanoparticles: role of Donnan membrane effect. Environ. Sci. Technol. 39, 6508–6515.

Dou, X., Mohan, D., Pittman, C.U., Yang, S., 2012. Remediating fluoride from water using hydrous zirconium oxide. Chem. Eng. J. 198–199, 236–245. https://doi.org/10.1016/j.cej.2012.05.084

Gabelich, C.J., Williams, M.D., Rahardianto, A., Franklin, J.C., Cohen, Y., 2007. High-recovery reverse osmosis desalination using intermediate chemical demineralization. J. Memb. Sci. 301, 131–141.

German, M.S., 2017. Hybrid anion exchange nanotechnology (HAIX- Nano) for concurrent trace contaminant removal with partial desalination : laboratory and field-scale investigations. Lehigh Univ. Diss.

Greenleaf, J.E., Lin, J.C., Sengupta, A.K., 2006. Two novel applications of ion exchange fibers: Arsenic removal and chemical-free softening of hard water. Environ. Prog. 25, 300–311. https://doi.org/10.1002/ep.10163

Greenleaf, J.E., SenGupta, A.K., 2009. Flue Gas Carbon Dioxide Sequestration during Water Softening with Ion-Exchange Fibers. J. Environ. Eng. 135, 386–396. https://doi.org/10.1061/(ASCE)EE.1943-7870.0000065

Guter, G.A., 1995. Nitrate removal from contaminated groundwater by anion exchange. Technomic Publishing Co. Inc.: Lancaster, PA.

Habuda-Stanić, M., Nujić, M., Santo, V., 2014. Nitrate removal from water using A520E

and A 100. Elektron. časopis građevinskog Fak. Osijek 8, 67–72.

Höll, W.H., 1988. Treatment of drinking water by the CARIX ion exchange process: Experience of two years of operation of the first full-scale plant, in: Proc. 49th Int. Water Conf. Pittsburgh, PA, 24. pp. 80–88.

Höll, W.H., Hagen, K., 1992. Municipal Drinking Water Treatment by the CARIX Ion Exchange Process BT - Ion Exchange Advances, in: Slater, M.J. (Ed.), . Springer Netherlands, Dordrecht, pp. 136–143.

Kunin, R., 1964. US3156644 expired Kunnie patent WBA CX CO2 desal and reg.

Lai, K., Bates, W., Bartels, C., 2009. Ft. lauderdale 12-MGD water treatment plant: Double hybrid RO and NF design. 2009 AWWA Membr. Technol. Conf. Expo. 1–12.

Li, P., Sengupta, A.K., 2000. Intraparticle diffusion during selective ion exchange with a macroporous exchanger. React. Funct. Polym. 44, 273–287. https://doi.org/10.1016/S1381-5148(99)00103-0

Metropolitan Water Reclamatin District of Greater Chicago, 1939. Fact Sheet.

Narasimhan, R., Agrawal, A., 2016. Pilot Testing of Nitrate Treatment Processes with Minimal Brine Waste [WWW Document]. URL http://www.waterrf.org/Pages/Projects.aspx?PID=4578

National Ground Water Association, 2010. NGWA Information Brief: Brackish Groundwater [WWW Document]. URL http://www.ngwa.org/Media-Center/briefs/Documents/Brackish_water_info_brief_2010.pdf

NOAA, 2019. Full Mauna Loa CO2 record [WWW Document]. URL https://www.esrl.noaa.gov/gmd/ccgg/trends/full.html

OCWD, 2018. OCWD Study [WWW Document]. URL https://www.ocwd.com/about/my-water-bill-and-service/

Orr, J.C., Fabry, V.J., Aumont, O., Bopp, L., Doney, S.C., Feely, R.A., Gnanadesikan, A., Gruber, N., Ishida, A., Joos, F., 2005. Anthropogenic ocean acidification over the twenty-first century and its impact on calcifying organisms. Nature 437, 681.

Padungthon, S., German, M., Wiriyathamcharoen, S., Sengupta, A.K., 2015. Polymeric anion exchanger supported hydrated Zr(IV) oxide nanoparticles: A reusable hybrid sorbent for selective trace arsenic removal. React. Funct. Polym. 93, 84–94. https://doi.org/10.1016/j.reactfunctpolym.2015.06.002

Padungthon, S., Greenleaf, J.E., Sengupta, a. K., 2011. Carbon dioxide sequestration through novel use of ion exchange fibers (IX-fibers). Chem. Eng. Res. Des. 89, 1891–1900. https://doi.org/10.1016/j.cherd.2010.11.012

Sarkar, S., Sengupta, A.K., Prakash, P., 2010. The Donnan membrane principle: Opportunities for sustainable engineered processes and materials. Environ. Sci. Technol. 44, 1161–1166. https://doi.org/10.1021/es9024029

Sendrowski, A., Boyer, T.H., 2013. Phosphate removal from urine using hybrid anion exchange resin. Desalination 322, 104–112. https://doi.org/10.1016/j.desal.2013.05.014

SenGupta, A.K., 2017. Ion Exchange in Environmental Processes, Ion Exchange in

Environmental Processes. John Wiley & Sons. https://doi.org/10.1002/9781119421252

SenGupta, A.K., 1995. Ion exchange technology: advances in pollution control. CRC Press.

Sengupta, A.K., Padungthon, S., 2015. Hybrid anion exchanger impregnated with hydrated zirconium oxide for selective removal of contaminating ligand and methods of manufacture and use thereof.

Sengupta, S., Pandit, A., 2011. Selective removal of phosphorus from wastewater combined with its recovery as a solid-phase fertilizer. Water Res. 45, 3318–3330. https://doi.org/10.1016/j.watres.2011.03.044

Smith, R.C., Sengupta, A.K., 2015a. Integrating tunable anion exchange with reverse osmosis for enhanced recovery during inland brackish water desalination. Lehigh Univ. Diss.

Smith, R.C., Sengupta, A.K., 2015b. Integrating tunable anion exchange with reverse osmosis for enhanced recovery during inland brackish water desalination. Environ. Sci. Technol. 49, 5637–5644. https://doi.org/10.1021/es505439p

State water resources control board, 2010. GAMA Program GROUNDWATER INFORMATION SHEET Salinity [WWW Document]. URL https://www.waterboards.ca.gov/gama/docs/coc_salinity.pdf

Su, X., Wang, H., Zhang, Y., 2013. Health risk assessment of nitrate contamination in groundwater: a case study of an agricultural area in Northeast China. Water Resour.

Manag. 27, 3025–3034.

Texas water development board, 2010. The desalination plant database of Texas [WWW Document]. URL http://www2.twdb.texas.gov/apps/desal/default.aspx

USEPA Web, 2019. Natioanl Secondary Drinking Water Regulations (NSDWRS) [WWW Document]. URL https://www.epa.gov/dwregdev/drinking-water-regulations-and-contaminants

veolia, 2014. CARIX-Economical and environmentally-friendly water softening [WWW Document]. URL http://technomaps.veoliawatertechnologies.com/carix/en/

Wentz, D.A., 2011. Nutrients from atmospheric and urban sources, fertilization, and livestock wastes can contribute to excessive algal growth in streams.

Werber, J.R., Deshmukh, A., Elimelech, M., 2016. The Critical Need for Increased Selectivity, Not Increased Water Permeability, for Desalination Membranes. Environ. Sci. Technol. Lett. 3, 112–120. https://doi.org/10.1021/acs.estlett.6b00050

Zhu, A., Christofides, P.D., Cohen, Y., 2009. Effect of thermodynamic restriction on energy cost Optimization of RO membrane water desalination. Ind. Eng. Chem. Res. 48, 6010–6021. https://doi.org/10.1021/ie800735q

VITA

Hang Dong was born on February 9, 1990 in Henan province, China. He earned his Bachelor's degree in Environmental Science from Henan University, China in June 2012 and came to Lehigh University at August to pursue a Master's degree under Dr. Derick Brown. He earned Master's degree in Environmental Engineering in May 2014 and passed the Fundamentals of Engineering Exam and became an Engineering in Training at the same year. He received Gibson Fellowship in September 2014 and started Ph.D. research with Dr. Arup SenGupta since October 2014.

During his time at Lehigh he was the Teaching Assistant and Research Assistant and published one first authored paper on Environmental Science & Technology Letters entitled " Hybrid Ion Exchange Desalination (HIX-Desal) of Impaired Brackish Water Using Pressurized Carbon Dioxide (CO2) as the Source of Energy and Regenerant" and one second authored paper on ACS Sustainable Chemistry & Engineering entitled "Treated Municipal Wastewater Reuse: A Holistic Approach Using Hybrid Ion Exchange (HIX) with Concurrent Nutrient Recovery and CO_2 Sequestration". He was a co-inventor on US patent application US20180273401A1: "Contaminants Removal with Simultaneous Desalination Using Carbon Dioxide Regenerated Hybrid Ion Exchanger Nanomaterials".